# Pre-clinical Drug Development of 9-aminoacridines for Malignant Glioma and Meropenem Prodrugs for Drug-Resistant Tuberculosis

A DISSERTATION
SUBMITTED TO THE FACULTY OF THE GRADUATE SCHOOL
OF THE UNIVERSITY OF MINNESOTA
BY

Aaron Matthew Teitelbaum

IN PARTIAL FULFILLMENT OF THE REQUIREMENTS
FOR THE DEGREE OF
DOCTOR OF PHILOSOPHY

Rory P. Remmel, Adviser

August 2012

**Acknowledgements**

This dissertation would not have been possible without the support from several influential people. First, I would like to express my sincere gratitude to Dr. Rory Remmel, my adviser. Over the last five years, I have learned an invaluable set of technical skills and scientific problem solving abilities, which have set the foundation for my future career as an academic scientist. Additionally, through his mentorship and guidance, I have learned how to effectively teach complex material and engage students within the classroom. His passion for teaching, advocacy for students, and willingness to always help are all qualities I would like to emulate during my career.

I would also like to acknowledge my committee members Drs. Courtney Aldrich, David Ferguson, and L'Aurelle Johnson for their support and insightful comments regarding my graduate work.

I am grateful for the previous and current members of the Center for Drug Design (CDD), namely Drs. Ce Shi, Kim Grimes, and Anja Meissner who have spent countless hours discussing and interpreting NMR spectra with me.

Additionally, I would have not survived graduate school without the support and aid from my classmates, friends, and lab members I have met during graduate school. I wish to thank Trinh (Amy) Doan, Mike Peterson, David Hermanson, Adam Benoit, Katie Pietsch, Hailey Gailon, Kathy Nelson, Alex Grill, Manoj Chiney, Harrison Tam, Theresa

Aliwarga, and Drs. Jin Zhou, Murali Subramanian, Melissa Kramer, Lucy Hodge, and Darcy Flora for all their help whether in the classroom, in the lab, or listening and giving insightful comments during a practice seminar.

Lastly, I would like to thank my family for their love, encouragement, and support during all aspects of my life, without which, none of this would be possible.

## Dedication

This dissertation is dedicated to my grandfather, Dr. Julius Paster.

## Abstract

The pre-clinical drug development of investigational molecules with encouraging *in vitro* efficacy require drug metabolism and pharmacokinetic experiments that ultimately characterize "what the body can do to the drug." In chapter one of this thesis, the absorption, distribution, and metabolic properties of a series of 9-amnoacridines (Acridine **1** – **4**) with potent anti-proliferative activity are described by investigating their metabolic stability, cellular accumulation in MDCK cells with or without transfected efflux transporters (PgP or BCRP), plasma protein binding, and tissue accumulation in mouse pharmacokinetic studies. Additionally, acridine **2** was chosen as the lead candidate and evaluated in a mouse orthotopic glioblastoma model.

Metabolic stability experiments in pooled human liver microsomes indicated slow rates of oxidation (apparent $t_{1/2}$ from 2.2 - 4.1 hours) and negligible glucuronidation. In addition, acridine **1**, **2**, and **4** accumulated in MDCK-WT cells with values 2.7, 2.2, and 4.3 times greater than propranolol. The accumulation of acridine **3** was equal to that of propranolol. In accumulation experiments with MDCK-MDR cells, it was discovered that acridine **1** and **3** were moderate substrates for Pgp whereas acridine **2** and **4** were not substrates. Accumulation experiments with MDCK cells overexpressing BCRP identified acridine **1**, **3**, and **4** as substrates for BCRP, but not **2**. Interestingly, it was discovered that the 9-aminoacridines were substrates for the organic cation transporter (OCT). A mouse pharmacokinetic study following a 60 mg/kg oral dose with Acridine 1 and 2 demonstrated low penetration into the brain ($C_{max}$ = 0.25 μM and 0.6 μM), but high uptake in kidney ($C_{max}$ = 30 μM and 300 μM) and liver ($C_{max}$ = 125 μM and 225 μM)

relative to total peak concentrations in plasma ($C_{max}$ = 2.25 μM and 20 μM). Subsequently, an intravenous pharmacokinetic study with Acridine 2 following a 15 mg/kg dose produced peak concentrations in the brain (1.7 μM), kidney (212 μM), and liver (78 μM) at 2.0 hours relative to a 2.0 μM peak concentration in the plasma. Acridine **2** bioavailability was 83.8%. Acridine **2** significantly increased the median survival of mice in an orthotopic glioblastoma model suggesting compounds in this series may offer new strategies for the design of chemotherapeutics for treating brain cancers with high oral bioavailability and improved efficacy.

Chapter 2 of this thesis describes the synthesis and evaluation of meropenem prodrugs for extensively drug-resistant tuberculosis (XDR-TB). *Mycobacterium tuberculosis* (*Mtb*), the causative agent of tuberculosis (TB), is the leading cause of bacterial infectious disease mortality worldwide. Due to the emergence of multi- and extensively drug-resistant strains of TB, new chemical agents are desperately needed. Although β-lactams are the most widely used group of antibiotics, they have never been systematically utilized in TB therapy due to their poor penetration of the mycobacterial cell wall as well as their inactivation by the chromosomally encoded β-lactamase (BlaC). In 2009, Hugonnet et al. shattered this long held dogma demonstrating that meropenem and clavulanate were highly effective against (XDR-TB) strains *in vitro*. Due to meropenem's short half-life (1 hr) and lack of oral bioavailability, the synthesis and evaluation of meropenem prodrugs as potential therapeutics for the treatment of TB are described.

The initial approach to improving the oral bioavailability of meropenem was to synthesize the isopropoxycarbonyloxymethyl (proxetil) ester of meropenem. Second generation prodrugs with more lipophilic promoieties (benzosuberyl, tetralyl, and indanyloxycarbonyloxymethyl) were subsequently synthesized as well as a simple benzyl ester derivative. The aqueous stability of prodrugs at biologically relevant pH 1.2 (stomach), 6.0 (intestinal), and 7.4 (blood) is reported in terms of prodrug half-life or percent remaining after a 2-hour incubation at 37 °C. The most stable prodrug at pH 7.4 and 6.0 was the proxetil ester of meropenem (6 – 11% degradation over 2 hours); however, the prodrugs containing the 1-benzosuberyl, 1-tetralyl, and 1-indanyloxycarbonyloxymethyl promoieties were all unstable in aqueous solution at pH 7.4 (half-lives of 139, 5.8 and < 1 min, respectively) and resulted in the formation of a racemic alcohol indicative of a $S_N1$ solvolysis mechanism. The prodrugs containing the 2-benzosuberyl, 2-tetralyl, and 2-indanyloxycarbonyloxymethyl promoieties were significantly more stable at physiological pH 7.4 and intestinal pH 6.0 (20 – 30% degradation in 2 hours) as a result of carbonate attachment at the 2-poistion and not the benzylic position. The plasma stability of the most aqueous stable prodrugs was very short (1 – 6 min) implying a rapid release of the parent compounds. Interestingly, the simple benzyl ester derivative had the longest stability (8 min) in plasma compared to all the other prodrugs. Experiments to determine the relative bioavailability of meropenem were conducted with the proxetil ester of meropenem as well as the 1-(*S*), 1-(*R*), and racemic 2- benzosuberyloxycarbonyloxymethyl prodrugs in jugular vein catheterized

guinea pigs. The bioavailabilities were calculated to be 1.9%, 6.2%, 4.4%, and 5.9%, respectively.

## Table of Contents

## List of Tables

## List of Figures

## List of Schemes

## List of Commonly Used Abbreviations

| | |
|---|---|
| AUC | Area under the curve |
| BlaC | β-Lactamase |
| BCRP | Breat Cancer Resistance Protein |
| CBS | Corey-Bakshi-Shibata |
| cLogP | Calculated Partition Coefficient |
| LogD | Distribution Coefficient |
| CAR | Constitutive Androstane Receptor |
| CYP | Cytochrome P450 |
| DACA | N-[2-(dimethylamino)ethyl]-acridine-4-carboxamide |
| DCM | Dichloromethane |
| DMSO | Dimethyl Sulfoxide |
| DOTS | Directly Observed Therpay - Shortcourse |
| EMB | Ethambutol |
| EtOAc | Ethyl Acetate |
| FBS | Fetal Bovine Serum |
| GF | GF120918 |
| GSH | Glutathione |
| HLM | Human Liver Microsomes |
| HPLC | High Performance Liquid Chromatography |
| IACUC | Institutional Animal Care and Use Commiteee |

| | |
|---|---|
| INH | Isoniazid |
| LC-MS | Liquid Chromatography Mas Spectrometry |
| LY | LY335979 |
| *m*-AMSA | Amsacrine |
| MES | 2-(*N*-morpholino)ethanesulfonic acid |
| MeOH | Methanol |
| MDCK | MadinDarby Canine Kidney |
| MTD | Maximum Tolerated Dose |
| Mero-Clav | Meropenem-Clavulanate |
| MDR1 | Multdrug Resistance Protein |
| MDR-TB | Multi-drug-resistant Tuberculosis |
| MIC | Minimum Inhibitory Concentration |
| MRP | Multidrug Reistance-Associated Protein |
| *Mtb* | *Mycobacterium Tuberculosis* |
| NMR | Nuclear Magnetic Resonance |
| NPLC | Normal Phase Liquid Chromatography |
| OCT | Organic Cation Tranporter |
| PB | Phenobarbital |
| Pgp | P-glycoprotein |
| PZA | Pyrazinamide |
| RIF | Rifampin |
| RPLC | Reversed Phase Liquid Chromatography |

| | |
|---|---|
| SERS | Surface Enhanced Raman Scattering |
| SPE | Solid Phase Extraction |
| TB | Tuberculosis |
| topo II | Topoisomerase II |
| Tris | Tris(hydroxymethyl)aminomethane |
| TOF-MS | Time of Flight-Mass Spectrometry |
| XDR-TB | Extensively Drug-Resistant Tuberculosis |

**Chapter 1: Pre-clinical Drug Development of 9-aminoacridines for Malignant Glioma**

## I. Acridine containing molecules as chemotherapeutic agents

- Overview

Since the 1970s, tricyclic acridine containing compounds have been investigated as small molecule chemotherapeutic agents.[1, 2] Due to the structurally planarity of the acridine core (**Figure 1**), the compounds are able to intercalate or insert between the base pairs of DNA and interfere with biological processes such as replication and transcription. Intercalation is a favorable process because the DNA-drug complex is stabilized by π-π stacking and charge transfer interactions with the DNA bases. In most cases, the stabilized structure can prevent the binding of topoisomerase or telomerase enzymes from interacting with the DNA, leading to programmed cell death. The following introduction will describe a series of examples of relatively successful acridine containing compounds, which have been clinically used to treat a variety of cancers. In each case, the pharmacology, *in vitro* and *in vivo* efficacy, as well as clinical applications will be described.

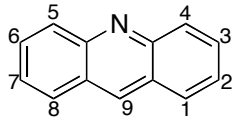


**Figure 1: Chemical Structure of Acridine**

- Amsacrine

Amsacrine (*m*-AMSA) (**Figure 2**) is a 9-anilinoacridine derivative and is the most widely studied acridine-containing drug to date. The pharmacology of *m*-AMSA has been rigorously investigated and studies have described this compound forms a ternary complex with DNA and topoisomerase II (topo II), trapping the "cleavable complex" during the topo II catalytic cycle.[3] In addition, Chourpa et al. utilized surface enhanced raman scattering (SERS) spectroscopy to provide evidence for DNA intercalation via π-πstacking interactions as well as the ionic interaction between the negatively charged phosphate backbone with the positively charged amino side chain of *m*-AMSA in the minor groove of DNA.[4] As a result of an acridine molecule's ability to bind and interact with DNA, several toxicity studies have been conducted to determine the safety of this compound.

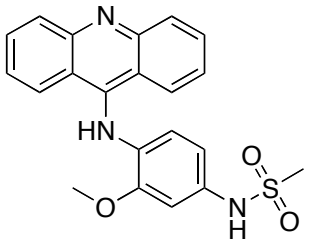


**Figure 2: Chemical Structure of *m*-AMSA**

To assess the toxicity of *m*-AMSA in small animals, male and female Wistar rats were dosed intravenously with 0.25, 1, and 3 mg/kg once daily over five consecutive days for 6 cycles followed by a twenty-three day recovery period during which no drug was administerd.[5] It was determined that at a dose of 3 mg/kg, 100% of males died by week 90 and 96% of females died by week 104 most notably by myelosuppression, chronic progressive neuropathy, and the development of tumors. The evident toxicity in the aforementioned animal study is mainly a result of the mutagenic effects of *m*-AMSA, accurately described by Mosesso and co-workers[6] in which they found significant

chromosomal aberrations in the form of translocations produced on chromosomes 2, 4, and 8 in human peripheral blood lymphocytes following exposure to *m*-AMSA.

Despite the animal toxicity profile and mutagenic nature of the *m*-AMSA, no significant toxicity was apparent in a study of 174 patients with acute myeloid leukemia (AML) exposed to a combination therapy of cytosine arabinoside, an anthracycline, and *m*-AMSA.[7] Several successful clinical applications of *m*-AMSA as a chemotherapeutic agent in combination with other medications have also been reported for treating relapsed childhood AML cases[8], acute promyleocytic leukemia[9], and adult lymphoblastic leukemia.[10] Most notably, 56 out of 166 (34%) children with induction-resistant or relapsed childhood AML completely responded to a therapy regimen that consisted of *m*-AMSA in combination with etoposide.[8]

The pharmacokinetics of *m*-AMSA were initially investigated in $B6DF_1$ mice following intravenous tail vein injection of 14.4, 28.9, and 57.7 μmol/kg.[11] Plasma protein binding as determined via equilibrium dialysis was 93.3%. Interestingly, as the dose of the compound increased, the clearances decreased, indicating dose-dependent elimination kinetics following a two-compartment model. Although the reason for this is unclear, it was assumed that the saturation of elimination pathways contributes to this type of kinetics. Cysyk and colleagues investigated the pharmacologic disposition of *m*-AMSA in mice and rats (10 mg/kg) following intravenous injections of radiolabeled *m*-AMSA with $^{14}C$ at the 9-position.[12] In each animal, biphasic kinetics were observed with an initial rapid elimination phase followed by a much slower elimination phase. Also, the majority of radioactivity was seen in the liver of the animals, followed by the spleen and

kidney. The primary elimination mechanism was biliary excretion with more than 50% of the dose eliminated as a glutathione conjugate by in 2 hours in rats. Also, therapeutic doses were seen to saturate the biliary transport system and liver GSH and GSH-transferase activity were reduced by 40% and 20%, respectively. The major metabolite identified was initially thought to be the 9-thioether of acridine, which was produced by the nucleophilic attack of GSH on the C-9 carbon, resulting from an addition/elimination reaction type mechanism. However, five years later Shoemaker and Cysyk[13] rebuked their previous description of the primary metabolite of *m*-AMSA being the 9-thioether acridine. In a more elegant experiment, both the C-9 or anilino position were labeled with $^{14}C$ and it was determined that the amount of radioactivity present in the bile of rats was same regardless of which position was labeled. The major metabolite was ultimately identified to be the glutathione conjugate off of the C-5 position of the parent molecule. Mechanistically, *m*-AMSA undergoes oxidation by cytochrome P450 to form a highly electrophilic quinone diimine, which subsequently is attacked by glutathione and excreted into the bile. These results were later confirmed by a study that looked at *m*-AMSA pharmacokinetics in rabbits in the presence of phenobarbital (PB), an activator of the constitutive androstane receptor (CAR), resulting in increased expression of CYP2B, and buthionine sulfoximine (BSO), an inhibitor of GSH biosynthesis.[14] In the presence of PB, the clearance of *m*-AMSA significantly increased by 46% while the clearance significantly decreased in the presence of BSO by 33%, ultimately confirming the data shown by Shoemaker that *m*-AMSA undergoes metabolism by oxidation followed by glutathione conjugation.

The pharmacokinetics of *m*-AMSA were additionally studied in 19 patients with disseminated neoplasms following an intravenous 10 mg of [9-$^{14}$C] *m*-AMSA.[15] Plasma pharmacokinetics indicated the elimination of *m*-AMSA from the plasma was biphasic with a distributional half-life of 0.27 hrs and a terminal elimination half-life of 7.4 hrs. The clearance was 140.8 mL/min/m$^2$ and the volume of distribution was calculated to 87.1 L/m$^2$, which is greater than the total body water and suggests *m*-AMSA extensively partitions into tissues. Also, 12% of unchanged dose was renally excreted 72-hrs after drug dosing; however, 35-50% of the administered $^{14}$C was excreted into the urine, most likely in the form of *m*-AMSA metabolites. Interestingly, both the initial half-life and elimination half-life increased (5.5-fold and 2.4, respectively) in patients with severe liver disease. In these patients, there was increased urinary excretion of unchanged *m*-AMSA (20%) and decreased plasma clearance (108 mL/min/m$^2$). Additionally, in patients with renal disease, only 1 – 4% of the administered dose was excreted unchanged in 72-hrs. Biliary excretion was also studied in two patients and 8.3% and 23.7% of the radioactive dose was found in the bile along with 0.5% and 1.6% of unchanged *m*-AMSA. In fact, the peak biliary concentration of $^{14}$C at 5 hrs following the dose was approximately 6-fold higher than the plasma concentrations in both of the patients. The pharmacokinetics of *m*-AMSA (200 mg/m$^2$) were additionally investigated in 10 patients also receiving cytarabine (ARA-C) and thioguanine (6-TG) for AML.[16] The concentration versus time profile was consistent with the previous animal and human studies illustrating biphasic kinetics with an initial or distributional half-life of 0.8 hrs and a terminal elimination half-life of 5.3 hrs following the first infusion. Interestingly, the clearance from plasma

significantly decreased and the terminal half-life increased following the third infusion but there was no change in the initial distributional half-life or volumes of distribution. The reason for this phenomenon is unclear but the speculation of saturated drug elimination as well as potential hepatocellular damage by mechanism-based inactivation of CYP450 may offer an explanation. The concentration of the dose excreted unchanged in the urine was 2 – 10%.

In a subsequent dose escalation (4 – 50 mg/m$^2$/day) study of 26 patients administered *m*-AMSA for three consecutive days, myelosuppression was recorded as the major form of toxicity with 75% of cases receiving the 25 mg/m$^2$/day dose having minimal myeleosuppression (granulocyte count > 1000/μL).[17] As the dose increased to 40 mg/m$^2$/day, 70% of cases resulted in moderate myleosupression (granulocyte count ~ 700μL). Other reported toxicities such as vomiting and nausea were minimal and unrelated to the dose escalation.

Currently, *m*-AMSA is prescribed to treat refractory acute lymphocytic and non-lymphocytic leukemias and both Hodgkin's and non-Hodgkin's lymphomas in other countries.[18-20]Additionally, *m*-AMSA is currently undergoing clinical trials for efficacy against hematological cancers in the United States.[21] However, *m*-AMSA has been shown to be ineffective against solid tumors[22] and several other anilinoacridine derivatives have been synthesized and investigated to combat this issue and improve efficacy.

- Asulacrine

The 4-methyl-5-N-methylcarboxamide derivative of *m*-AMSA, commonly known as asulacrine (**Figure 3**), was initially synthesized by Bagueley and colleagues[23] in an effort to improve efficacy against solid tumors. Asulacrine was reported to have $IC_{50}$ values of 6.7 nM and 800 nM against the T-47D human breast carcinoma and the murine leukemia P388/ADR cell lines, respectively. The mechanism of action for asulacrine is similar to that of *m*-AMSA, a DNA intercalator as well as an inhibitor of topo II;[24] however, it is interesting that such a similar molecule displayed high efficacy against solid tumors in P388 leukemia inoculated mice.[23] This difference has been attributed the additional ring substituents off the 4 and 5 positions of asulacrine which increased the association constant for calf thymus DNA (2.1 x $10^6$ $M^{-1}$) sixteen-fold compared with *m*-AMSA (1.3 x $10^5$ $M^{-1}$).[23] Additionally, when 20 mg/kg of asulacrine were administered via intraperitoneal (ip) injection on day 1, 5, and 9 to mice pre-inoculated with P388 leukemia, it was found that 3/6 mice survived (50%) the study after 50 days. Comparatively, 0/6 mice survived (0%) following ip administration of *m*-AMSA (13.3 mg/kg) or daunorubicin (2.7 mg/kg) and only 1/6 (17%) mice survived following ip administration of adriamycin (3.9 mg/kg). Similarly, 14/17 (84%) of mice pre-inoculated with Lewis lung carcinoma survived for 60 days following ip injections of asulacrine on the day 1, 5, and 9 on the study while no animals survived when dosed with *m*-AMSA. In subsequent murine tumor model studies (lung, colon, and mammary

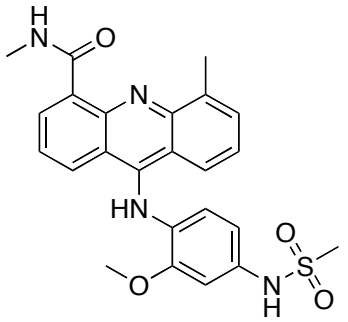

**Figure 3: Chemical Structure of Asulacrine**

carcinomas) it was found that asulacrine was effective against 84% of the models investigated while also being superior to *m*-AMSA.[25] Further in vivo murine tumor studies provided evidence that asulacrine in combination with cisplatin or carboplatin was highly synergistic and effective than dosing a single agent alone indicating that asulacrine and platinum agents may have clinical significance.[26] The pharmacokinetics of asulacrine was investigated in male B6D2F1 mice following the iv injection of either 14.4, 28.9, and 57.7 μmol/kg.[11] As shown with, *m*-AMSA, dose-dependent elimination kinetics were observed and as the half-life increased, clearance decreased with increasing the dose (dose-dependent elimination kinetics). The plasma protein binding of asulacrine was reported to be 99.94 %, which is significantly higher than what was observed for *m*-AMSA (93.3%). The clinical pharmacokinetics of asulacrine were investigated in a phase 1 trial consisting of 16 patients with solid tumors (breast, pancreas, melanoma, stomach, and non-small cell lung carcinoma).[27] For the dose ranges of 13-270 mg/m$^2$, the kinetics were biphasic and the distributional and elimination half-lives were 0.5 and 2.6 hours, respectively. The clearance was reported as 158 mL/hr and the volume of distribution was 319 mL/kg. Additionally, less than 1% of the dose was excreted unchanged in the urine, suggesting hepatic excretion; however, hepatobiliary was never investigated and most likely is the route of elimination. Phase 2 efficacy studies in 16 patients with non-small cell lung cancer identified one response (6.25%) when treated daily with 216 mg/m$^2$ as a 15-minute infusion for three days repeated every three weeks.[28] An additional study was also disappointing when out of 132 cancer patients with either breast, stomach, pancreas, non-small cell lung, small cell lung, colon, head and

neck, or melanoma, only 4 responses (3.0%) were seen following a 270 mg/m$^2$ weekly infusion of asulacrine.[29]

- DACA

DACA (XR-5000), an acrdinecarboxamide derivative (**Figure 4**), made it furthest into the clinic compared to any other acridine containing molecules. Atwell et al.[30] first reported the synthesis of *N*-[2-(dialkylamino)alkyl]-acridine-4-carboxamides including DACA, and their encouraging *in vitro* efficacy against murine leukemia cells (4.3 – 17900 nM) and human colon tumor cells (54 – 2900 nM). Also, the in vivo efficacy of each derivative was determined following ip doses on day 5, 9, and 13 following ip inoculations of P388 leukemia cells or Lewis lung carcinoma cells in mice. The survival of the animals was remarkable with several derivatives essential curing the cancer-induced mice as evidenced by their extended survival compared to vehicle controls. Similar to *m*-AMSA and asulacrine, DACA is also a specific inhibitor of topo II, trapping the cleavable complex leading to double strand DNA beaks.[31] Interestingly, it was determined that acridinecarboxamide derivatives that possess an amino substituent at the 9 position as well as an overall +2 charge at physiological pH such AAC (**Figure 4**), has a 6-fold increase in binding affinity to DNA compared to the deamino derivative, DACA, which has an overall positive charge of +1 at physiological pH.[32, 33] The interactions with DNA for both compounds, AAC and DACA, is an enthalpy-favored process with binding enthalpies of -6.2 kcal mol$^{-1}$ for each compound. However, the

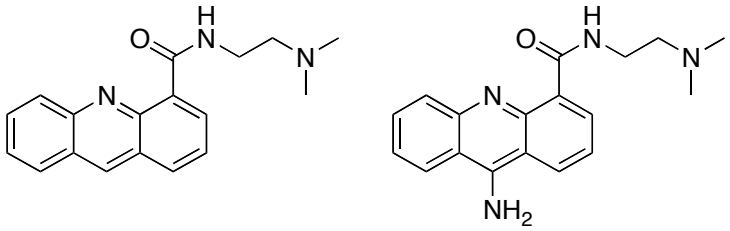


**Figure 4: Chemical Structures of DACA and AAC**

major difference in energetics between these compounds is in regards to the binding entropy, which is five-fold higher for AAC due to the "enhanced counterion displacement coupled with the loss of water from the minor groove of DNA." Despite the higher binding affinity of AAC, DACA was pushed further into clinical development due to the metabolic liability of an aromatic amine located at the 9-position. In addition, DACA was shown to be effective against Jurkat multidrug-resistant leukemia cell lines with an $IC_{50}$ value of 380 nM,[34] and this result is most likely due to DACA having poor substrate specificity for the efflux transporter P-glycoprotein (Pgp) encoded by the *ABCB1* gene as well as multidrug resistance-associated protein (MRP).[35] Efficacy against MDR-expressing cell lines has all also been attributed to DACA's extremely fast uptake into carcinoma cells due to inherent lipophilic nature of the compound.[36] The primary route of metabolism for DACA is oxidation at the C-9 position to ultimately form the acridone metabolite.[37] Interestingly, this metabolite was only produced in the mouse hepatic 9000g supernatant or cytosolic fractions, but not the microsomal fraction. Metabolite formation was inhibited in cytosolic incubations in the presence of menandione, but not allopurinol, strongly indicating the role of aldehyde oxidase in the metabolism of DACA. Evans et al[38] reported the free fraction of DACA in human plasma to be only 3.4 ± 0.2% with most of the molecule binding non-specifically to $\alpha_1$-acid glycoprotein. Initial pharmacokinetic studies in 22 patients given intravenous doses 36 mg/m$^2$ – 165 mg/m$^2$ per day for three consecutive days of radiolabeled $^{14}$C DACA indicated a rapid clearance from plasma due the formation of several unidentified metabolites.[39] McCrystal and co-workers[40] conducted the first phase 1 study of DACA in 31 patients with varying solid tumors, e.g.

breast, ovary, rectum, and pancreas. The maximum tolerated dose (MTD) of 750 mg/m$^2$ was determined during a 3-hour infusion therapy tri-weekly with an escalating dose range of 18 – 1000 mg/m$^2$. During the infusion, patients reported arm pain and mild facial discomfort which subsided following the halt of the infusion. It is interesting to note that no anti-proliferative activity was noticed in any of the patients, which most likely was caused by an insufficient dosage of DACA. In a similar Phase 1 study, 41 patents with refractory metastatic solid tumors were dosed intravenously with DACA (9 mg/m$^2$ – 800 mg/m$^2$) on a tri-weekly basis for three weeks and the most common side effect was pain in the infusion arm at the MTD of 800 mg/m$^2$.[41] Again, no positive responses were observed. The pharmacokinetics in plasma were fit to two-compartment model for a majority of the patients although the plasma concentration versus time profile appears to follow first order kinetics. The $AUC_{\infty}$, clearance, $C_{max}$, and $T_{max}$ were 21.5 ± 10.7 μg mL$^{-1}$ h, 76.26 ± 34.1 L/hr, 4.84 ± 4.09 μg mL$^{-1}$, and 3.72 ± 1.67 h, respectively for the 800 mg/m$^2$ MTD.[41] Despite an encouraging low toxicity profile and high *in vitro* efficacy, DACA was not further developed due to lack of efficacy in patients with either advanced colorectal cancer, non-small cell lung cancer, advanced ovarian cancer, and glioblastoma multiforme[42-45].

- 9-aminoacridnes

Professor David Ferguson's group at the University of Minnesota has identified a series of 9-aminoacrdine compounds that have specific activity against topo II and function by catalytic inhibition, similar to aclarubicin.[46] Four compounds (**Figure 5**) were chosen to be investigated as potential agents to treat pancreatic cancer based on their superior

inhibition of topo II catalyzed reaction assays and acceptable cytotoxicity. Compounds **1 – 4** (**Figure 5**) showed low micomolar activity (1-18 μM) against several pancreatic cell lines and provided encouraging evidence for their therapeutic utility[47] (**Table 1**). In addition, the same four compounds were investigated in a variety of cancer cell lines (prostate, colon, liver, non-small lung, breast, melanoma, ovarian, and kidney) and low micromolar activity ranging from 4.1 – 55.9 were identified as $EC_{50}$ values.[47]

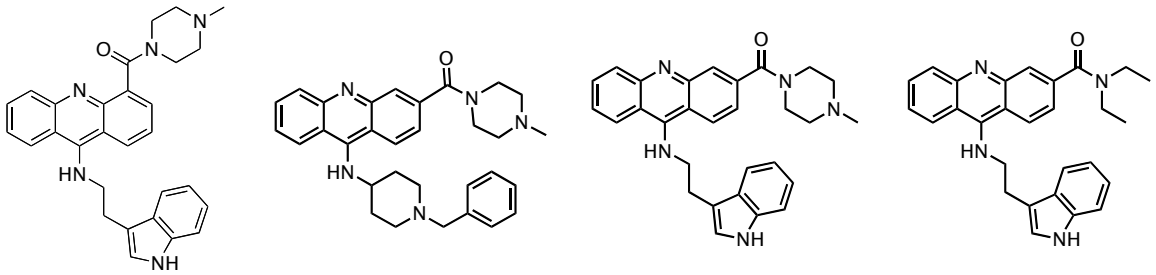

**Acridine 1** **Acridine 2** **Acridine 3** **Acridine 4**

**Figure 5: Chemical Structures of 9-aminoacridines**

| Cell line | $EC_{50} \pm SE$ (μM) | | | |
|---|---|---|---|---|
| | 1 | 2 | 3 | 4 |
| DU145 | 37.2 ± 12.1 | 32.4 ± 8.8 | 16.6 ± 5.0 | 11.9 ± 2.9 |
| HCT-116 | 29.0 ± 8.7 | 29.2 ± 4.1 | 27.6 ± 5.3 | 11.2 ± 2.6 |
| Hepa1c1c7 | 55.9 ± 5.3 | 26.9 ± 6.6 | 24.8 ± 9.0 | 11.2 ± 3.0 |
| H460 | 16.0 ± 6.9 | 38.5 ± 3.6 | 31.8 ± 3.2 | 18.8 ± 2.3 |
| MCF-7 | 37.2 ± 6.2 | 25.7 ± 5.0 | 19.2 ± 3.1 | 13.5 ± 2.7 |
| SU86.86 | 6.8 ± 2.2 | 21.2 ± 5.1 | 16.3 ± 3.5 | 16.2 ± 2.9 |
| MEL | 16.7 ± 4.1 | 14.6 ± 3.2 | 5.30 ± 2.5 | 16.0 ± 2.9 |
| OCL-3 | 39.8 ± 8.6 | 20.3 ± 4.6 | 15.3 ± 3.8 | 18.3 ± 2.8 |
| REH | 19.7 ± 4.9 | 21.0 ± 4.5 | 4.10 ± 0.5 | 15.5 ± 2.8 |

**Table 1: Acridine 1 - 4 efficacy against a variety of cancer cell lines**
Cancer cells: DU-145 (prostate),HCT-116 (colon), Hepa-1c1c (liver), H460 (non-small lung), MCF-7 (breast), SU86.86 (pancreatic), MEL (melanoma), OCL-3 (ovarian), and REH (kidney). Values reported are $EC_{50} \pm SE$ (μM).

## II. Aims of the Present Work

In collaboration with Dr. David Ferguson at the University of Minnesota, our research group investigated the absorption, distribution, and metabolic characteristics of acridines **1 - 4** in an effort to further them along the drug discovery pipeline. Experiments including metabolic stability, MDCK cell accumulation in wild type cells and cell that overexpress Pgp and BCRP, plasma protein binding, and tissue distribution in mouse pharmacokinetic studies were all conducted. The data generated from these studies provided metabolic and pharmacokinetic profiles, which could ultimately be utilized to select a lead compound for further *in vivo* efficacy experiments. Also, in collaboration with Dr. John Ohlfest at the University of Minnesota, the $IC_{50}$ values of the four compounds against primary malignant glioma cells were measured (2.8 – 4.5 μM),[48] and the results prompted an subsequent *in vivo* efficacy study involving an orthotopic human glioma mouse model.

## III. Materials and Methods

- Chemical materials

Acridines **1** - **4** (**Figure 5**) were synthesized as previously described.[46] Tamoxifen was purchased from MP Biomedicals (Solon, OH). Quinidine, amitriptyline, verapamil, atenolol, sotalol, nadalol, metorprolol, and propranolol were all purchased from Sigma-Aldrich (St. Louis, MO). Talinolol was purchased from Toronto Research Chemicals (Toronto, Ontario). LY335979 trichloride (LY) and GF120918 (GF) were gifts from Dr. Elmquist's laboratory at the University of Minnesota. Solvents and reagents for liquid chromatography included HPLC grade acetonitrile (Sigma Aldrich, St. Louis, MO), 1-heptane sulfonate sodium salt (Regis Technologies, Morton Grove, IL), and 98% formic acid (Fluka Analytical, St. Louis, MO). Aqueous reagents were prepared with water purified from a Millipore Elix UV Water Purification System (Millipore, Billerica, MA).

- HPLC method development
    - Acridines

The HPLC system was composed of an Agilent 1100 Liquid Chromatograph (Agilent Technologies, Santa Clara, CA), a Phenomenex Gemeni C6-Phenyl 100mm x 2.0mm, 5µm reversed-phase column (Phenomenex, Torrance, CA), and a Shimadzu UV/Vis detector (Shimadzu, Kyoto, Japan) with the wavelength set at 434 nm. Mobile phase A consisted of a 0.05% formic acid aqueous solution containing 5 mM 1-heptane sulfonate, pH 2.8 and mobile phase B was

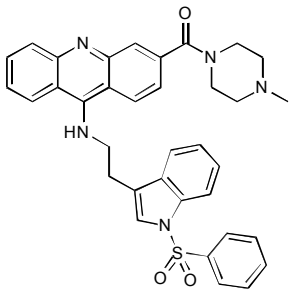


**Figure 6: Chemical Structure of Acridine Sulfonamide Internal Standard**

acetonitrile. Acridine **1**, **2**, **4** and a sulfonamide derivative (**Figure 6**) internal standard eluted at 4.06, 5.22. and 6.38 minutes, respectively (**Figure 7**) with the following gradient elution: 30% B to 75% B over 8 minutes with a flow rate of 0.3 mL/min and re-equilibration at 30% for 2.0 minutes prior to the next injection. The data was analyzed with ChromPerfect software (Justice Innovations, Denville, NJ).

- β-blockers

The same HPLC system as described above was utilized for the separation of atenolol, sotolol (IS), nadolol, metoprolol, talinolol, and propranolol. A Thermo Betasil C18 100mm x 2.1mm, 5μm reversed-phase column (Thermo Fisher Scientific, Rockford, IL) and a fluorescence detector (Jasco, Great Dunmow, Essex UK) were employed for the separation. Mobile phase A consisted of 0.05% ammonium formate and mobile phase B was acetonitrile. Atenolol, sotalol, nadolol, metoprolol, talinolol, and propranolol eluted at 2.91, 3.55, 8.87, 9.71, 11.40, and 11.88 minutes, respectively (**Figure 14**) with the following gradient elution: 3% B to 10% B over 10 min, 20% B to 35% B from 10.01 min to 12 min, and a re-equilibration at 3% for 3 min prior to the next injection. Due to the difference in fluorescence sensitivity of talinolol and propranolol from the other β-blockers, the detection wavelength was changed during the chromatography. From 0 – 10 minutes the wavelengths were set at an excitation of 230 nm and an excitation of 302 nm. From 10.5 – 15 minutes, the wavelength were set at an excitation of 249 nm and an emission of 333 nm. The data was analyzed with ChromPerfect software (Justice Innovations, Denville, NJ).

- Microsomal stability

Pooled human liver microsomes (HLMs) (BD Biosciencs, San Jose, CA) were incubated at 37 °C with acridine **1 - 4** (added in DMSO, final DMSO concentration was < 0.1%) for 120 minutes in the presence of NADPH (EMD Chemicals, Inc., Gibbstown, NJ). The final incubation volume was 0.25 mL and contained the following reagents: 1 μM acridine **1 - 4**, 0.25 mg protein/mL pooled human liver microsomes, 50 mM potassium phosphate buffer, pH 7.4, 1 mM NADPH, and 5 mM $MgCl_2$. All samples were prepared on ice in triplicate, pre-incubated for two min at 37 °C, followed by the addition of NADPH. Incubations were removed at 5, 10, 15, 30, 45, 60, 90, and 120 min, and quenched with 0.25 mL of ice-cold acetonitrile containing the internal standard. Each incubation was added to a 0.2 μM micro-spin filter tube (Chrom Tech, Inc., Apple Valley, MN) and spun at 13,000*g* for 5 min to remove precipitated proteins. The filtrate was then subjected to HPLC-Vis analysis.

- Intracellular accumulation in MDCKII cells

Wild type, MDR1-transfected, and Bcrp1-transfected Madin-Darby canine kidney (MDCKII) cells were kindly provided by Dr. William Elmquist's laboratory at the University of Minnesota. Wild type cells were cultured in DMEM (Mediatech, Inc., Herndon, VA) supplemented with 10% fetal bovine serum (FBS), penicillin (100 U/mL) and streptomycin (100 μg/mL) (Sigma-Aldrich, St. Louis, MO) and incubated at 37 °C and 5% $CO_2$. MDR1-transfected cells were cultured as described above but with the addition of colchicine to the media (final concentration 0.22 μM). Colchicine is added to

the media because it will kill any WT cells that remain in the culture; however, the MDR-1 transfected cells will survive because colchicine is a substrate for MDR-1. Bcrp1-transfected cells were cultured with DMEM/F12 media supplemented with FBS and antibiotics. Cultures were passed successively in T-75 tissue culture flasks (Becton Dickinson, San Jose, CA). Accumulation experiments were performed in 12 or 24-well polystyrene tissue culture plates (Sarstedt, Inc., Newton, NC). All cells were seeded at a density of 2 x $10^6$ cells/well and the media was changed every other day until confluent monolayers were formed. At the start of the experiment, the media was removed from each well by aspiration and the monolayers were washed two times with warmed 37 °C cell assay buffer, pH 7.4 (122 mM NaCl, 25 mM $NaHCO_3$, 10 mM glucose, 10 mM HEPES, 3 mM KCl, 1.2 mM $MgSO_4$, 1.4 mM $CaCl_2$, 0.4 mM $KH_2PO_4$). 1.0 mL of cell assay buffer was added to each monolayer and the plates were pre-incubated for 15 min at 37 °C in an orbital shaker with mild agitation (60 rpm). Subsequently, the media was aspirated and the experiment began by the addition of 1.0 mL of 5 μM acridine **1 - 4** in cell assay buffer. Plates were agitated at 60 rpm and 37 °C in an orbital shaker for 120 min. At the end of 120 min, the drug solutions were immediately aspirated from each well and the wells were washed three times with 1.0 mL ice-cold phosphate buffered saline. The cells were then lysed by the addition of 0.5 mL 1% Triton X-100 solution. Five hundred μL of acetonitrile were added to a 500 μL aliquot of cell lysate from each well to precipitate proteins. Samples were spun at 13,000*g* for two min and the supernatant was subjected to HPLC-Vis analysis. In addition, the BCA protein assay (Pierce Biotechnology, Inc., Rockford, IL) was utilized to measure protein concentrations

in each cell lysate and normalize acridine concentrations from cell monolayers. Acridine concentrations need to be normalized to total protein concentration because the wild type cells grow at different rates compared to the transfected cells. Acridine accumulation was expressed as the amount of acridine (μmols) per microgram of cellular protein. For the Pgp and BCRP inhibition experiments, cells were treated during both the pre-incubation and incubation times with 1 μM of LY335979 or 5 μM GF120918 respectively. Acridine uptake in the presence of organic cation transporter substrates (70 μM amitriptyline, 100 μM verapamil, 100 μM tamoxifen, 174 μM quinidine) were also investigated in the wild type cells. The uptake experiment of β-blockers (atenolol, nadolol, metoprolol, talinolol, and propranolol) in MDCK-WT cells was performed identically to the accumulation experiment of the acridines.

- Plasma protein binding

The binding of acridine **1 - 4** to human plasma proteins was investigated by an ultracentrifugation technique. Acridine **1 - 4** were added to blank human plasma to achieve a 5 μM concentration. In triplicate, 500 μL of each solution were added to Millipore Centrifree UF Devices (Millipore, Billerica, MA) and centrifuged at 2000*g* for 30 min. The resulting ultrafiltrate was subjected to HPLC-Vis analysis.

- Drug formulation and administration

Oral doses of acridine **1** were prepared in a 0.1M phosphate buffer, pH 3.0 containing 30% polyethylene glycol 200 (Sigma-Aldrich, St. Louis, MO). Oral doses of acridine **2** were prepared in a 0.1M phosphate buffer, pH 3.0. Each dose contained 1.2 mg acridine/200 μL formulation solution (60 mg/kg) and was administered to mice by oral gavage. Intravenous doses of acridine **2** were prepared in filter sterilized water containing 40% hydroxypropyl beta-cyclodextrin (Cerestar, Hammond, IN). Each dose contained 0.3 mg acridine/100 μL (15 mg/kg) and was administered via tail vein injection.

- Animals

42 female C57BL/6J mice (stock #: 000664) and 12 female B6.CB17-*Prkdc*$^{scid}$*/SzJ* mice (stock #: 01913) (Jackson Labs, Bar Harbor, ME) were utilized for the acridine pharmacokinetic investigations and glioma efficacy experiments, respectively. Animals were 6 - 8 weeks old (20 – 24 g) at the time of the experiment and were maintained under controlled temperature and humidity while having unlimited access to food and water in a pathogen free storage facility. The Institutional Animal Care and Use Committee (IACUC) of the University of Minnesota approved all animal procedures.

- Sample collection

Single oral and iv dose pharmacokinetic experiments: Following acridine **1** or **2** administration by oral gavage, mice were sacrificed at 1, 2, 4, 8, and 24 hours (three mice per time point) by an overdose of ketamine/xylazine (1 dose: . Blood was collected into

heparinized vacutainers (BD Biosciences, San Jose, CA) by cardiac puncture. Following aortic perfusion with PBS, the liver, kidney, and brain were excised from the mouse and immediately snap frozen in liquid nitrogen. Acridine **2** was administered via tail vein injection and mice were sacrificed at 0.25, 0.5, 2, 8, 24, and 72 hrs by an overdose of ketamine/xylazine. Blood and organs were collected as previously described. Plasma was fractionated from whole blood by centrifugation at 2000*g*. Each organ was separately weighed in a homogenization test tube and a volume of PBS 3x the organ weight was added. Following homogenization, the tissue homogenates were filtered through gauze to remove any particulates.

- Sample preparation

To 0.1 mL of plasma and 0.8 mL of tissue homogenate were added 0.1 mL and 0.8 mL of methanol containing an acridine sulfonamide internal standard, respectively. The samples were vortexed, refrigerated for 30 min, and centrifuged at 13,000*g* for 10 min. The supernatants were then subjected to the following solid phase extraction (SPE) protocol: C18 Bond Elut (1.0 mL 100 mg) SPE cartridges (Varian, Lake Forest, CA) were conditioned with 1.0 mL 100% methanol and equilibrated with 1.0 mL 0.05% formic acid. 0.1 - 0.2 mL of plasma and 1.0 mL of tissue homogenate supernatants were loaded onto the cartridge. The cartridges were then washed with 0.5 mL of 30% methanol followed by an additional wash with 70% methanol. Acridines were eluted with 0.5 mL 2% ammonium hydroxide in methanol. Samples were dried under a nitrogen atmosphere at 37°C and reconstituted in 0.1 mL of the HPLC mobile phase.

- In vivo efficacy

50,000 P9-F cells suspended in 1 μL of PBS were injected into the right hemisphere of the brain parenchyma of 6 - 8 week old female C57BL/6J SCID mice[49]. Briefly, mice were anesthetized with an IP injection of a cocktail of 54 mg/mL ketamine and 9.2 mg/mL xylazine and subsequently placed in a Kopf stereotactic head frame. The scalp was swabbed with betadine and a midline incision was made with a scalpel. A burr hole was placed 2.5 mm lateral and 0.5 mm anterior from sagittal midline-located bregma. A Hamilton syringe (26 g) was used to deliver P9-F cells to a 3.3 mm depth from the skull surface to about the middle of the caudate-putamen. Each mouse was randomized and administered a 200 μL dose of acridine **2** via oral gavage on a two-week dosing schedule (days 1-5, 8-12). A 30 mg/kg dose was administered for the first week followed by a 60 mg/kg dose for the second week. Control mice were administered 200 μL of 0.1M phosphate buffer, pH 3. Mice were closely observed for the duration of the experiment and sacrificed upon any visual morbidity. The Kaplan-Meier curve was generated with GraphPad Prism software.

- Pharmacokinetic calculations

The area under the plasma concentration-time curve (AUC) was calculated with the WinNonLin software v5.0.1 (Pharsight, St. Louis, MO). Acridine **2** bioavailability was calculated by the following equation: $F = (AUC_{po} \times Dose_{iv}) / (AUC_{iv} \times Dose_{po})$. Elimination half-life ($t_{1/2}$,) clearance (Cl), and volume of distribution ($V_d$) were calculated by the following equations: $t_{1/2} = (\ln 2 / k_e)$ where $k_e$ = fractional rate of elimination, Cl = Dose / AUC, $V_d$ = Dose / $C_0$ where $C_0$ is the concentration at time 0.

- Statistical Analysis

An unpaired Student's *t*-test was used to compare the differences of experimental groups. Data are expressed as the mean ± standard deviation. Survival was tested by Log-Rank test. Statistical significance (indicated by an *) was determined by a $p < 0.05$.

## IV. Results

- Bioanalytical method development

Before any experimental work is conducted on investigational compounds or drugs, a bioanalytical method must be established. The primary function of an analytical method is to accurately quantitate an analyte(s) from a biological matrix such as plasma or tissue homogenate. A common approach for analyzing drugs or investigational compounds is by high performance liquid chromatography (HPLC) coupled with UV/Vis, fluorescence detection or mass spectrometry. Typically, assay development begins with establishing a chromatographic method followed by the development of an extraction procedure. Next, validation of the assay by the generation of triplicate standard curves is performed to determine accuracy and precision. Once the assay is validated, samples and standards will be analyzed simultaneously.

A short separation of acridine **1**, **2**, **4**, and an acridine sulfonamide internal standard was established in six min **(Figure 7)** on a Phenomenex Gemeni C6-Phenyl 100mm x 2.0mm, 5µm reversed-phase column. Due to the high lipophilicity of the acridine **1** - **4**, an ion-pairing reagent (1-heptane sulfonate) was added to the mobile to improve the chromatographic peak shape and prevent peak tailing. Additionally, the acridines are an orange color and detection was achieved at 434 nm with a visible wavelength detector.

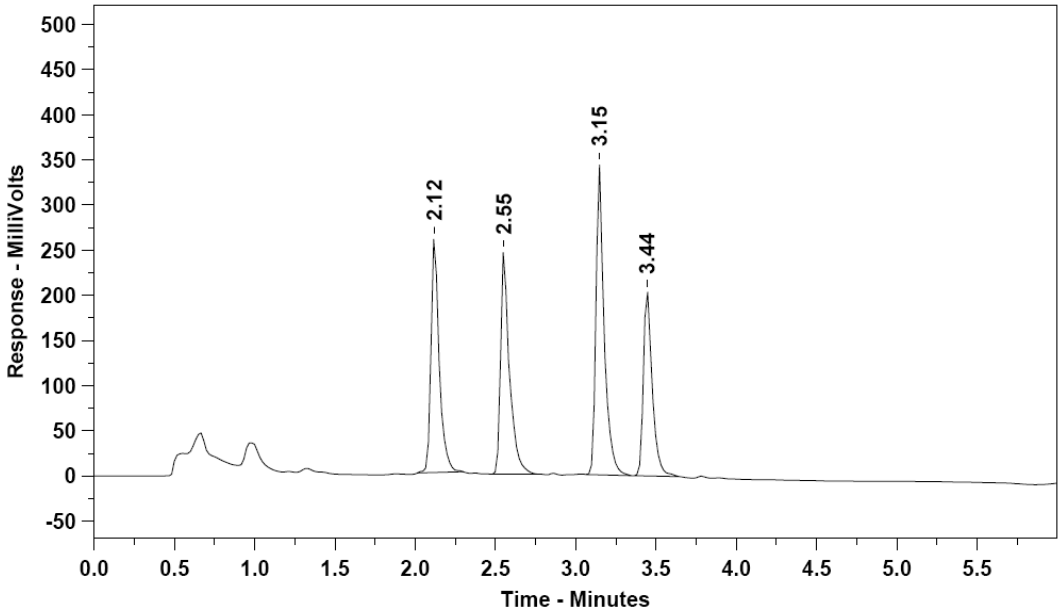


**Figure 7: Chromatograpic Separation of Acridine 2, 1/3, IS, and 4**

Following the successful separation of the acridines, an extraction procedure was developed (see sample preparation in materials and methods) with C18 solid phase extraction cartridges. The extraction efficiency from human plasma is illustrated in **Figure 8**. All acridines were extracted out of human plasma with a >75% extraction efficiency. Acridine **2**, the most polar acridine, had the lowest extraction efficiency (76%), while the other more nonpolar acridines had high extraction efficiencies (>94%). Extraction efficiencies out of tissue homogenates (brain, kidney, liver) were also shown to have similar efficiencies to human plasma.

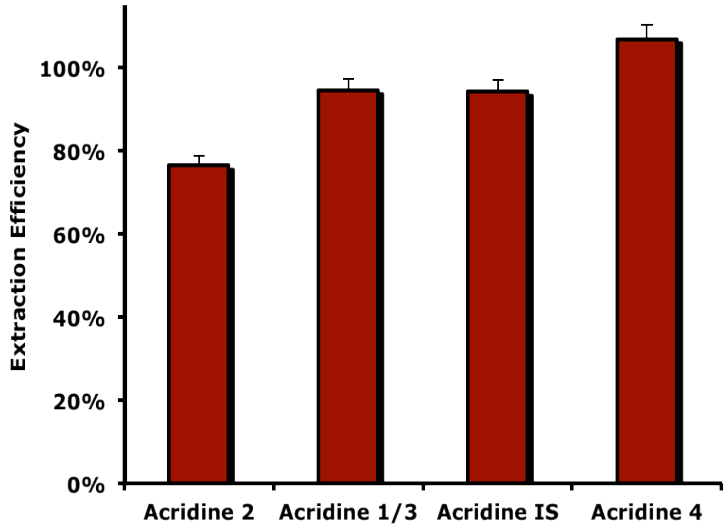


**Figure 8: Extraction Efficiency of Acridines 1 - 4 from Human Plasma**

With the above chromatographic method and extraction procedure, the assay was validated by the generation of triplicate standard curves. **Figure 9** illustrates a representative example of a standard curve for each acridine. All $r^2$ values were greater than 0.999 for each compound and the coefficients of variation for each concentration (0.3125 µM – 10 µM) was <5%. The limit of detection for the assay was 0.05 µM

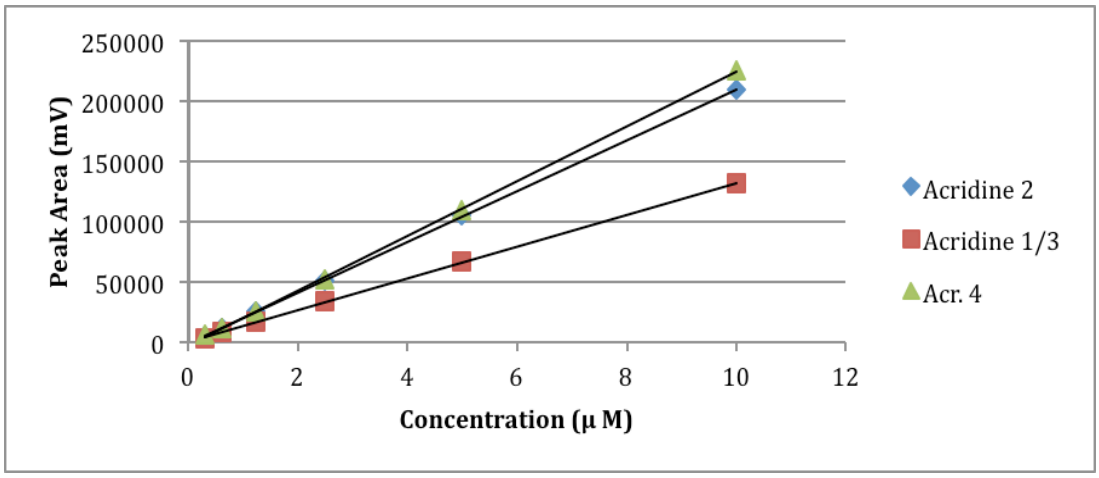


**Figure 9: Standard Curves for Acridine 1, 2, 4 Extracted Out Of Brain Tissue Homogenate**

- Metabolic Stability

Acridines **1 - 4** (1.0 μM) were incubated in pooled HLMs (0.25 mg protein $mL^{-1}$), for 120 minutes in the presence of 1 mM NADPH. Following protein precipitation by the addition of acetonitrile containing an internal standard and HPLC-Vis analysis, no significant metabolites were identified. Half-lives were calculated to be 1.9, 5.8, 3.9 and 2.9 hours for acridine **1**, **2**, **3** and **4**, respectively (**Figure 10**). Metabolic stability of acridines **1 - 4** in HLMs supplemented with UDPGA also did not show the formation of any glucuronide metabolites. (Data not shown). The conversion of Flurbiprofen to 4'OH Flurbiprofen was monitored as a positive control in microsomes supplemented with NADPH.

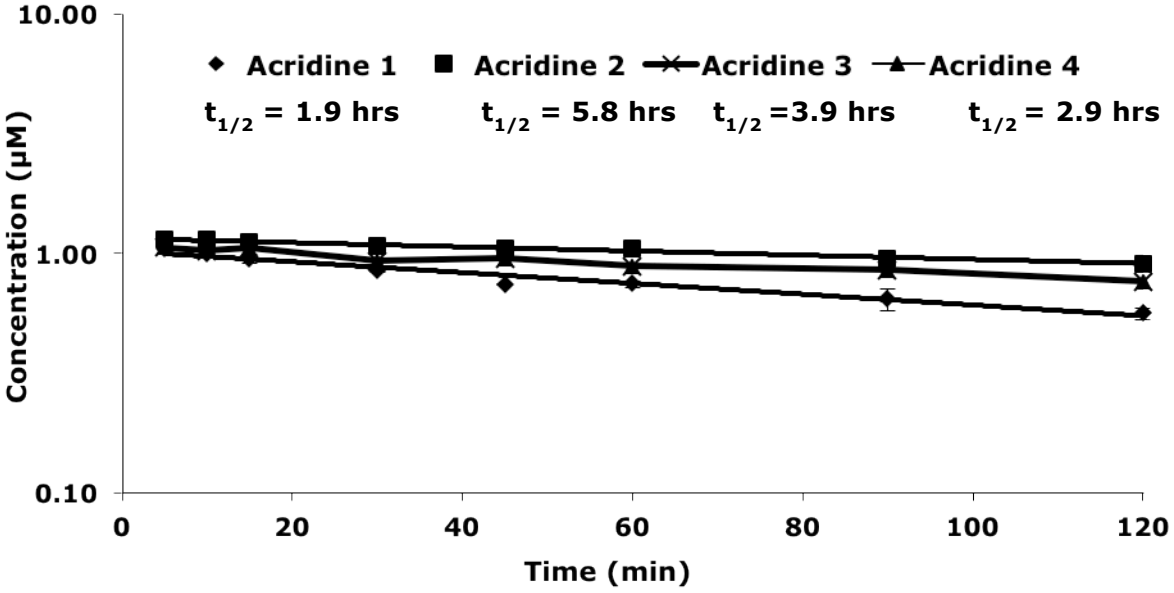


**Figure 10: Oxidative Metabolic Stability of 1 μM Acridine 1 - 4 in HLM**
*Symbols* are the mean ± standard deviation of triplicate samples. Lines were fit to a monoexponential equation and half-lives were calculated by dividing the ln 2 by the fractional rate of elemination $k_e$

- Intracellular Accumulation

Acridine cellular uptake was investigated by measuring accumulation in MDCK cells. To determine if the compounds were substrates for p-glycoprotein (Pgp) or breast cancer resistant protein (BCRP), MDCK cells overexpressed with the respective efflux transporters were utilized (**Figures 11-13**).

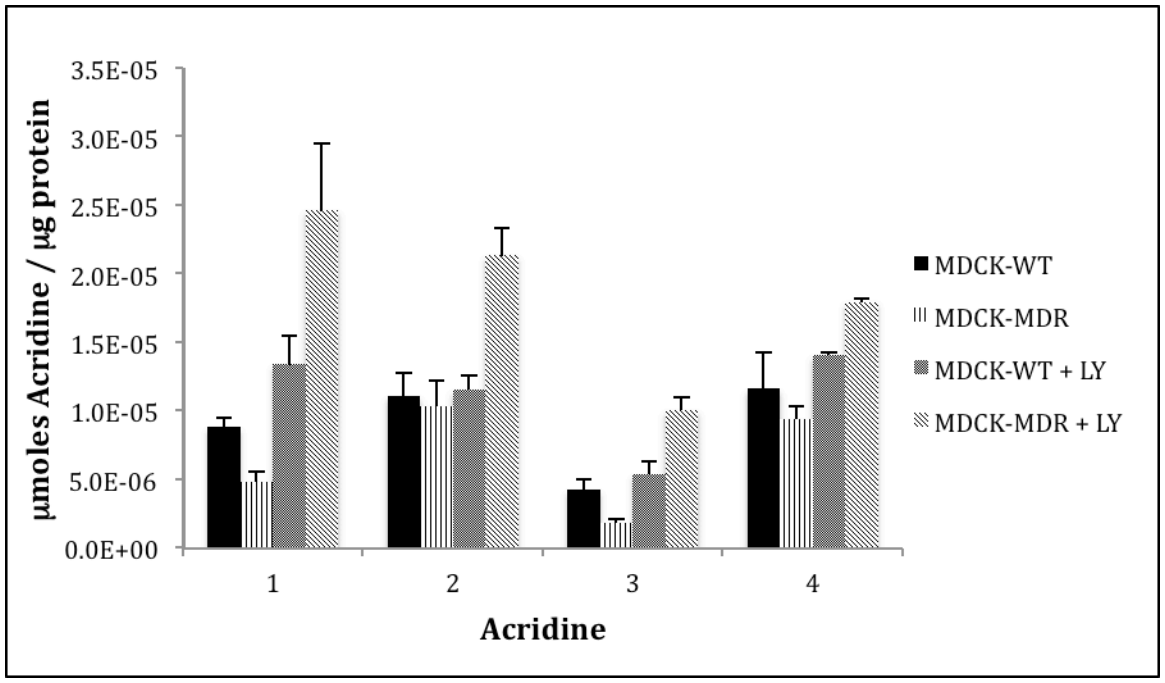


**Figure 11: Acridine 1 - 4 Accumulation in MDCK-WT and MDCK-MDR1 transfected cells in the presence of absence of the selective P-glycoprotein (Pgp) inhibitor LY335979**

In this experiment, it was determined that acridine **1**, **2**, and **4** similarly accumulated in MDCK-WT cells while acridine **3** had the lowest accumulation. Interestingly, the accumulation of acridine **1** and **3** significantly decreased in the presence of overexpressed Pgp (MDR-1), indicating these two compounds may be substrates for the efflux transporter protein. In WT cells co-incubated with a Pgp inhibitor (LY), accumulation of the acridines all increased implying endogenous basal levels of Pgp, may affect acridine

uptake. Lastly, in MDCK-MDR cells co-incubated with LY, accumulation of acridines significantly increased again implying the role of Pgp in affecting the uptake of the acridines in MDCK cells.

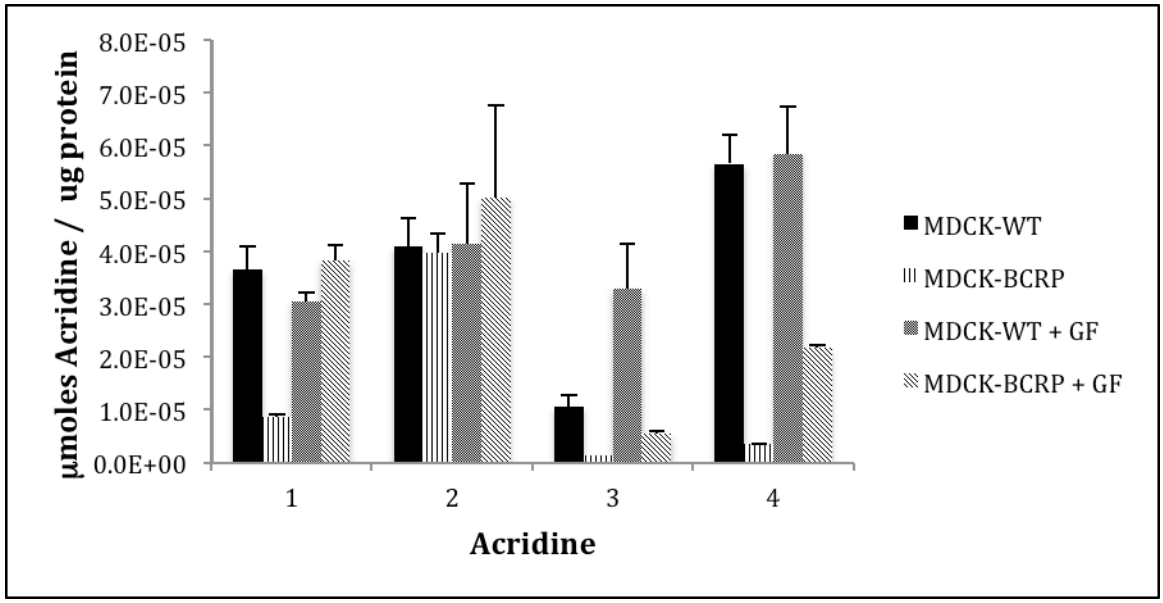


**Figure 12: Accumulation of Acridine 1 - 4 in MDCK-WT and MDCK-Bcrp1-transfected cells in the presence of absence of the BCRP inhibitor GF120918 (GF)**

As depicted in the previous experiment, acridines **1**, **2**, and **4** all similarly accumulated in MDCK-WT cells while acridine **3** showed the least accumulation. In MDCK cells overexpressed with BCRP, acridine **1**, **3**, and **4** did not accumulate indicating that they are substrates for BCRP. Accumulation was restored in the presence of the BCRP inhibitor GF120918.

In addition, the acridines were thought to be substrates for the organic cation transporter due to the weakly basic nature of acridine containing compounds. To test this hypothesis, acridine **1** and **2** were incubated in MDCK-WT cells in the presence of various organic cation transporter (OCT) substrates and acridine accumulation was measured (**Figure 13**). Acridine accumulation significantly decreased in the presence of all OCT substrates providing evidence that acridine **1** and **2** are substrates for this transporter.

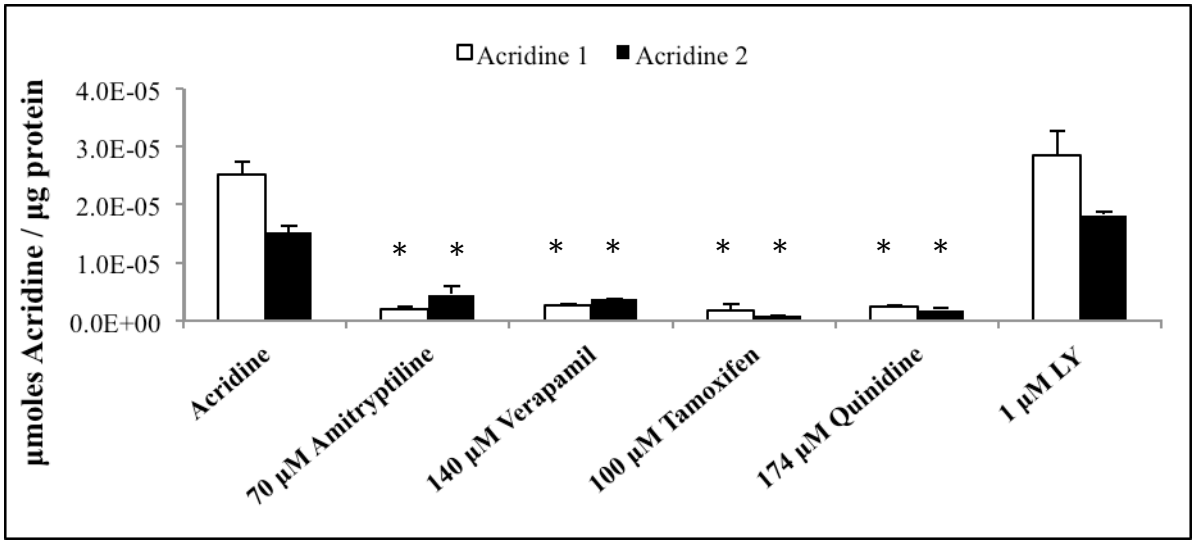


**Figure 13: Accumulation of Acridine 1 - 4 in MDCK-WT in the presence of OCT Substrates**

Acridine permeability was investigated by comparing their accumulation in MDCK cells with a series of β-blockers (atenolol, nadolol, metoprolol, talinolol, and propranolol), which have known permeability. An HPLC method with fluorescence detection was developed for the quantitation of β-blockers from the MDCK cell lysate (**Figure 14**) and the lipophilic dependent accumulation of the β-blockers are depicted in (**Figure 15**). It was ultimately determined that acridine **1**, **2**, and **4** accumulated 2.7, 2.2, and 4.3 times more than propranolol, respectively indicating these compounds are highly permeable. Acridine **3** accumulated equally to propranolol again indicating high permeability.

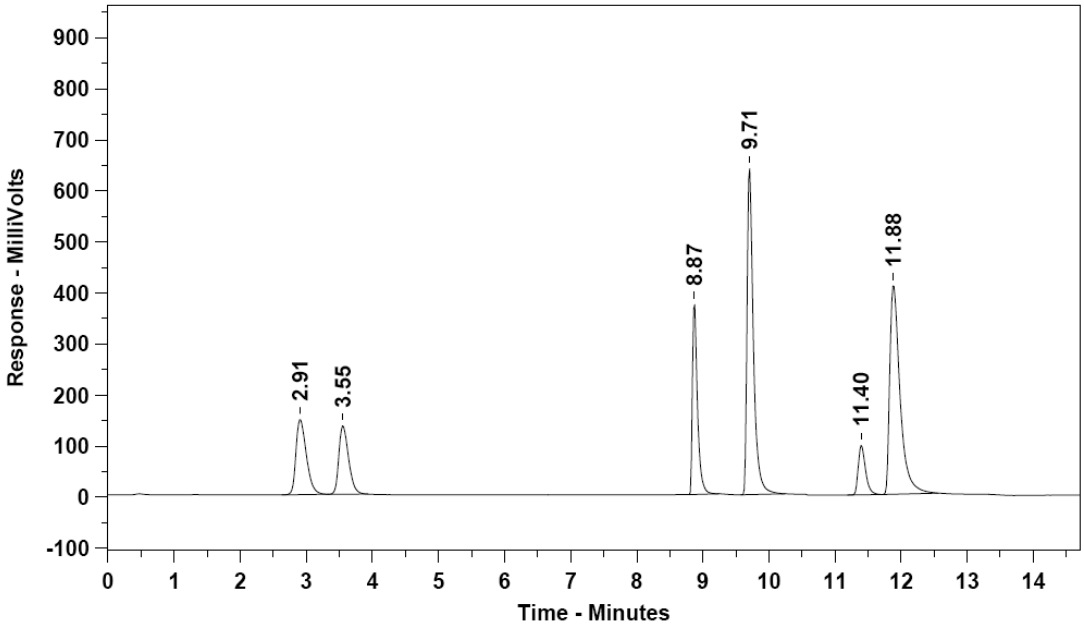


**Figure 14: HPLC-Fl Chromatogram of 6 β-blockers (atenolol, sotalol, nadolol, metoprolol, talinolol and propranolol) with differing lipophilicities**
β-blockers (5.0 μM): atenolol (2.91 min), sotalol (3.55 min), nadolol (8.87 min), metoprolol (9.71 min), talinolol (11.40 min), and propranolol (11.88 min).

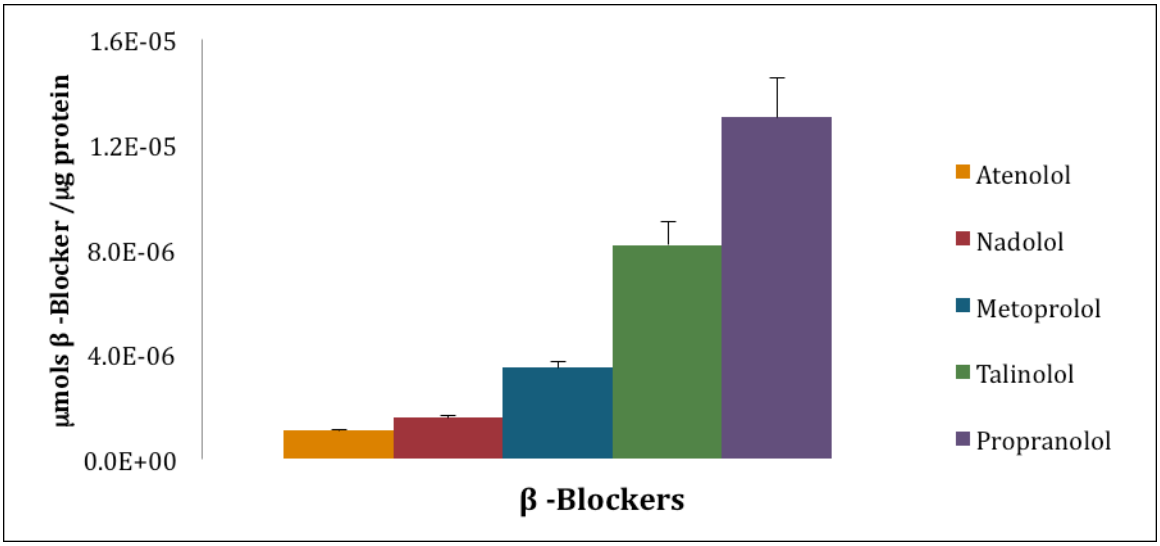


**Figure 15: Lipophilic dependent permeability of six β-blockers in MDCK-WT cells.**

- Plasma Protein Binding

Human plasma protein binding as determined by membrane ultrafiltration was 97.7%, 95.3 %, 97.7%, and 99.3% for Acridine **1 - 4**, respectively (**Figure 16**).

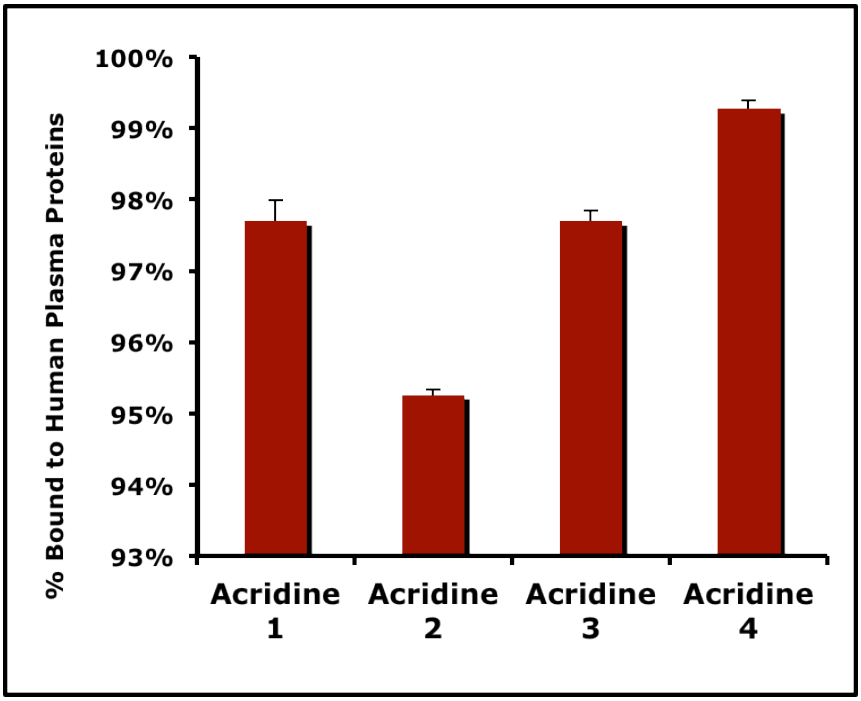


**Figure 16: Acridine binding to human plasma proteins by a membrane ultracentrifugation technique**

- Mouse pharmacokinetics
  - Acridine 1 Oral Dose

The acridine **1** concentration vs. time profiles for plasma, brain, liver, and kidney are presented in **Figure 17 A-D**. The profiles display a clear mono-exponential decline of acridine **1** indicating a one-compartment model. Following a single 60 mg/kg oral dose of acridine **1**, the $C_{max}$ values of acridine **1** in brain, liver, and kidneys were 0.2, 125, and 30 μM, respectively and the free concentration of acridine 1 in the plasma was 0.052 μM. The half-life of acridine **1** in plasma and tissue was calculated to be approximately 4.0 hrs. All other pharmacokinetic parameters in plasma are described in **Table 2**.

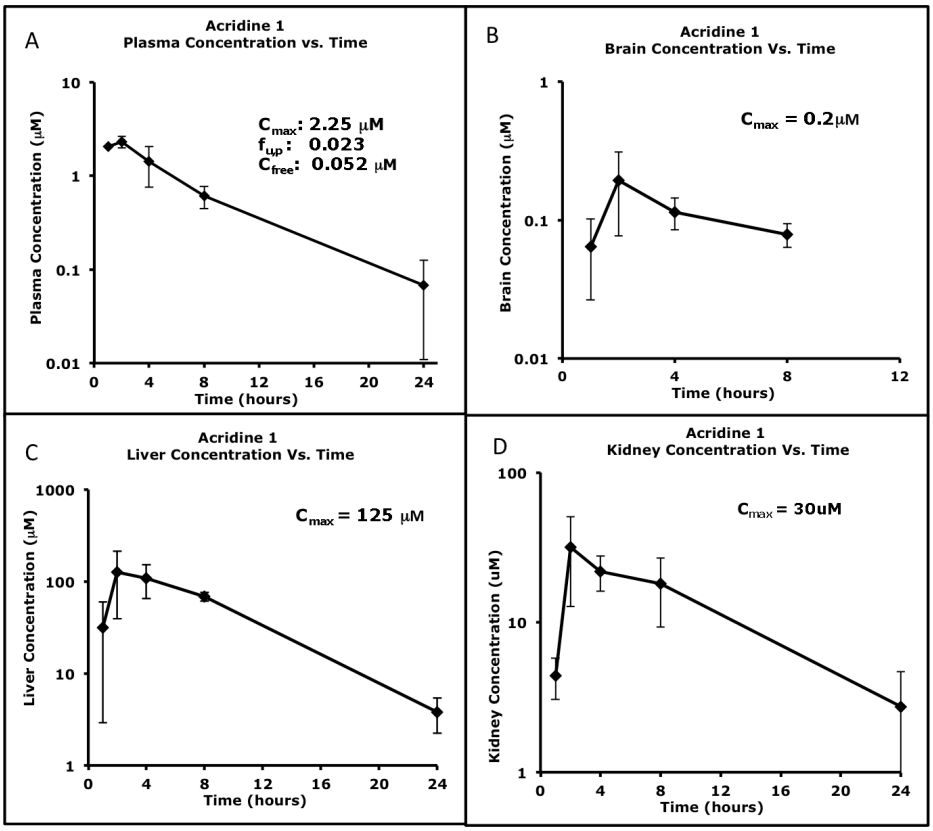


**Figure 17: Plasma, brain, liver, and kidney concentration of Acridne 1 Following a 60 mg/kg oral dose of Acridine 1**

- Acridine 2 Oral and IV dose

**Figure 18 A-D** depicts the concentration vs. time profiles for plasma, brain, liver, and kidney in murine administration of a single oral (60 mg/kg) or IV (15 mg/kg) dose of acridine **2**. The plasma profile display a two-compartment model with a both a distributional and elimination phase. The plasma half-life of acridine **2** (22.2 hrs) was approximately 5 times longer than acridine **1** (4.46 hrs). Following the IV dose, a distributional half-life (4.68 hrs) was calculated instead of a terminal half-life because the concentration at the 72-hr time point was beyond the limit of detection for the assay. All other plasma pharmacokinetic parameters are described in **Table 2**.

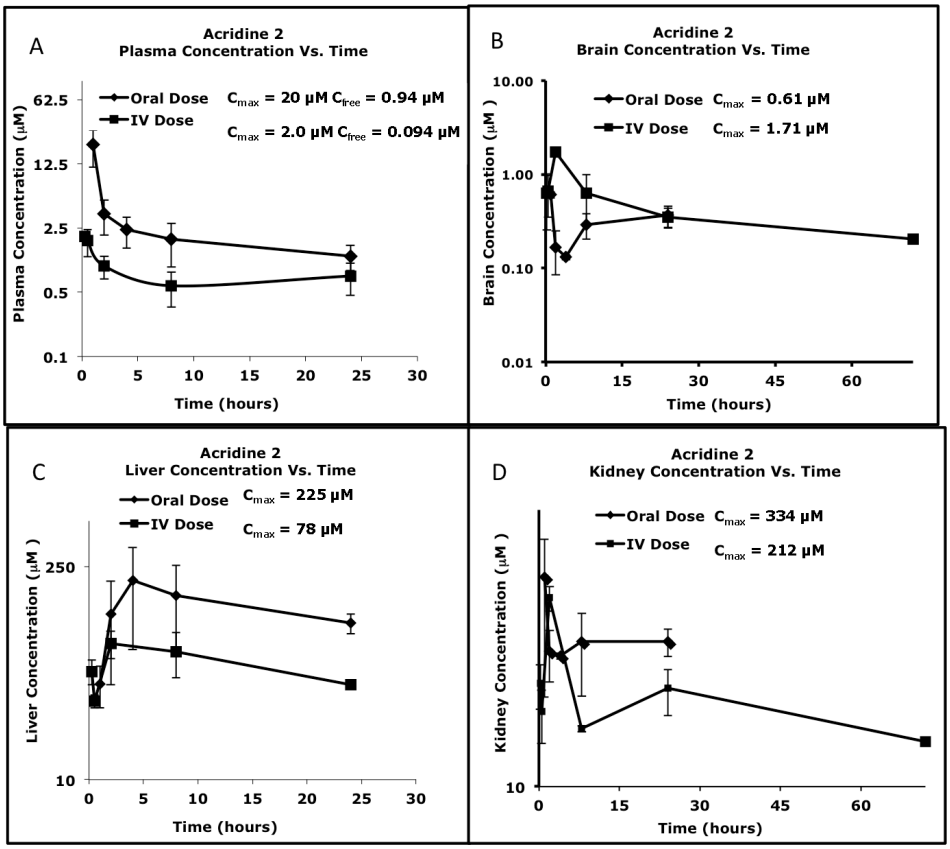


**Figure 18: Plasma, brain, liver, and kidney concentration of Acridine 2 following a 60 mg/mg oral dose and 15 mg/kg IV dose**

| Compound | Acridine 1 | Acridine 2 | Acridine 2 |
|---|---|---|---|
| Route | Oral | Oral | IV |
| Dose (mg/kg) | 60 | 60 | 15 |
| $t_{1/2}$ (hr) | 4.5 | 22.2 | 4.68* |
| Cl (L/hr) | 0.153** | 0.033** | 0.039 |
| $AUC_{0-24}$ hr*µmol/L | 16.91 | 61.6 | 18.4 |
| Volume of Distribution (L) | N/A | N/A | 0.266 |
| Bioavailability (F) | N/A | | 86% |
| $C_{free}$ µM Plasma | 0.052 | 0.94 | 0.094 |
| $C_{max}$ µM Brain | 0.2 | 0.61 | 1.7 |
| $C_{max}$ µM Liver | 125 | 225 | 78 |
| $C_{max}$ µM Kidney | 30 | 334 | 212 |

**Table 2: Pharmacokinetic parameters calculated for the oral and IV dosing of Acridine 1 and 2 to mice. * indicates a distributional half-life ** indicates the apparent oral clearance (Cl/F)**

- In vivo efficacy

Mice bearing glioma were treated with acridine **2** via oral gavage. Mice were dosed once daily, M-F for two weeks. During the first week, the mice were treated with 30 mg/kg of acridine **2** followed by 60 mg/kg during the second week. All of the untreated mice died within two weeks of glioma implantation; however, there was a significant increase in the lenghth survival ($p < 0.0375$) of mice treated with acridine **2** (**Figure 19**).

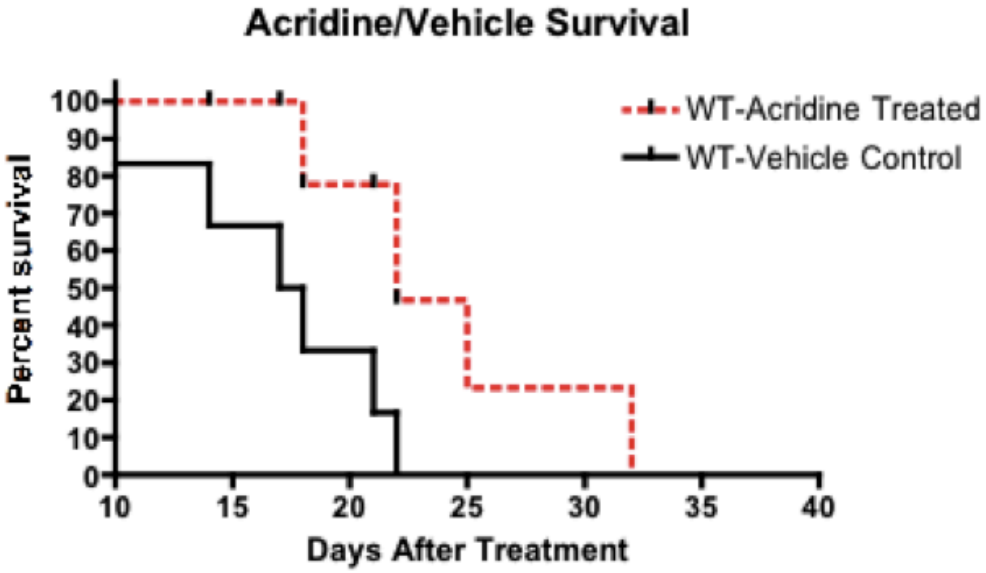


**Figure 19: Kaplan-Meier survival curve of untreated and acridine 2 treated mice**
$P < 0.05$ for the median survival between treated and untreated animals

## V. Discussion

Dr. Ferguson's research group at the University of Minnesota discovered a series of small molecule 9-aminoacridine based compounds with low micromolar $IC_{50}$ values (2.8 – 4.5 μM) against human glioma cell lines.[48] In fact, these values are significantly lower than the reported glioma cell $IC_{50}$ value for temozolomide (1.7 mM), the current drug used to treat patients with malignant glioma.[50] Despite the moderate success of temozolomide treatment, undesirable side effects such as aplastic anemia,[51-53] hepatic encephalopathy,[54] and urticarial hypersensitivity[55] have been reported. Several other types of small molecule chemotherapeutic agents for malignant glioma have been investigated only to find a modest increase in patient survival and/or problems with toxicity.[56-58] As a result of the encouraging results from the *in vitro* work with acridines **1 – 4**, it would be ideal to test each of their respective efficacies in a mouse orthotopic glioblastoma model designed by Dr. John Ohlfest at the University of Minnesota. However, due to significant cost and experimental time, we decided to perform the necessary drug metabolism and pharmacokinetic experiments to select a lead candidate for the *in vivo* efficacy experiment.

Metabolic stability experiments in pooled human liver microsomes (**Figure 10**) indicate the acridines undergo slow rates of oxidation and negligible glucuronidation. Structurally, the acridines appear to be metabolically labile; however, no significant metabolites were identified in microsome or cytosolic preparations. The main reason postulated for this result is the high lipophilicity (cLogP values: 4-5) of the acridine compounds, which can cause them to bind non-specifically to membranes or proteins.

Also, the half-lives of acridines **1, 3,** and **4** were significantly longer than acridine **2** and may be attributed to the lack of steric bulk around the 9-amino substituent. The long metabolic half-lives were encouraging results because the compounds have the potential to be absorbed into the systemic circulation without any significant first pass metabolism following an oral dose.

MDCK cells were chosen as a model to investigate acridine absorption due to their ability to grow as monolayers and form tight junctions analogous to intestinal epithelial cells. Molecules with high lipophilicity generally are able to penetrate cellular membranes and it was expected the acridines would have little trouble entering cells. Acridine **1**, **2**, and **4** all accumulated in MDCK-WT cells with values 2.7, 2.2, and 4.3 times greater than propranolol, a β-blocker characterized by the biopharmaceutical classification system as having "high" permeability. The accumulation of acridine **3** was about equivalent to propranolol. MDCK cells can also be overexpressed with efflux transporter proteins such as Pgp and BCRP to investigate whether compounds are potential efflux transporter substrates. In accumulation experiments with MDCK-MDR cells, it was discovered that the accumulation of acridine **1** and **3** significantly decreased compared to their accumulation in wild-type cells. The accumulation was significantly restored in the presence of the LY335979, a Pgp inhibitor. This data suggests that that acridine **1** and **3** are moderate substrates for Pgp whereas acridine **2** and **4** are not substrates. Accumulation experiments with MDCK cells overexpressing BCRP were also conducted and it was found that only acridine **2** was not a substrate for BCRP. The difference in efflux transporter substrate specificity can be attributed to the overall charge

on the acridine at physiological pH. Under these conditions, the piperidine nitrogen of acridine **2** is more easily ionized than the indole nitrogen of acridine **1, 3,** or **4**, and thus accounts for the greater overall positive charge of acridine **2**. Also, preliminary experiments have been performed that suggest acridines are substrates for an organic cation transporter (**Figure 13**). It is believed that OCT-2 is the predominant isoform involved in acridine transport because MDCK cells have been previously shown to express OCT-2 specifically, with little to no expression of the other isoforms (OCT-1 and OCT-3).[59]

Plasma protein binding experiments were subsequently conducted to determine the free fraction of acridine in the plasma. It is important to remember that only the free fraction of drug is available to cross membranes into tissues and exert a therapeutic effect. Similar to the studies described with *m*-AMSA, asulacrine, and DACA, acridines **1** – **4** were all highly bound to plasma proteins. Acridine **2**, the most polar compound in the series, was the least bound with a free fraction of 0.047.

Based on the results from the metabolic stability, MDCK accumulation, and plasma protein binding studies, it was decided to move acridine **1** and **2** further along the development pipeline and investigate their pharmacokinetics in mice. Acridine **3** was not chosen mainly because of the lowest accumulation in MDCK cells as well as its potential as a Pgp and BCRP substrate. Acridine **4** was not taken forward due to specificity for BCRP as well as the highest plasma protein binding compared to the other compounds in the series.

Oral doses (60 mg/kg) of Acridine **1** or **2** were chosen as initial investigational doses due to prior experiments in a mouse prostate cancer model, which determined a 60 mg/kg dose to be non-toxic. The pharmacokinetics in plasma following an oral dose of acridine **1** indicated a one-compartment model and mono-exponential elimination of **1** from the plasma. The liver and kidney concentrations were very high (125 μM and 30 μM, respectively) as expected from previous pharmacokinetic work *m*-AMSA and DACA in small animals.[12, 60] Acridine **1** was able to cross the blood-brain barrier and a maximum concentration of 0.2 μM was achieved. The pharmacokinetics in plasma following an oral dose of acridine **2** were more consistent with the dose-dependent kinetics described for *m*-AMSA, and asulacrine.[11] The kinetics of **2** were biphasic with an initial distributional phase in which **2** is rapidly taken up into the tissues from the plasma followed by a long drawn out terminal elimination phase. Free concentrations in plasma, liver, kidney, and brain were 0.94 μM, 225 μM, 334 μM, and 0.6 μM, respectively. The free concentrations of acridine **1** and **2** in plasma were lower than concentrations in the brain while the concentrations in liver and kidney were dramatically higher than brain or plasma concentrations. It is hypothesized that the acridines gain access to the brain by passive diffusion due to their high lipophilicity: (ClogP values of 5.52 and 5.28 for acridine **1** and **2**, respectively). Lin and colleagues recently discovered that both OCT-1 and OCT-2 are expressed on the luminal side of brain microvessel endothelium isolated from humans, mice, and rats.[61] In addition to passive diffusion, the acridines may be entering the brain through the OCT uptake transporters expressed on the luminal membrane of the brain capillary endothelial cells. Efflux may explain the higher

concentration achieved in the brain for acridine **2**. In comparing cellular concentrations of compounds **1** and **2** in Pgp and BCRP overexpression systems (**Figures 12-13**), acridine **1** had a lower accumulation in brain, consistent with the *in vitro* data indicating it is a more favorable substrate for Pgp and BCRP efflux than acridine **2**. Also, acridine **2** is less highly bound to human plasma proteins than acridine **1** (95.26% and 97.7%, respectively). In addition, there is a 4.7-fold difference in apparent oral clearance (Cl/F) and a 4.9-fold difference in half-life between **1** and **2** due to a change in metabolic or biliary clearance, protein binding, or altered bioavailability. Metabolic clearance data (**Figure 10**) indicates **1** is metabolized more rapidly than **2**, suggesting the main difference in CL/F is due to a change in clearance rather than a change in F. As a result of the higher brain concentration of **2**, an iv study was conducted in an effort to ultimately calculate absolute bioavailability. The oral and iv pharmacokinetic experiments indicate **2** is readily bioavailable (F = 86%) and can dosed orally in animal efficacy experiments.

Mouse pharmacokinetic studies led us to choose acridine **2** for *in vivo* efficacy experiments due to its higher brain penetration and limited efflux by Pgp and BCRP compared with acridine **1**. Acridine **2** significantly increased the median survival of mice in an orthotopic glioblastoma model (**Figure 19**). To our knowledge, this is the first evidence of *in vivo* efficacy against malignant glioma from both a topoisomerase II inhibitor and acridine-containing compound. Although DACA and pyrazoloacridine (PA), a nitracrine derivative, were administered to patients with malignant glioma, the BBB permeability was never initially investigated. The CLogP values of DACA and PA

are 3.1 and 4.2, respectively and thus are less lipophilic than acridine **1** and **2**. This may explain the failure of DACA and PA to show efficacy against glioma. Alternatively, they may be better substrates for efflux pumps. Other topoisomerase II inhibitors such as etoposide, doxorubicin, and mitoxantrone are thought to suffer from high efflux (Pgp and BCRP), limiting their application in the clinic. [62]

## VI. Conclusions and Future Directions

The work presented in this chapter describes a drug discovery investigation of 9-amino acridine based compounds with the potential to treat malignant glioma. Overall, the results suggest compounds in this series may offer new strategies for the design of chemotherapeutics for treating brain cancers with high oral bioavailability and improved efficacy. Although acridine **2** was found to effective in a mouse brain cancer model, many metabolic and pharmacokinetic questions still remain to be answered for the acridine series. For instance, in each of the cases reported for *m*-AMSA, asulacrine, and DACA, the primary mechanism of clearance is via the biliary route. Due to the molecular similarity of the compounds described in this work with the previously investigated acridine based compounds, it is reasonable to suggest biliary clearance as route of elimination for acridines **1** – **4**. Experiments involving bile duct cannulated animals would be a reasonable method to investigate the elimination pathway hypothesis. Additionally, metabolites eliminated into the bile as glutathione conjugates could also be identified with the aid of liquid chromatography-mass spectrometry (LC-MS) techniques as well as GSH trapping experiments in microsomal preparations. Oxidative metabolite identification experiments via microsomal or cytosolic enzymes are also necessary to determine an overall metabolic profile for the investigational compounds.

Additional experiments are required to more completely understand the role OCT plays in mediating transport of acridines across physiological membranes as well as the blood brain barrier. An initial experiment should investigate the acridine substrate specificity for the three different isoforms of OCT by looking at transport in cells transfected with each respective isoform. Dr. Carolyn Fairbanks, a professor in the

pharmaceutics department at the University of Minnesota, has previously investigated the disposition of agmatine and polyamines in human embryonic kidney cells (HEK293) stably transfected with the human isoforms of OCT-1 and OCT-2. A collaboration with her group may provide some useful information regarding the transport of acridines via the OCT transport system. In addition, Dr. Kathy Giacommini, a professor at the University of California San Francisco, is one of the world's leading expert's on drug transport and she may be able to offer some advice regarding the transport of acridines through the blood-brain barrier. Additionally, Taconic sells a relatively expensive OCT1-2 knockout mouse model, which can be utilized to unequivocally test the hypothesis that acridine brain accumulation is greater when OCT is present in the animal. Acridine **2** does bear an additional positive charge, which may have a significant impact on distribution and elimination, especially if OCT transport is involved.

A potential concern from the pharmacokinetic investigations was the high concentration of acridine found in the liver and kidney of the animals. As a result of the mutagenic nature of the acridines, liver and kidney toxicity studies are certainly warranted. One method to identify liver or kidney damage would be to submit the organs for histopathological analysis. Another method to investigate possible toxicity is to look at serum biomarkers for liver and kidney injury. Alanine aminotransferase (ALT) is a common biomarker for liver injury and one could look at the ALT levels from the blood of mice with an ALT assay kit sold the Cayman Chemical Company (item # 700260). Neutrophil gelatinase-associated lipocalin (NGAL) and kidney injury molecule-1 (KIM1) are serum and urinary biomarkers, respectively and can be utilized to determine kidney

injury following a dose of an investigational compound. A mouse NGAL ELISA kit sold by Bioporto Diagnostics (item # Kit 042) and a mouse KIM1 assay kit is sold by Genway Biotech, Inc (item # GWB374Z36).

Lastly, an optimized dosing regimen to increase brain concentrations and achieve improved therapeutic levels is worth investigating. Ideally, the therapeutic level in the brain should be equivalent or above the $IC_{50}$ value. It would be interesting to know what the drug concentration level was in the brain following the dosing regimen reported the *in vivo* efficacy study as well as other optimized regimens such as multiple daily dosing or increasing the single oral daily dose. By improving the dosing regimen, adequate levels of drug will be in the brain to exert therapeutic effects and prolong the live of mice in efficacy experiments.

## VII. References


1. Denny, W. A. Acridine derivatives as chemotherapeutic agents. *Curr Med Chem* **2002,** 9, 1655-65.

2. Belmont, P.; Bosson, J.; Godet, T.; Tiano, M. Acridine and acridone derivatives, anticancer properties and synthetic methods: where are we now? *Anticancer Agents Med Chem* **2007,** 7, 139-69.

3. Liu, L. F. DNA topoisomerase poisons as antitumor drugs. *Annu Rev Biochem* **1989,** 58, 351-75.

4. Chourpa, I. Specific Molecular Interactions of Acridine Drugs in Complexes with Topoisomerase II and DNA. SERS ad Resonance Rama Study of m-AMSA in comparison with o-AMSA. *Journal of Raman Spectroscopy* **1995,** 26, 813-819.

5. Graziano, M. J.; Courtney, C. L.; Meierhenry, E. F.; Kheoh, T.; Pegg, D. G.; Gough, A. W. Carcinogenicity of the anticancer topoisomerase inhibitor, amsacrine, in Wistar rats. *Fundam Appl Toxicol* **1996,** 32, 53-65.

6. Mosesso, P.; Darroudi, F.; van den Berg, M.; Vermeulen, S.; Palitti, F.; Natarajan, A. T. Induction of chromosomal aberrations (unstable and stable) by inhibitors of topoisomerase II, m-AMSA and VP16, using conventional Giemsa staining and chromosome painting techniques. *Mutagenesis* **1998,** 13, 39-43.

7. de Nully Brown, P.; Hoffmann, T.; Hansen, O. P.; Boesen, A. M.; Gronbaek, K.; Hippe, E.; Jensen, M. K.; Thorling, K.; Storm, H. H.; Pedersen-Bjergaard, J. Long-term survival and development of secondary malignancies in patients with acute myeloid leukemia treated with aclarubicin or daunorubicin plus cytosine arabinoside followed by intensive consolidation chemotherapy in a Danish national phase III trial. Danish Society of Haematology Study Group on AML. *Leukemia* **1997,** 11, 37-41.

8. Steuber, C. P.; Krischer, J.; Holbrook, T.; Camitta, B.; Land, V.; Sexauer, C.; Mahoney, D.; Weinstein, H. Therapy of refractory or recurrent childhood acute myeloid leukemia using amsacrine and etoposide with or without azacitidine: a Pediatric Oncology Group randomized phase II study. *J Clin Oncol* **1996,** 14, 1521-5.

9. Estey, E.; Thall, P. F.; Pierce, S.; Kantarjian, H.; Keating, M. Treatment of newly diagnosed acute promyelocytic leukemia without cytarabine. *J Clin Oncol* **1997,** 15, 483-90.

10. Mollgard, L.; Tidefelt, U.; Sundman-Engberg, B.; Lofgren, C.; Lehman, S.; Paul, C. High single dose of mitoxantrone and cytarabine in acute non-lymphocytic leukemia: a pharmacokinetic and clinical study. *Ther Drug Monit* **1998,** 20, 640-5.

11. Kestell, P.; Paxton, J. W.; Evans, P. C.; Young, D.; Jurlina, J. L.; Robertson, I. G.; Baguley, B. C. Disposition of amsacrine and its analogue 9-([2-methoxy-4-[(methylsulfonyl)amino]phenyl]amino)-N,5-dimethyl-4- acridinecarboxamide (CI-921) in plasma, liver, and Lewis lung tumors in mice. *Cancer Res* **1990,** 50, 503-8.

12. Cysyk, R. L.; Shoemaker, D.; Adamson, R. H. The pharmacologic disposition of 4'-(9-acridinylamino)methanesulfon-m-anisidide in mice and rats. *Drug Metab Dispos* **1977,** 5, 579-90.

13. Shoemaker, D. D.; Cysyk, R. L.; Padmanabhan, S.; Bhat, H. B.; Malspeis, L. Identification of the principal biliary metabolite of 4'-(9-acridinylamino)methanesulfon-m-anisidide in rats. *Drug Metab Dispos* **1982,** 10, 35-9.

14. Paxton, J. W.; Foote, S. E.; Singh, R. M. The effect of buthionine sulphoximine, cimetidine and phenobarbitone on the disposition of amsacrine in the rabbit. *Cancer Chemother Pharmacol* **1986,** 18, 208-12.

15. Hall, S. W.; Friedman, J.; Legha, S. S.; Benjamin, R. S.; Gutterman, J. U.; Loo, T. L. Human pharmacokinetics of a new acridine derivative, 4'-(9-acridinylamino)methanesulfon-m-anisidide (NSC 249992). *Cancer Res* **1983,** 43, 3422-6.

16. Jurlina, J. L.; Varcoe, A. R.; Paxton, J. W. Pharmacokinetics of amsacrine in patients receiving combined chemotherapy for treatment of acute myelogenous leukemia. *Cancer Chemother Pharmacol* **1985,** 14, 21-5.

17. Legha, S. S.; Gutterman, J. U.; Hall, S. W.; Benjamin, R. S.; Burgess, M. A.; Valdivieso, M.; Bodey, G. P. Phase 1 clinical investigation of 4'-(9-acridinylamino)methanesulfon-m-anisidide (NSC 249992), a new acridine derivative. *Cancer Res* **1978,** 38, 3712-6.

18. Jehn, U.; Heinemann, V. New drugs in the treatment of acute and chronic leukemia with some emphasis on m-AMSA. *Anticancer Res* **1991,** 11, 705-11.

19. Kell, J. Treatment of relapsed acute myeloid leukaemia. *Rev Recent Clin Trials* **2006,** 1, 103-11.

20. Verma, D.; Kantarjian, H.; Faderl, S.; O'Brien, S.; Pierce, S.; Vu, K.; Freireich, E.; Keating, M.; Cortes, J.; Ravandi, F. Late relapses in acute myeloid leukemia: analysis of characteristics and outcome. *Leuk Lymphoma* 51, 778-82.

21. Trials, N. C. I. C. http://www.cancer.gov/clinicaltrials/search/results?/protocolsearchid=9234167. In 2011.

22. Jelic, S.; Nikolic-Tomasevic, Z.; Kovcin, V.; Milanovic, N.; Tomasevic, Z.; Jovanovic, V.; Vlajic, M. A two-step reevaluation of high-dose amsacrine for advanced carcinoma of the upper aerodigestive tract: a pilot phase II study. *J Chemother* **1997,** 9, 364-70.

23. Baguley, B. C.; Denny, W. A.; Atwell, G. J.; Finlay, G. J.; Rewcastle, G. W.; Twigden, S. J.; Wilson, W. R. Synthesis, antitumor activity, and DNA binding properties of a new derivative of amsacrine, N-5-dimethyl-9-[(2-methoxy-4-methylsulfonylamino) phenylamino]-4-acridinecarboxamide. *Cancer Res* **1984,** 44, 3245-51.

24. Covey, J. M.; Kohn, K. W.; Kerrigan, D.; Tilchen, E. J.; Pommier, Y. Topoisomerase II-mediated DNA damage produced by 4'-(9-acridinylamino)methanesulfon-m-anisidide and related acridines in L1210 cells and isolated nuclei: relation to cytotoxicity. *Cancer Res* **1988,** 48, 860-5.

25. Leopold, W. R., 3rd; Corbett, T. H.; Griswold, D. P., Jr.; Plowman, J.; Baguley, B. C. Experimental antitumor activity of the amsacrine analogue CI-921. *J Natl Cancer Inst* **1987,** 79, 343-9.

26. Elliot, W. L. Enhanced therapeutic effect of amsalog (CI-921) in combination with cisplatin in vitro and in vivo. *Oncology Reports* **1998,** 3, 1153.

27. Paxton, J. W.; Hardy, J. R.; Evans, P. C.; Harvey, V. J.; Baguley, B. C. The clinical pharmacokinetics of N-5-dimethyl-9-[(2-methoxy-4-methyl-sulfonylamino)phenylamino]-4 -acridinecarboxamide (CI-921) in a phase 1 trial. *Cancer Chemother Pharmacol* **1988,** 22, 235-40.

28. Harvey, V. J.; Hardy, J. R.; Smith, S.; Grove, W.; Baguley, B. C. Phase II study of the amsacrine analogue CI-921 (NSC 343499) in non-small cell lung cancer. *Eur J Cancer* **1991,** 27, 1617-20.

29. Sklarin, N. T.; Wiernik, P. H.; Grove, W. R.; Benson, L.; Mittelman, A.; Maroun, J. A.; Stewart, J. A.; Robert, F.; Doroshow, J. H.; Rosen, P. J.; et al. A phase II trial of CI-921 in advanced malignancies. *Invest New Drugs* **1992,** 10, 309-12.

30. Atwell, G. J.; Rewcastle, G. W.; Baguley, B. C.; Denny, W. A. Potential antitumor agents. 50. In vivo solid-tumor activity of derivatives of N-[2-(dimethylamino)ethyl]acridine-4-carboxamide. *J Med Chem* **1987,** 30, 664-9.

31. Schneider, E.; Darkin, S. J.; Lawson, P. A.; Ching, L. M.; Ralph, R. K.; Baguley, B. C. Cell line selectivity and DNA breakage properties of the antitumour agent N-[2-(dimethylamino)ethyl]acridine-4-carboxamide: role of DNA topoisomerase II. *Eur J Cancer Clin Oncol* **1988,** 24, 1783-90.

32. Crenshaw, J. M.; Graves, D. E.; Denny, W. A. Interactions of acridine antitumor agents with DNA: binding energies and groove preferences. *Biochemistry* **1995,** 34, 13682-7.

33. Bridewell, D. J.; Finlay, G. J.; Baguley, B. C. Mechanism of cytotoxicity of N-[2-(dimethylamino)ethyl] acridine-4-carboxamide and of its 7-chloro derivative: the roles of topoisomerases I and II. *Cancer Chemother Pharmacol* **1999,** 43, 302-8.

34. Finlay, G. J.; Marshall, E.; Matthews, J. H.; Paull, K. D.; Baguley, B. C. In vitro assessment of N-[2-(dimethylamino)ethyl]acridine-4-carboxamide, a DNA-intercalating antitumour drug with reduced sensitivity to multidrug resistance. *Cancer Chemother Pharmacol* **1993,** 31, 401-6.

35. Davey, R. A.; Su, G. M.; Hargrave, R. M.; Harvie, R. M.; Baguley, B. C.; Davey, M. W. The potential of N-[2-(dimethylamino)ethyl]acridine-4-carboxamide to circumvent three multidrug-resistance phenotypes in vitro. *Cancer Chemother Pharmacol* **1997,** 39, 424-30.

36. Haldane, A.; Finlay, G. J.; Hay, M. P.; Denny, W. A.; Baguley, B. C. Cellular uptake of N-[2-(dimethylamino)ethyl]acridine-4-carboxamide (DACA). *Anticancer Drug Des* **1999,** 14, 275-80.

37. Robertson, I. G.; Palmer, B. D.; Officer, M.; Siegers, D. J.; Paxton, J. W.; Shaw, G. J. Cytosol mediated metabolism of the experimental antitumor agent acridine carboxamide to the 9-acridone derivative. *Biochem Pharmacol* **1991,** 42, 1879-84.

38. Evans, S. M.; Robertson, I. G.; Paxton, J. W. Plasma protein binding of the experimental antitumour agent acridine-4-carboxamide in man, dog, rat and rabbit. *J Pharm Pharmacol* **1994,** 46, 63-7.

39. Brady, F.; Luthra, S. K.; Brown, G.; Osman, S.; Harte, R. J.; Denny, W. A.; Baguley, B. C.; Jones, T.; Price, P. M. Carbon-11 labelling of the antitumour agent N-[2-(dimethylamino)ethyl]acridine-4-carboxamide (DACA) and determination of plasma metabolites in man. *Appl Radiat Isot* **1997,** 48, 487-92.

40. McCrystal, M. R.; Evans, B. D.; Harvey, V. J.; Thompson, P. I.; Porter, D. J.; Baguley, B. C. Phase I study of the cytotoxic agent N-[2-(dimethylamino)ethyl]acridine-4-carboxamide. *Cancer Chemother Pharmacol* **1999,** 44, 39-44.

41. Twelves, C. J.; Gardner, C.; Flavin, A.; Sludden, J.; Dennis, I.; de Bono, J.; Beale, P.; Vasey, P.; Hutchison, C.; Macham, M. A.; Rodriguez, A.; Judson, I.; Bleehen, N. M. Phase I and pharmacokinetic study of DACA (XR5000): a novel inhibitor of topoisomerase I and II. CRC Phase I/II Committee. *Br J Cancer* **1999,** 80, 1786-91.

42. Caponigro, F.; Dittrich, C.; Sorensen, J. B.; Schellens, J. H.; Duffaud, F.; Paz Ares, L.; Lacombe, D.; de Balincourt, C.; Fumoleau, P. Phase II study of XR 5000, an inhibitor of topoisomerases I and II, in advanced colorectal cancer. *Eur J Cancer* **2002,** 38, 70-4.

43. Dittrich, C.; Coudert, B.; Paz-Ares, L.; Caponigro, F.; Salzberg, M.; Gamucci, T.; Paoletti, X.; Hermans, C.; Lacombe, D.; Fumoleau, P. Phase II study of XR 5000 (DACA), an inhibitor of topoisomerase I and II, administered as a 120-h infusion in patients with non-small cell lung cancer. *Eur J Cancer* **2003,** 39, 330-4.

44. Dittrich, C.; Dieras, V.; Kerbrat, P.; Punt, C.; Sorio, R.; Caponigro, F.; Paoletti, X.; de Balincourt, C.; Lacombe, D.; Fumoleau, P. Phase II study of XR5000 (DACA), an inhibitor of topoisomerase I and II, administered as a 120-h infusion in patients with advanced ovarian cancer. *Invest New Drugs* **2003,** 21, 347-52.

45. Twelves, C.; Campone, M.; Coudert, B.; Van den Bent, M.; de Jonge, M.; Dittrich, C.; Rampling, R.; Sorio, R.; Lacombe, D.; de Balincourt, C.; Fumoleau, P. Phase II study of XR5000 (DACA) administered as a 120-h infusion in patients with recurrent glioblastoma multiforme. *Ann Oncol* **2002,** 13, 777-80.

46. Goodell, J. R.; Madhok, A. A.; Hiasa, H.; Ferguson, D. M. Synthesis and evaluation of acridine- and acridone-based anti-herpes agents with topoisomerase activity. *Bioorg Med Chem* **2006,** 14, 5467-80.

47. Galvez-Peralta, M.; Hackbarth, J. S.; Flatten, K. S.; Kaufmann, S. H.; Hiasa, H.; Xing, C.; Ferguson, D. M. On the role of topoisomerase I in mediating the cytotoxicity of 9-aminoacridine-based anticancer agents. *Bioorg Med Chem Lett* **2009,** 19, 4459-62.

48. Teitelbaum, A. M.; Gallardo, J. L.; Bedi, J.; Giri, R.; Benoit, A. R.; Olin, M. R.; Morizio, K. M.; Ohlfest, J. R.; Remmel, R. P.; Ferguson, D. M. 9-Amino acridine pharmacokinetics, brain distribution, and in vitro/in vivo efficacy against malignant glioma. *Cancer Chemother Pharmacol* 69, 1519-27.

49. Olin, M. R.; Andersen, B. M.; Zellmer, D. M.; Grogan, P. T.; Popescu, F. E.; Xiong, Z.; Forster, C. L.; Seiler, C.; SantaCruz, K. S.; Chen, W.; Blazar, B. R.; Ohlfest, J. R. Superior efficacy of tumor cell vaccines grown in physiologic oxygen. *Clin Cancer Res* 16, 4800-8.

50. Liu, G.; Yuan, X.; Zeng, Z.; Tunici, P.; Ng, H.; Abdulkadir, I. R.; Lu, L.; Irvin, D.; Black, K. L.; Yu, J. S. Analysis of gene expression and chemoresistance of CD133+ cancer stem cells in glioblastoma. *Mol Cancer* **2006,** 5, 67.

51. Jalali, R.; Singh, P.; Menon, H.; Gujral, S. Unexpected case of aplastic anemia in a patient with glioblastoma multiforme treated with Temozolomide. *J Neurooncol* **2007,** 85, 105-7.

52. George, B. J.; Eichinger, J. B.; Richard, T. J. A rare case of aplastic anemia caused by temozolomide. *South Med J* **2009,** 102, 974-6.

53. Kopecky, J.; Priester, P.; Slovacek, L.; Petera, J.; Kopecky, O.; Macingova, Z. Aplastic anemia as a cause of death in a patient with glioblastoma multiforme treated with temozolomide. *Strahlenther Onkol* **2010,** 186, 452-7.

54. Goldbecker, A.; Tryc, A. B.; Raab, P.; Worthmann, H.; Herrmann, J.; Weissenborn, K. Hepatic encephalopathy after treatment with temozolomide. *J Neurooncol* **2011,** 103, 163-6.

55. Pothiawala, S.; Hsu, M. Y.; Yang, C.; Kesari, S.; Ibrahimi, O. A. Urticarial hypersensitivity reaction caused by temozolomide. *J Drugs Dermatol* 9, 1142-4.

56. Galanis, E.; Buckner, J. C. Enzastaurin in the treatment of recurrent glioblastoma: a promise that did not materialize. *J Clin Oncol* **2010,** 28, 1097-8.

57. Neyns, B.; Sadones, J.; Chaskis, C.; Dujardin, M.; Everaert, H.; Lv, S.; Duerinck, J.; Tynninen, O.; Nupponen, N.; Michotte, A.; De Greve, J. Phase II study of sunitinib malate in patients with recurrent high-grade glioma. *J Neurooncol* 103, 491-501.

58. Murray, L. J.; Bridgewater, C. H.; Levy, D. Carboplatin chemotherapy in patients with recurrent high-grade glioma. *Clin Oncol (R Coll Radiol)* 23, 55-61.

59. Shu, Y.; Bello, C. L.; Mangravite, L. M.; Feng, B.; Giacomini, K. M. Functional characteristics and steroid hormone-mediated regulation of an organic cation transporter in Madin-Darby canine kidney cells. *J Pharmacol Exp Ther* **2001,** 299, 392-8.

60. Evans, S. M.; Young, D.; Robertson, I. G.; Paxton, J. W. Intraperitoneal administration of the antitumour agent N-[2-(dimethylamino)ethyl]acridine-4-carboxamide in the mouse: bioavailability, pharmacokinetics and toxicity after a single dose. *Cancer Chemother Pharmacol* **1992,** 31, 32-6.

61. Lin, C. J.; Tai, Y.; Huang, M. T.; Tsai, Y. F.; Hsu, H. J.; Tzen, K. Y.; Liou, H. H. Cellular localization of the organic cation transporters, OCT1 and OCT2, in brain microvessel endothelial cells and its implication for MPTP transport across the blood-brain barrier and MPTP-induced dopaminergic toxicity in rodents. *J Neurochem* **2010,** 114, 717-27.

62. Loscher, W.; Potschka, H. Role of drug efflux transporters in the brain for drug disposition and treatment of brain diseases. *Prog Neurobiol* **2005,** 76, 22-76.

## Chapter 2: Meropenem Prodrugs for Drug-Resistant Tuberculosis

### I. Introduction

*Mycobacterium tuberculosis* (*Mtb*), the bacterium responsible for the disease tuberculosis (TB), is the leading cause of bacterial infectious diseases mortality responsible for approximately 1.4 million deaths in 2010, the most recent year for which statistics are available. The estimated incidence of TB in 2010, defined by the number of new and relapse cases arising per year, is 8.8 million cases worldwide with most of the cases occurring in Asia and Africa. In addition, about 13% (1 million) of TB cases occur among people living with HIV.[1]

Despite these staggering statistics, TB is a curable and treatable disease with several chemotherapeutic agents having excellent efficacy against the bacteria. The first line agents, described in the Directly Observed Treatment Shortcourse (DOTS) program, are comprised of isoniazid (INH), rifampin (RIF), ethambutol (EMB), and pyrazinamide (PZA), which are currently administered to patients as a combination therapy. However, *Mtb* is a complex organism, which has consistently eluded several chemotherapeutic regimens due to the development of resistance. The development of multi-drug resistant TB (MDR-TB) arose due to improper patient compliance of the DOTS combination therapy and/or the use of only monotherapy to treat the disease.[2] MDR-TB is defined as resistance to isoniazid and rifampicin, the two most active first-line agents and consequently, the treatment of MDR-TB involves the use of second-line agents such as the injectable aminoglycosides streptomycin, kanamycin, amikacin, or the cyclic

penatpeptide capreomycin with an additional fluorquinolone such as norfloxacin, ciprofloxacin, levofloxacin, and moxifloxacin. As a result of the treatment of MDR-TB with poorly effective second-line agents and fluroquinolones, extensively drug resistant TB (XDR-TB) evolved and is characterized by the resistance to INH and RIF, any fluroquinolone, and at least one second-line agent.[3] Additionally, patients with XDR-TB are subjected to treatment with drugs that have shown effectiveness *in vitro* from their own clinical isolates. In most case, the bacterostatics cycloserine, ethionamide, and *para*-aminosalicylic acid are required in addition to other agents such as clofazimine, linezolid, amoxicillin/clavulanate, imipenem, and clarithromycin.[4] Also, there are have been some recent reports of totally drug-resistant TB (TDR-TB), in which no chemotherapeutic treatments are available.[5, 6] Clearly, there is an imperative requirement for the development of new anti-TB drugs.

β-lactam containing antibiotics are the most widely and effective utilized chemotherapy to treat bacterial infections. Members of the β-lactam class function by inhibiting the bacterial $_{D,D}$- transpeptidases (a type of penicllin binding protein), which aid in the final step of cell wall biosynthesis.[7] The use of β-lactams for the clinical treatment of TB is limited for a variety of reasons. Initially, it was thought that low permeability through the mycobacterial cell wall due to the hydrophilic nature of β-lactams was the reason for ineffectiveness.[8, 9] However, Chambers and colleagues[10] measured the permeability coefficients of some cephalosporins and penicillins with differing hydrophobicity and found the rates through the cell wall were comparable to *P. aeruginosa*, but 100-fold less than *E. coli*. It was ultimately determined that the

mycobacterial cell wall was not solely responsible for the ineffectiveness of β-lactams and the major culprit was due to the existence of an intrinsic extended spectrum β-lactamase (BlaC). In experiments where the *blaC* gene was knocked out, *Mtb* became significantly more susceptibility (16-32-fold) to penicllins, cephalosporins, and carbapenems.[11] Consequently, it was postulated that a β-lactam/β-lactamase inhibitor combination might be useful in the treatment of TB.

The first successful *in vitro* study regarding a β-lactam/β-lactamase inhibitor combination therapy against *Mtb* was reported in 1983 and it was found that the amoxicillin (β-lactam) and clavulanate (β-lactamase inhibitor) was bactericidal against 14/15 tested *Mtb* isolates.[12] The first evidence of clinical success from a β-lactam/β-lactamase drug therapy was reported by Chambers et al. in 1998.[13] Following the treatment of ten patients who solely received amoxicillin/clavulanate (1000 mg/250 mg orally three times daily) for seven days, the amount of *Mtb* in their sputum cultures was reduced over two days at a mean rate of $0.34 \pm 0.03$ $\log_{10}$ cfu/mL/day. Comparatively, treatment with INH was about 2-fold times better ($0.60 \pm 0.30$ $\log_{10}$ cfu/mL/day); however, the encouraging results supported the previous *in vitro* work regarding the successful combination of a β-lactam/ β-lactamase drug therapy.[14, 15] There have been other successful clinical reports regarding the amoxicillin/clavulanate combination; however, the therapy was given in addition to other first line drugs and the data has largely remained inconclusive.[16, 17]

In 2007, Hugonnet and co-workers[18] cloned and expressed the *bla*C gene and characterized kinetic parameters with known β-lactamse inhibitors (tazobactam,

sulbactam, and clavulanate) as well as other β-lactam antibiotics. The major finding of this work was the discovery that clavulanate (**Figure 20**) irreversibly inactivates BlaC whereas sulbactam and tazobactam have other modes of transient inhibition which ultimately result in the formation of an active enzyme. Also, it was determined that BlaC has an extraordinary substrate specificity and was able to hydrolyze penicillins at the diffusion-limited rate as well as cephalosporins and carbapenems. Most interestingly, meropenem (a carbapenem) (**Figure 20**) was hydrolyzed five orders of magnitude more slowly than ampicillin. A more detailed kinetic analysis of BlaC inhibition by meropenem is described by Hugonnet et al.[19] in which the $K_m$ and $k_{cat}$ were determined to be 3.4 μM and 0.08 $min^{-1}$, respectively. Due to the extremely slow turnover rate, meropenem was investigated as an inhibitor of BlaC by conducting inhibition experiments with nitrocefin, a probe substrate for β-lactamases. It was ultimately confirmed that meropenem was a tight-binding inhibitor of nitrocefin hydrolysis and the encouraging results gave rise to the idea that a meropenem-clavulanate (mero-clav) combination therapy could have utility in the treatment of TB. This hypothesis was tested by determining the minimum inhibitory concentration (MIC) values of *Mtb* H37Rv by meropenem in the presence of clavulanate (2.5 μg/mL). As a result of the low MIC reported (0.32 μg/mL), the mero/clav combination was tested against *Mtb* Erdman for five consecutive days under aerobic growth conditions and

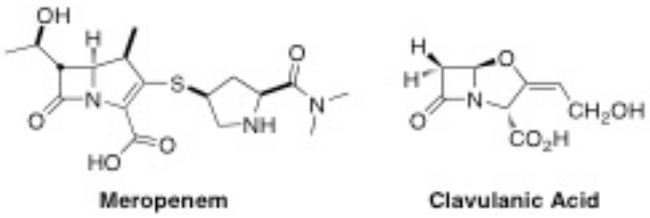


**Figure 1: Chemical Structures of Meropenem and Clavulanic Acid**

complete sterilization of cultures was seen following 9-12 days after treatment. Additionally, mero/clav was successful in reducing the viability of *Mtb* in the non-replicative or dormant state under anaerobic conditions. The highly encouraging results of these experiments prompted further studies of the mero/clav combination against extensively-drug-resistant clinical isolates of *Mtb*. The MIC values reported against 13 clinical XDR-TB isolates by meropenem was < 1 μg/mL in the presence of clavulanate (2.5 μg/mL). Additionally, a recent report validated the mero/clav combination as a successful treatment in mice infected with *Mtb* H37rv, which was more efficacious than linezolid alone. Moreover, two recent clinical case reports describe the successful use of this combination along with other first and second line agents in patients with XDR-TB from the Russian Federation.[20, 21] Clearly, a mero/clav combination therapy for the treatment of TB has exceptional clinical potential.

## II. Aims of the Present Work

The major caveat to the treatment of TB with meropenem is the requirement of multiple intravenous infusions due to meropenem's short one hour half-life[22] and negligible oral absorption. Intravenous dosing is impractical for underserved populations where TB is the most prevalent. Also,

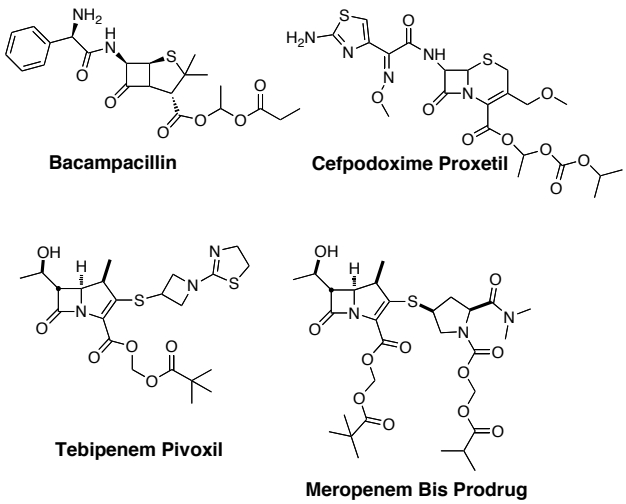


**Figure 20: Chemical Structures of Bacampacillin, Cefpodoxme Proxetil, Tebipenem Pivoxil, and a Meropenem bis prodrug**

meropenem is a highly polar zwitterionic molecule (Log D < -2.5)[23] and inherently unstable in aqueous conditions. Consequently, the intravenous product (Merrem®) must be given within 3 hours following aqueous reconstitution. Aqueous degradation products include β-lactam ring-opening (major) and dimerization from an intramolecular aminolysis reaction with two molecules of meropenem.[24] Consequently, oral forms of meropenem are required to improve stability and intravenous dosing issues and provide a reasonable dosing regimen (preferably once or twice daily).

A standard approach to improving the oral absorption of β-lactams is to synthesize a corresponding prodrug, with the ultimate goal of achieving greater lipophilicity to enhance diffusion through membranes within the gastrointestinal tract. Daehne and co-workers[25] were the first to report the improved oral absorption of ampicillin (a penicllin) in humans by the prodrug concept. This important discovery led to the development of three oral ampicillin prodrugs, pivampicillin, talmapicillin, and bacampacillin (**Figure 21**), which significantly improved the blood levels of ampicllin by 2-3-fold compared to an oral dose of ampicillin. Additionally, prodrugs of cephalosporin antibiotics such as cefuroxime axetil (Ceftin), cefditoren pivoxil (Spectrocef), and cefpodoxime proxetil (Vantin) (**Figure 21**) have be en developed and are currently used in the clinic today to treat a variety of bacterial infections. Most recently, prodrugs of the carbapenem class of antibiotics have been investigated to improve the overall absorption of the parent carbapenem.[26] The most successful oral carabapenem in development to date is tebipenem pivoxil (**Figure 21)**, which showed bioavailabilites of 71, 59, and 35% in the mouse, dog, and monkey, respectively.[27] Although pivoxil esters have been used as

successful promoieties to improve the lipophilicity of β-lactam antibiotics, the released pivalic acid is a concern when trying to develop an oral antibiotic for chronic therapy. Pivalic acid enters into the branched-chained fatty acid acyl carnitine pathway and forms pivaloyl CoA, which is excreted as pivaloyl carnitine.[28] Carnitine plays an essential role in fatty acid beta-oxidation, energy metabolism, and mitochondrial function and depletions have led to serious side effects.[29-33] In addition, meropenem bis prodrugs with a pivoxil ester attached to the carboxylate and various alkylcarbonyloxymethyl esters attached to the pyrrolidine nitrogen have previously been synthesized, and the bioavailability values ranged from (27.0 – 29.5%) in the rat and 24.4 – 38.4% in the beagle dog.[23] A representative example of a meropenem bis prodrug is shown in **Figure 21**. The following work focuses on the synthesis of a proxetil ester as well as novel bicyclic (benzosuberyl, tetralyl, and indanyl) alkyloxycarbonyloxy promoietes of meropenem in an effort to add significant lipophilicity to the parent molecule and ultimately improve oral absorption. We chose the bicyclo promoieties based historically on the first broad-spectrum penicillin prodrug carbencillin indanyl (Geocillin) and the ability to release a soft leaving group. Upon ester hydrolysis, a bicyclic alcohol is formed that can be glucuronidated and rapidly excreted from the blood.[34] Additionally, the biologically relevant pH dependent stability and plasma stability of the synthesized prodrugs will be discussed. Lastly, bioavailability experiments in jugular vein catheterized guinea pigs with select prodrugs were conducted and the results of these studies will be presented.

## III. Materials and Methods

- Chemistry

All chemicals utilized for synthetic reactions were purchased from Sigma-Aldrich (St. Louis, MO). Meropenem and was purchased from A.G Scientific (San Diego, CA). Flash chromatography was performed using a Combiflash Companion® equipped with flash column silica cartridges with the indicated solvent system. Solvents for purification (DCM, MeOH, EtOAc, Hexanes, and $NH_4OH$) were all purchased from Fisher Scientific (Pittsburgh, PA). $^{1}H$ and $^{13}C$ NMR spectra were obtained from a Varian 600 MHz spectrometer. Proton chemical shifts (δ) are reported in ppm from an internal standard of chloroform (7.26) or dichloromethane (5.32). Carbon chemical shifts are reported using an internal standard of residual chloroform (77.23) or dichloromethane (54.00). Proton chemical data are reported as follows: chemical shift, multiplicity (s = singlet, d = doublet, t = triplet, q = quartet, m = multiplet, br = broad, ovlp = overlapping), coupling constant, and integration. High-resolution mass spectra were obtained on an Agilent TOF II TOF/MS instrument equipped with an ESI probe.

- High Performance Liquid Chromatography

Solvents and reagents for liquid chromatography included HPLC grade methanol, isopropanol, and *n*-heptanes, (Sigma-Aldrich, St. Louis, MO), ammonium acetate (Fisher Scientific, Pittsburgh, PA), and acetic acid (Pharmco, Brookfield, CT).

- Reversed-phase HPLC:

The HPLC system was composed of an Agilent 1100 Liquid Chromatograph (Agilent Technologies, Santa Clara, CA), a Phenomenex Gemini-NX 150 x 4.6 mm, 5 μM reversed-phase column (Phenomenx, Torrence, CA), and a Shimadzu UV/Vis detector (Shimadzu, Kyoto, Japan) set at 300 nm. Ammonium acetate (25 mM, pH 4.8) and methanol were the aqueous (A) and organic (B) components of the mobile phase. Meropenem, acetaminophen (MP Biomedicals, Inc., Solon, OH), and prodrugs (**17-24, 37-40)** eluted at 4.3, 5.7, and 7.5-8.5 min, respectively, with the following step gradient elution: 15% B over 5.0 min, 95% B from 5.01 – 8.5 min, and re-equilibration at 15% B from 8.51 - 10.0 min prior to the next injection. The detection wavelength was set at 300 nm and the flow rate was 1.0 mL / min. The separation of meropenem proxetil diastereomers was achieved utilizing the following gradient elution timetable: 15% B over 5.0 min, 50% B from 5.01 min – 12.0 min, and re-equiliration at 15% from 12.01 min to 15.0 min. (**Figure 22**). The diastereomers eluted at 10.85 min and 11.59 minutes.

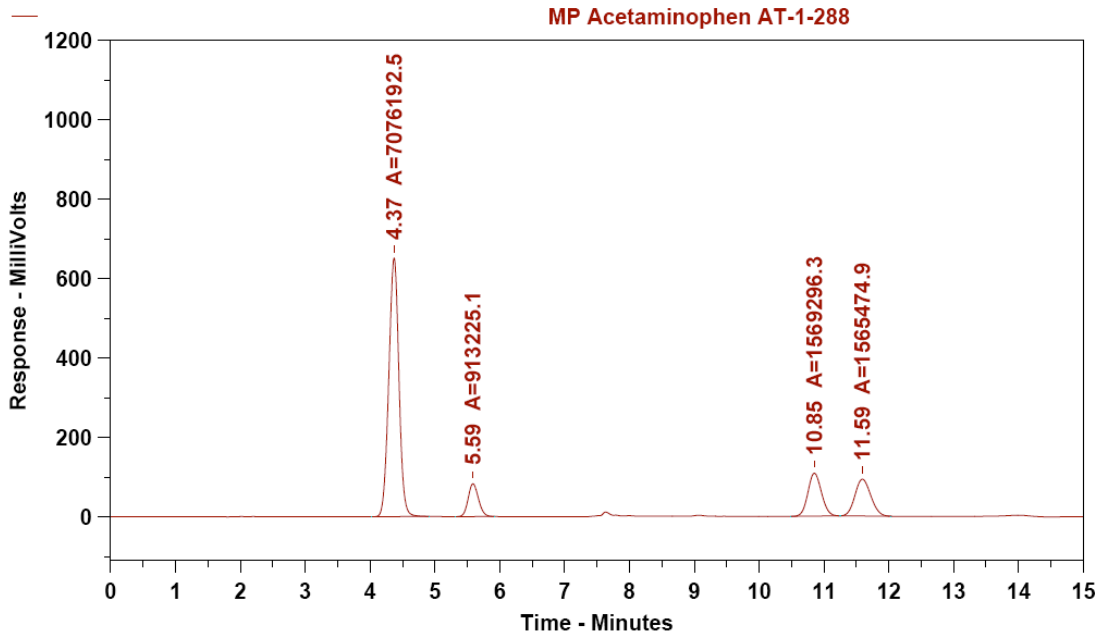


**Figure 21: HPLC chromatogram illustrating the separation of meropenem, acetaminophen, and the diastereomers of compound 2**

- Chiral HPLC

Chromatography was performed on a Shimdazu chromatograph system consisting of a SIL-10A autosampler, LC-10AD and LC-10AT binary pump system (Shimadzu, Columbia, MD), and a Spectra Focus UV/Vis optical scanning detector (Spectra-Physics, Santa Clara, CA). Chiral separations were achieved using a Chiralcel OJ 250 x 4.6mm, 10 µM column (Daicel Chemical Industries, Tokyo, Japan) with n-heptane and isopropanol as mobile phase A and B, respectively. Flow rates were 1.0 mL/min.

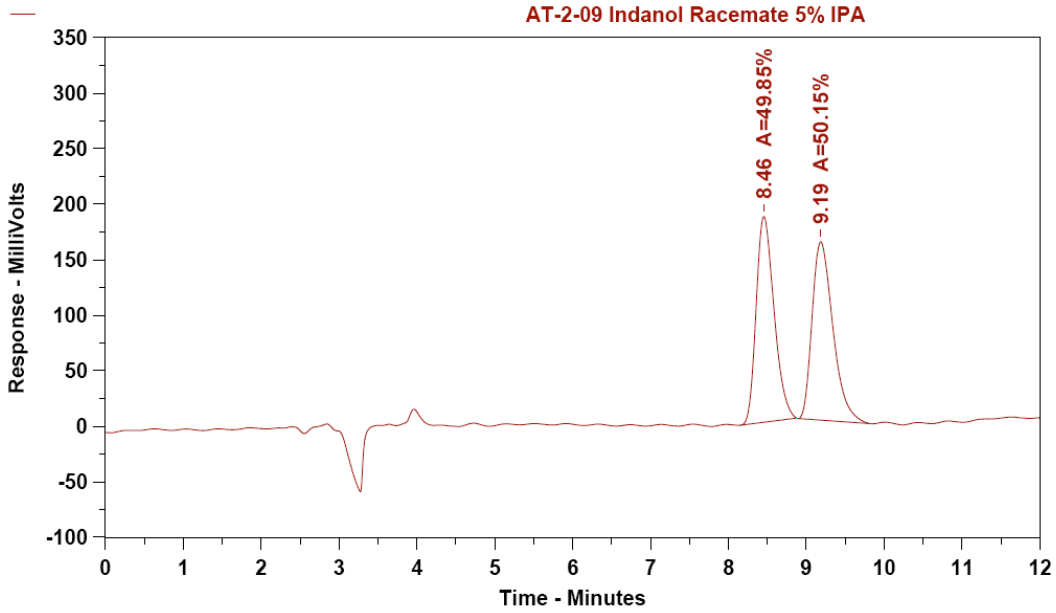


**Figure 22: Chromatogram illustrating the separation of 1-indanol enantiomers by NP-HPLC**
Method 1: 5% IPA/*n*-heptane isocratic separation of (*S*)-1-indanol and (*R*)-1-indanol at 8.46 and 9.19 min, respectively with the detection set at 254 nm

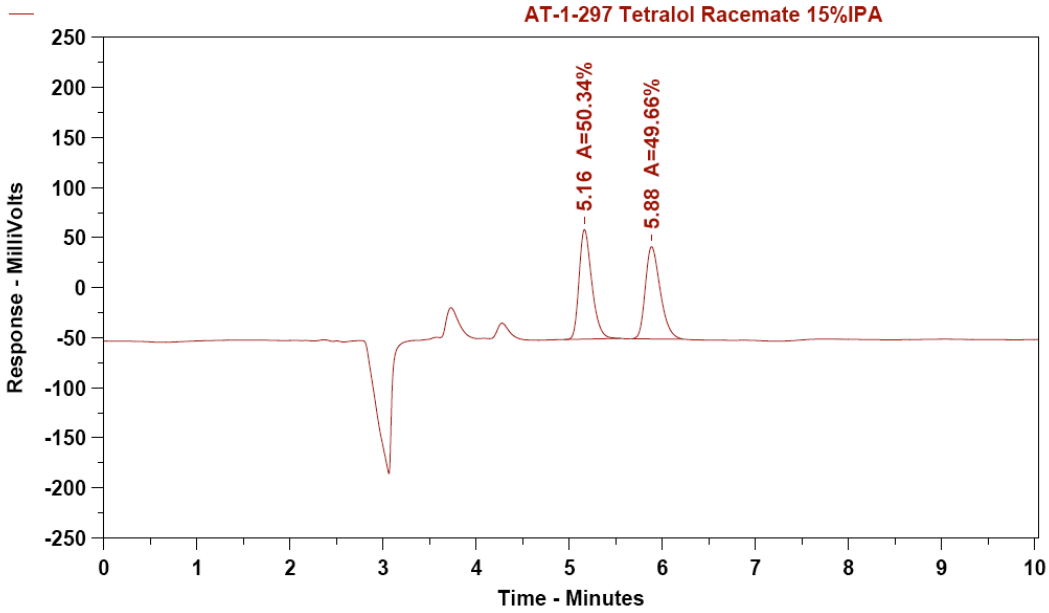


**Figure 23: Chromatogram illustrating the separation of 1-tetralol enantiomers by NP-HPLC**
Method 2: 15% IPA/n-heptane isocratic separation of (*S*)- 1-tetralol, (*R*)-1-tetralol at 5.16 and 5.88 min, respectively, with the detection set at 254 nm.

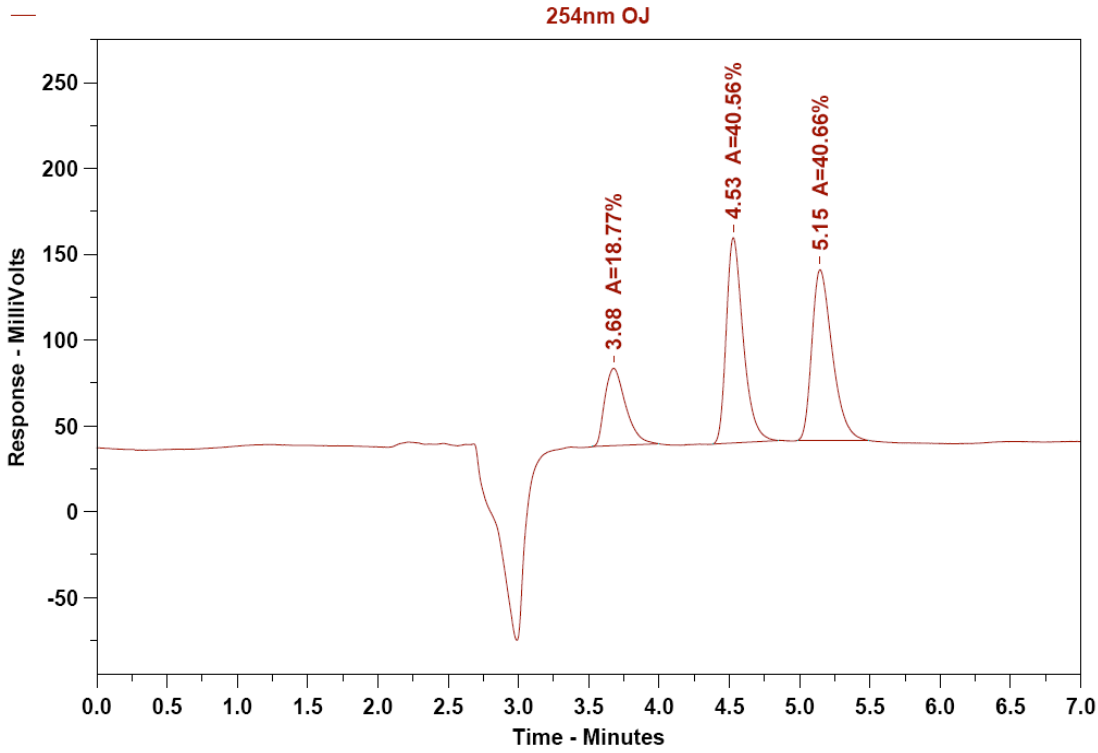


**Figure 24: Chromatogram illustrating the separation of 1-benzosuberol enantiomers by NP-HPLC** Method 3: 25% IPA/*n*-heptane isocratic separation of (*S*)-1-benzosuberol and (*R*)-1-benzosuberol at 4.53 and 5.15 min, respectively, with the detection set at 254 nm

- Prodrug aqueous stability

Reagents for prodrug stability included hydrochloric acid (Fisher Scientific, Pittsburgh, PA), sodium chloride, 2-(*N*-morpholino)ethanesulfonic acid (MES), tris(hydroxymethyl)aminomethane (Tris) (Sigma-Aldrich, St. Louis, MO). Meropenem and prodrugs (**X-X**) (100 µM) were incubated at 37 °C in simulated gastric fluid (pH 1.2)[35] 100 mM MES pH 6.0, and 100 mM Tris, pH 7.4. In duplicate, samples (980 µL) were pre-incubated for 2 min at 37 °C followed by the addition of 20 µL of a 5.0 mM DMSO stock solution of meropenem or prodrug. The final incubation volume was 1.0 mL and aliquots (100 µL) were removed from the incubation solution at 0, 5, 10, 15, 30,

45, 60, and 120 min, and immediately injected (85 μL) onto the HPLC. Stability was determined by calculating the half-life of the parent compound or the percentage of prodrug remaining after the final incubation time.

- Prodrug plasma stability

The stability of selected prodrugs was investigated in Dunkin Hartley female pooled guinea pig plasma (BioChemed, Winchester, VA). In duplicate, plasma (1.0 mL) was pre-incubated for 2 min at 37 °C followed by the addition of 20 μL of a 5.0 mM stock solution of prodrug. Aliquots (100 μL) were withdrawn at 0, 2.5, 5,10, 15, and 30 min and immediately quenched with an equal volume of acetonitrile to precipitate the proteins. The samples were filtered through nylon 0.2 μM spin filters (Chrom Tech, Inc., Apple Valley, Minnesota) and 100 μL of the filtrate was injected onto the HPLC. The stability of the prodrugs was determined by calculating the half-lives of the parent compounds.

- Animal Studies

Double jugular vein catheterized female guinea pigs weighing 400 – 500 g (Charles River Laboratories, Wilmington, MA) were utilized for the meropenem prodrug bioavailability investigations. The animals were allowed to acclimate for 24 hours and were maintained under controlled temperature and humidity while having unlimited access to food and water in a pathogen free storage facility. All catheters were maintained by following the

Vascular Catheterizations: Handling Instructions provided by Charles River Laboratories. The Institutional Animal Care and Use Committee (IACUC) of the University of Minnesota approved all animal procedures.

- Drug formulation and administration

Intravenous doses of meropenem (50 mg/kg) were prepared in USP grade sterile water for injection (Phoenix, St. Joseph, MO) and 0.5 mL of the solution was administered into the left catheter of the guinea pig over a period of 30 seconds via a tuberculin syringe with a 22 gauge blunted needle. Subsequently, 0.2 mL of sterile USP 0.9% sodium chloride (Baxter, Deerfield, IL) was infused into the catheter followed by 40 – 50 μL of a heparin (500 units/mL) / dextrose catheter lock solution (SAI Infusion Technologies). Oral doses of prodrugs (100 mg/kg) were prepared in 100 mM sodium phosphate, pH 6.0 solution containing 50% hydroxypropyl beta-cyclodextrin (Cerestar, Hammond, In) and 1.0 mL of the formulation was administered to the guinea pig via the following procedure. The guinea pig's neck was gently cradled between the thumb and index finger of the left hand while the dosing syringe was placed in the back left side of the guinea pig's mouth with the right hand. The formulation was slowly dispensed from the syringe over a period of 30 second to 1 minute and the noticeable swallowing felt by the left hand indicated a successful drug administration. Also, guinea pigs may chew on the syringe while it's in their mouth, also indicative of animal swallowing.

- Sample collection

Following the IV bolus dose of Meropenem (50 mg/kg), 0.5 mL of blood was removed from the right catheter of the animal via a tuberculin syringe with a 22 gauge blunted needle at 5, 10, 15, 30, 45, 60, 90, and 120 min. Following the oral dose of prodrug (100 mg/kg), 0.5 mL of blood was removed from the right catheter of the animal via a tuberculin syringe with a 22 gauge blunted needle at 15, 30, 45, 60,90,120, 240, and 360 min. Blood was immediately transferred to a vacutainer containing 3 mg of sodium fluoride (esterase inhibitor) and 6 mg of disodium EDTA (Becton Dickinson, Franklin Lakes, NJ). The blood was transferred to a 0.5 mL tubes and spun at 2,000*g* for 5 minutes in a microcentrifuge (Eppendorf, Enfield, CT) to separate the plasma from the hematocrit. Subsequently, 100 µL of plasma were added to 100 µL of MES buffer, pH 6.0 containing 2 mM Bis-(4-nitrophenyl) phosphate (Sigma Aldrich, St. Louis, MO) as an esterase inhibitor. The samples were then stored at -80 until sample further analysis.

- Sample preparation

To the 200 µL sample were added 200 µL of acetonitrile containing acetaminophen (100 µM) as the internal standard. The sample was vortexed for ten seconds and subsequently transferred to a 0.2 µM micro-spin filter (Chrom Tech, Inc., Apple Valley, MN) and spun at 13,000*g* for 5 min to remove the precipitated proteins. The filtrates were then evaporated on a Savant SpeedVac Concentrator (Thermo Scientific, Asheville, NC). The residues were reconstituted in 100 µL of 100 mM MES pH 6.0 and subjected to HPLC analysis.

- Standard Preparation

A 4.0 mM stock solution of meropenem trihydrate was prepared in 100 mM MES, pH 6.0 and serially diluted to 7.8 μM. Standard solutions (400, 200, 100, 50, 25, 12.5, 6.25, 3.13, 1.56, and 0.78 μM) were prepared by spiking 100 μL of blank guinea pig plasma with 10 μL of the appropriate diluted stock solution. After precipitating the proteins with 200 μL of acetonitrile containing the acetaminophen internal standard, the samples were prepared as previously described.

- Pharmacokinetic calculations

Pharmacokinetic analysis of the meropenem concentrations were calculated by a non compartmental analysis with the WinNonLin software (PharSight, St. Louis , MO). AUC values were determined by the trapezoidal rule with estimation of the terminal phase area by dividing the concentration of the last time point by the elimination rate constant ($k_e$). The bioavailability (F) was determined by the following equation: $F = AUC_{oral}*Dose_{IV}/AUC_{IV}*Dose_{oral}$. Elimination half-life ($t_{1/2}$,) clearance (Cl), and volume of distribution ($V_d$) were calculated by the following equations: $t_{1/2} = (\ln 2 / k_e)$ where $k_e$ = fractional rate of elimination, $Cl = Dose / AUC_{iv}$, $V_d = Dose / C_0$ where $C_0$ is the concentration at time 0, $Cl/F = Dose/AUC_{p.o.}$

## IV. Results

- Chemistry

The synthesis of meropenem proxetil (**2**) was completed by reacting meropenem (**1**) with 1.1 equivalents of freshly prepared 1-iodethyl isopropyl carbonate[36] and 4 equivalents of $Cs_2CO_3$ in DMF at 0 °C for 30 minutes (**Scheme 1**). Under these conditions, a total conversion of 98% was observed via HPLC analysis. Interestingly, the use of 1-8 equivalents of sodium or potassium carbonate as inorganic bases did not produce the product at an acceptable conversion rate (41-72%) compared with 4 equivalents of $Cs_2CO_3$ (**Table 3**). The purification of (**2**) from the reaction mixture was achieved by evaporating the DMF at 25 °C followed by immediate silica gel purification with 10% methanol/DCM and 1% $NH_4OH$ as the mobile phase.

**Scheme 1: Synthesis of meropenem proxetil**

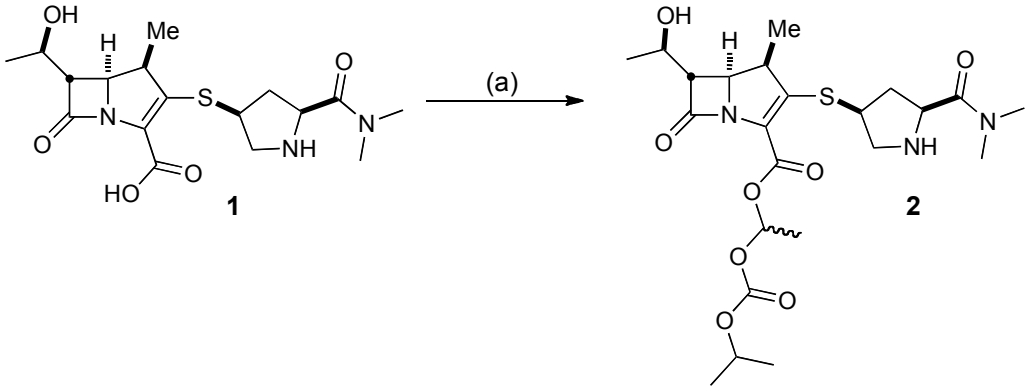


Reaction conditions: (a) 1-Iodoethyl isopropyl carbonate,[16] $Cs_2CO_3$, DMF, 0 °C, 30 min, 64%

**Table 3: Investigation of inorganic bases for the alkylation of meropenem with 1-iodoethyl isopropyl carbonate**

| Base | Equivalents | Reaction time (min) | % Conversion HPLC |
|---|---|---|---|
| $K_2CO_3$ | 1 | 120 | 41 |
| | 2 | 120 | 51 |
| | 4 | 45 | 62 |
| | 8 | 45 | 72 |
| $Na_2CO_3$ | 4 | 60 | 67 |
| $Cs_2CO_3$ | 2 | 60 | 81 |
| | 4 | 30 | 98 |

The synthesis of (*R*)/(*S*) 1-indanyl, 1-tetralyl, and benzosuberyloxycarbonyloxymethyl meropenem prodrugs are outlined in **Scheme 2**. Initially, ketones **3-5** were enantioselectively reduced to the corresponding alcohols with the (*R*) or (*S*) Corey-Bakshi-Shibata (CBS) catalyst and borane dimethylsulfide as the reducing agent.[37] Subsequently, the alcohols were acylated with chloromethyl carbonate in excellent yields to produce the 1-indanyl, 1-tetralyl, and 1-benzosuberyl chloromethyl carbonates **9-11**. Next, the iodo derivatives were synthesized via a halogen-exchange Finklestein reaction in excellent yields as well. Finally, the carboxylate of meropenem was successfully

alkylated with 2.3 equivalents of the corresponding iodomethyl or iodoethyl carbonate compound and 4 equivalents of $Cs_2CO_3$ in DMF at 0 °C resulting in a 90- 95% conversion in 30 minutes. The reaction mixture was evaporated and subsequently purified by the aforementioned procedure to afford pure prodrugs **17-22** as white foams in moderate to excellent yields.

**Scheme 2: Synthesis of 1-indanyl, 1-tetralyl, and 1-benzosuberyloxycarbonyloxymethyl prodrugs**

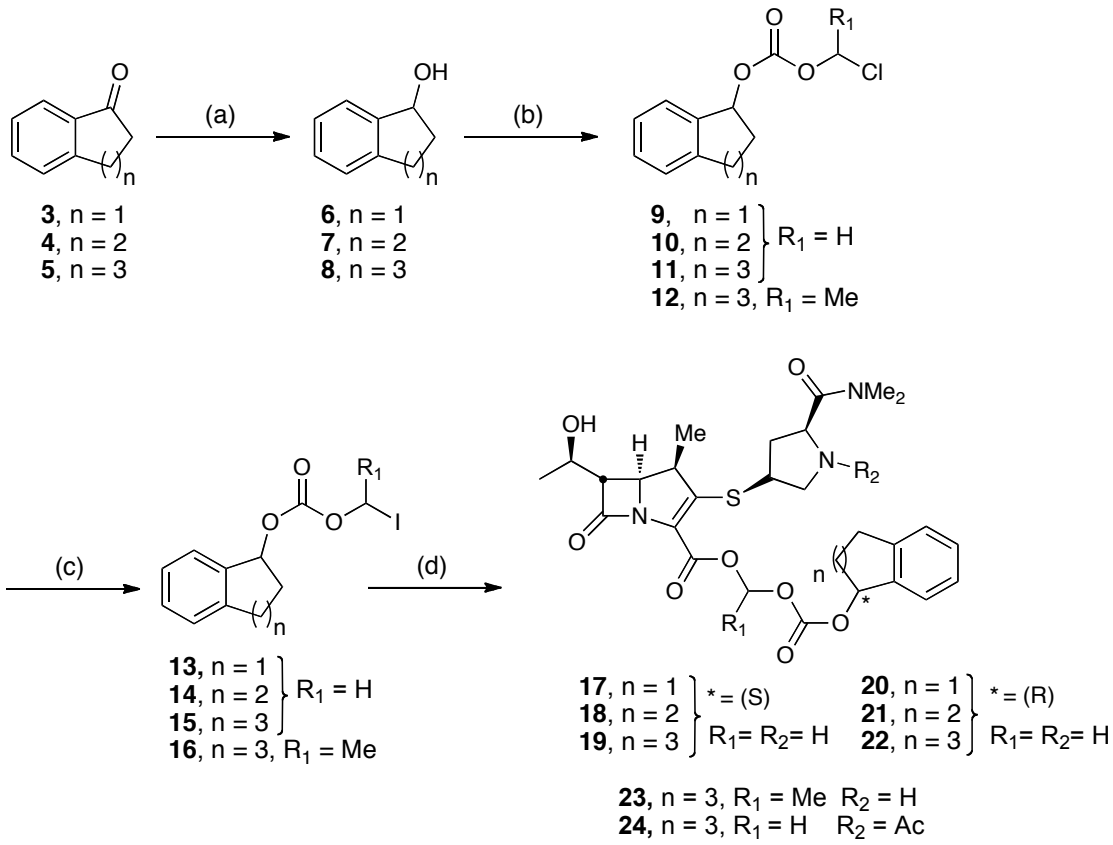


Reaction conditions: (a) (±)-CBS, $BH_3$•$SMe_3$, THF, 0 °C – rt, quant. yield; (b) for **12**: $ClCO_2CH(CH_3)Cl$, pyridine, DCM, rt, 30 min, 85%; for **9-11**: $ClCO_2CH_2Cl$, pyridine, DCM, rt, 30 min, 76-98%; (c) NaI, acetone, 40 °C, 5 hrs, 25% (**16**) 70-95% (**13-15**); (d) for **17-23**: **1**, $Cs_2CO_3$, DMF, 0 °C, 30 min, 57 - 84%; for **24**: *i*) $Ac_2O$, **1**, DMF, 0 °C, 15 min; *ii*) then add **16,** 30 min, 0 °C, 62%

The synthesis of (*R*) or (*S*) 2-indanyl, 2-tetralyl, and 2-benzosuberyloxycarbonyloxy meropenem prodrugs (**37-40**) are presented in **Scheme 3**. 2-benzosuberone (**27)** was synthesized in three steps from 1-tetralone (**26**) by following established procedures described elsewhere.[38, 39] The enantioselective reduction of 2-benzosuberone and 2-tetralone to corresponding (*R*) and (*S*) alcohols was attempted with the (*R*) or (*S*) CBS catalyst and borane dimethyl sulfide as the reducing agent by the aforementioned procedure.[37] Interestingly, no enantioselectivity was identified by chiral HPLC for the reduction of 2-benzosuberone as only the racemic alcohol was produced. Similarly, the enantioselective ratio for 2-tetralone was only 7:3. The difference in enantioselectivity between the 1 and 2-ketones may be attributed to the difference in their respective aryl ketone substituent sizes.[37] Since 2-indanone (**25**) is an achiral molecule, no enantioselective reduction is required and a simple $NaBH_4$ reduction in MeOH afforded the corresponding achiral alcohol **28**. The synthesis of the chloromethyl and iodomethyl carbonate intermediates, and subsequent final prodrug molecules were achieved as previously reported in **Scheme 1**. The benzyl ester derivative (**42**) was synthesized by a protection/deprotection strategy because iodobenzene was too reactive for a single step alkylation. (**Scheme 4**)

**Scheme 3: Synthesis of 2-indanyl, 2-tetrayl, and 2-benzosuberyloxycarbonyloxymethyl prodrugs**

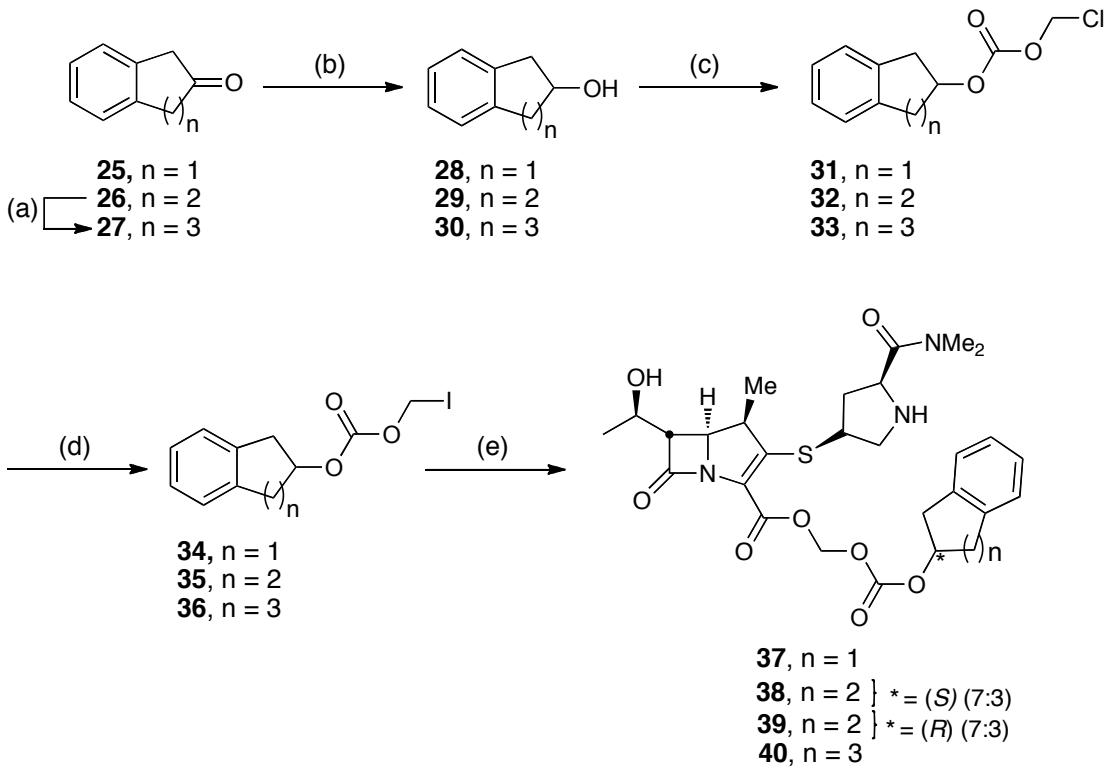


Reaction Conditions: (a) Ref 38-39; (b) for **25**: $NaBH_4$ MeOH, rt, 97%; for **26-27**: CBS, $BH_3$•$SMe_3$, THF, 0 °C – rt, 68 – 89%; (c) $ClCO_2CH_2Cl$, pyridine, DCM, rt, 30 min, 70-94%; (d) NaI, acetone, 40 °C, 5 hrs, 62-70%; (e) **1**, $Cs_2CO_3$, DMF, 0 °C, 30 min, 68 - 84%

**Scheme 4: Synthesis of meropenem benzyl ester**

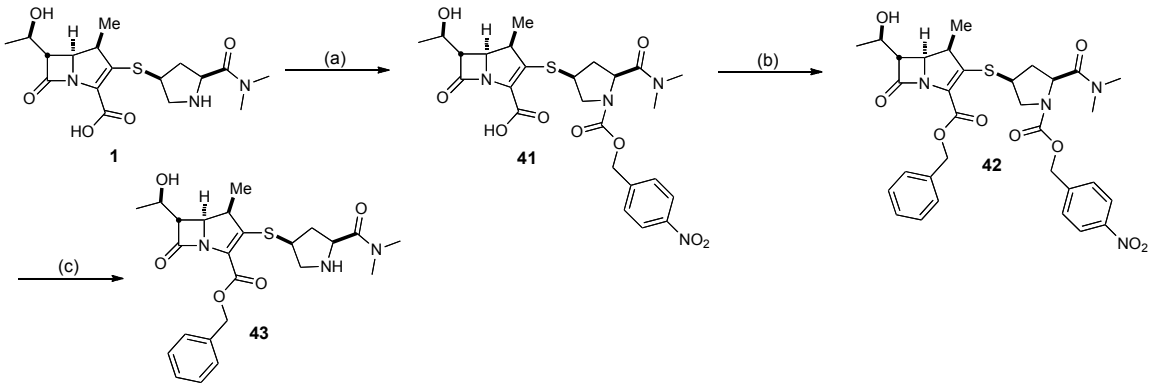


Reaction Conditions: (a) *i*) *p*-nitrobenzyl chloroformate, $NaHCO_3$, THF/$H_2O$, 0 °C, 20 min;(b) Benzyl iodide, DMF, 30 min, rt, 63%; (b) $Na_2S_2O_4$, MeCN/EtOH/$H_2O$ (1:1:1), rt, 10 min, 22%

- Prodrug aqueous stability

We initially evaluated the aqueous stability of our first synthesized prodrug, meropenem proxetil (**2).** At physiological pH 7.4, only 9 and 11% of each diastereomer was hydrolyzed to **(1)** in a period of 2 hours. At intestinal pH 6.0, there was also not any significant degradation. In simulated gastric fluid (pH 1.2), the half-life of each diasteromer was 9.2 and 7.2 minutes. To our surprise, the major degradation product was identified to be the β-lactam ring-opened metabolite with the proxetil promoiety still intact.

The aqueous stability of the 1-bicyclo series of meropenem prodrugs was subsequently investigated. Interestingly, the stability of prodrugs (**17-22)** decreased as the ring size decreased at both physiological and intestinal pH. The major degradation product identified was the expected parent compound meropenem as well as the corresponding alcohol. A representative example of prodrug degradation, meropenem and bicyclic alcohol formation is shown with compound (**19)** in **Scheme 5**. To improve

the stability of the 1-benzosuberol prodrugs, we hypothesized that the addition of a methyl group at the original methylene position (analogous to the proxetil ester) would reduce the hydrolysis rate. Interestingly, the prodrug with the additional methyl (**23**) improved the stability about 2-fold at physiological and intestinal pH; however, this modification also results in the addition of a stereocenter in the prodrug. It was also postulated that the secondary nitrogen in the pyrrolidine ring may intramolecularly attack the electrophilic carbonate or carboxyl group of the promoiety resulting in the hydrolysis of the promoiety. Consequently, the N-acetylated derivative (**24**) was synthesized; however, there was no significant change in the hydrolysis rate (**Table 4**). To fully understand the mechanism of hydrolysis, (**19**) was incubated at 37 °C for 4 hours in 25 mM HEPES, pH 7.4 and the solution was subsequently evaporated to dryness. The residue was dissolved in n-heptane and injected onto a normal phase HPLC column with the conditions described in Chiral HPLC method 3. To our surprise, the racemic alcohol was identified demonstrating that hydrolysis takes place via a $S_N1$ solvolysis mechanism (**Scheme 5**) and not via attack on the carbonate or carboxylate functional groups. In simulated gastric fluid, pH 1.2, the stability of the (*S*) and (R)-1-benzsoberyl series was 9.6 min and 10.4 min, respectively.

As a result of the poor aqueous stability of the 1-series of bicyclic prodrugs, we synthesized an additional series starting from the 2-ketones in an effort to avoid the benzylic position. Prodrugs (**37-40**) had remarkable stability at physiological and intestinal pH compared with the 1-series due to their inability to form benzylic cations in aqueous solution. Additionally, stability was investigated in simulated gastric fluid to

determine the rate of hydrolysis in the stomach. In each case, the major degradation product identified was the ring-opened metabolite with the promoiety still intact, similar to what was observed with meropenem proxetil (**2**).

**Table 4: Aqueous stability of meropenem and prodrugs at pH 7.4, 6.0, and 1.2**

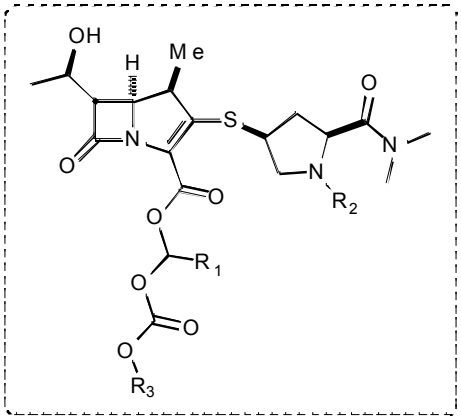


| Compound | HEPES pH 7.4 | MES pH 6.0 | SGF pH 1.2 |
|---|---|---|---|
| $R_1$=$R_2$=H $R_3$ = *i*-Pr (**2**) | 91[a] | 94[a] | 7.2 |
| $R_1$=$R_2$=H $R_3$ = *i*-Pr (**2**) | 89[a] | 92[a] | 9.1 |
| $R_1$=$R_2$=H $R_3$ = (*S*)-1-benzosuberyl (**19**) | 69 | 34 | 9.6 |
| $R_1$=$R_2$=H $R_3$ = (*R*)-1-benzosuberyl (**22**) | 69 | 37 | 10.4 |
| $R_1$=Me $R_2$=H $R_3$= (*S*)-1-benzosuberyl (**23**) | 139 | n.d | n.d |
| $R_1$=Me $R_2$=H $R_3$= (*S*)-1-benzosuberyl (**23**) | 173 | n.d | n.d |
| $R_1$=H $R_2$=Ac $R_3$= (*S*)-1-benzosuberyl (**24**) | 58 | n.d | n.d |
| $R_1$=$R_2$=H $R_3$ = (*S*)-1-tetralyl (**18**) | 1.4 | 0.92 | n.d |
| $R_1$=$R_2$=H $R_3$ = (*R*)-1-tetralyl (**21**) | 1.5 | 0.98 | n.d |
| $R_1$=$R_2$=H $R_3$ = (*S*)-1-indanyl (**17**) | <1 | n.d | n.d |
| $R_1$=$R_2$=H $R_3$ = (*R*)-1-indanyl (**20**) | <1 | n.d | n.d |
| $R_1$=$R_2$=H $R_3$ = 2-benzosuberyl (**40**) | 80[a] | 96[a] | 19.8 |
| $R_1$=$R_2$=H $R_3$ = 2-tetralyl (**38**) | 78[a] | 94[a] | 14.1 |
| $R_1$=$R_2$=H $R_3$ = 2-indanyl (**37**) | 70[a] | 95[a] | 13.1 |
| Benzyl ester (**42**) | 95[a] | 92[a] | 10.3 |

The hydrolysis of the prodrugs followed first-order degradation kinetics and the fractional rate of degradation (*k*) was determined by plotting the log of prodrug peak area vs. time. Half-lives (min) were determined by dividing the natural log of 2 by *k* (fractional rate of hydrolysis). If a half-life was unable to be calculated, the % of prodrug remaining after a120 min incubation is reported.[a] n.d = not don

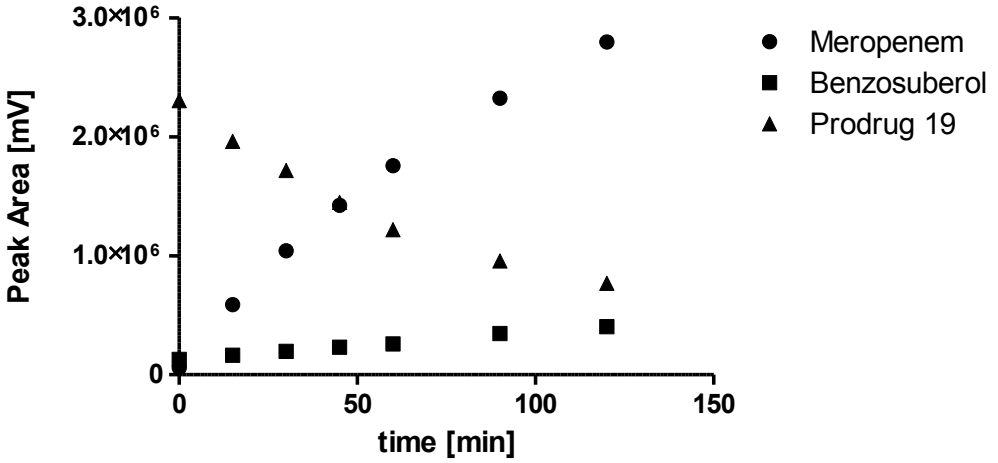


**Figure 25: Aqueous Stability of Prodrug 19, (*S*)-1-Benzosuberyloxycarbonyloxymethyl meropenemate at pH 7.4**

**Scheme 5: Proposed mechanism for the (*S*)-1-Benzosuberyloxycarbonyloxymethyl meropenemate hydrolysis**

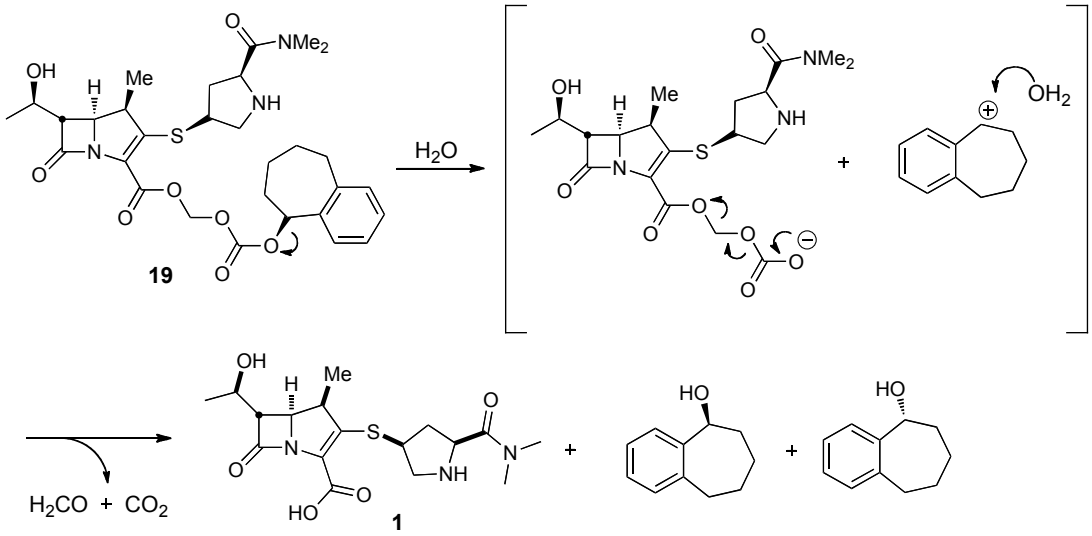


A proposed chemical mechanism illustrated the formation of racemic products from an $S_N1$ solvolysis reaction with **19.**

- Prodrug stability in guinea pig plasma

The prodrugs with the longest stability in aqueous solution at physiological and intestinal pH were further investigated for their stability in guinea pig plasma. The diastereomers of meropenem proxetil (**2**) had significantly different plasma stabilities, 6.48 and 1.48 min, and can be attributed to their different specificities for carboxylesterases as previously described for the proxetil and axetil promoieties.[40] The half-lives of compounds **2**, **19**, **22**, **37**, **39**, and **40** were calculated to be from 0.88 – 1.9, indicating poor plasma stability. Interestingly, the simple benzyl ester derivative survived the longest in the guinea pig plasma compared with the other prodrugs.

**Table 5: Stability of meropenem and selected prodrugs in guinea pig plasma**

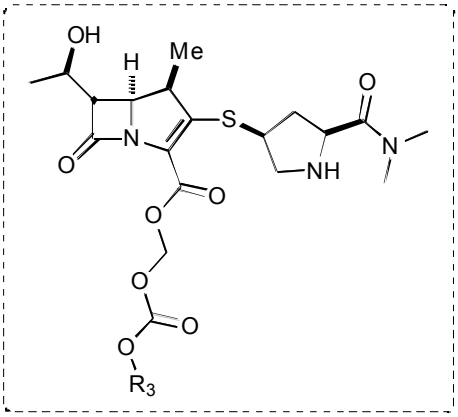


| **Compound** | $t_{1/2}$ (min) |
|---|---|
| $R_3$ = *i*-Pr (Diastereomer 1) (**2**) | 6.5 |
| $R_3$ = *i*-Pr (Diastereomer 2) (**2**) | 1.4 |
| $R_3$ = (*S*)-1-benzosuberyl (**19**) | 1.3 |
| $R_3$ = (*R*)-1-benzosuberyl (**22**) | 0.88 |
| $R_3$ = 2-benzosuberyl (**40**) | 1.9 |
| $R_3$ = 2-tetralyl (**38**) | 1.7 |
| $R_3$ = 2-indanyl (**37**) | 0.99 |
| Benzyl ester (**43**) | 8.7 |

- Bioavailability experiments in guinea pigs

Initially, the pharmacokinetics of meropenem in double jugular vein catheterized guinea pigs were investigated following a 50 mg/kg iv bolus dose. As expected, meropenem was rapidly eliminated from the plasma and presumably excreted into the urine as the parent drug or ring-opened metabolite. Subsequently, the proxetil ester of meropenem (**2**) as well as the most non-polar prodrugs (**19, 22, 40**) were orally dosed to guinea pigs in an effort to determine the relative bioavailability for meropenem after dosing of the prodrug. The calculated pharmacokinetic parameters and representative plasma vs. concentration time profiles are described below.

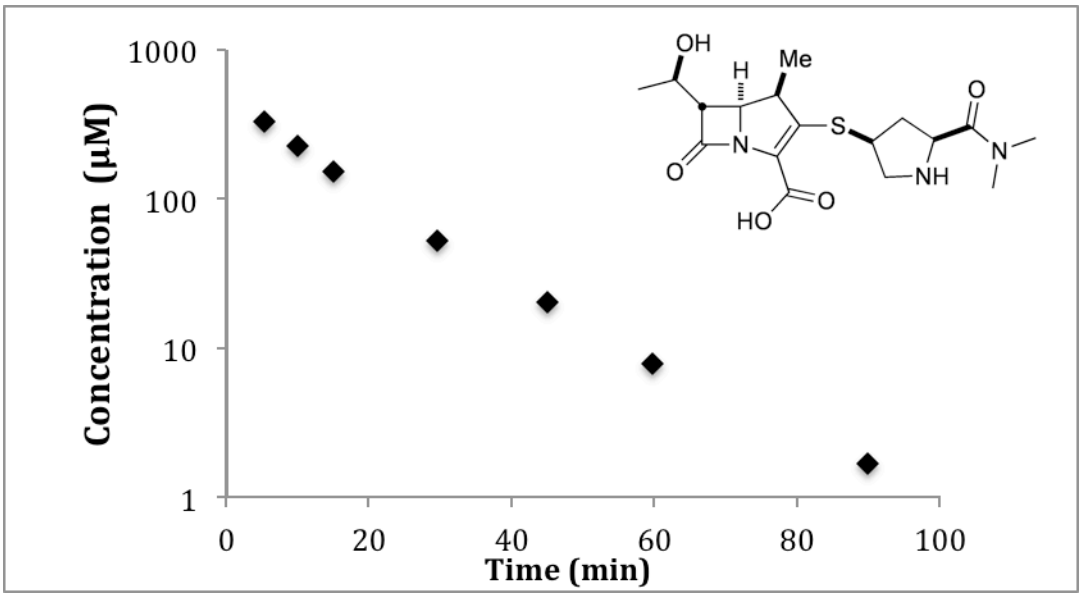


**Figure 26: Concentration vs. time profile for guinea pig G following an IV bolus dose (50 mg/kg) of meropenem trihydrate**

| Guinea Pig ("Miss") | Body Weight (g) | Dose (mg/kg) | $C_0$ (µM) | $t_{1/2}$ (min) | Volume (mL/kg) | Clearance mL/min/kg | $AUC_{0-\infty}$ (min*µmol/L) |
|---|---|---|---|---|---|---|---|
| B | 491.4 | 51.9 | 370 | 11.00 | 209 | 13.1 | 4429.8 |
| C | 448.3 | 52.6 | 497 | 11.04 | 125 | 7.8 | 6895.0 |
| D | 496.0 | 57.3 | 651 | 11.35 | 117 | 7.1 | 9097.4 |
| E | 457.6 | 58.2 | 569 | 11.30 | 130 | 7.9 | 7647.9 |
| F | 414.8 | 50.8 | 383 | 12.7 | 222 | 12.1 | 3974.1 |
| G | 417.2 | 50.8 | 417 | 12.93 | 163 | 8.7 | 5440.9 |
| H | 446.2 | 50.5 | 283 | 8.4 | 156 | 12.8 | 4001.6 |
| I | 467.1 | 50.5 | 418 | 7.8 | 156 | 13.9 | 3871.1 |
| AVG | 454.8 | 52.8 | 448 | 10.8 | 160 | 10.4 | 5669.7 |
| S.D. | 30.1 | 3.1 | 118.2 | 1.8 | 38.3 | 2.8 | 1987.3 |

**Table 6: Pharmacokinetic parameters following an IV bolus dose (50 mg/kg) of meropenem trihydrate**

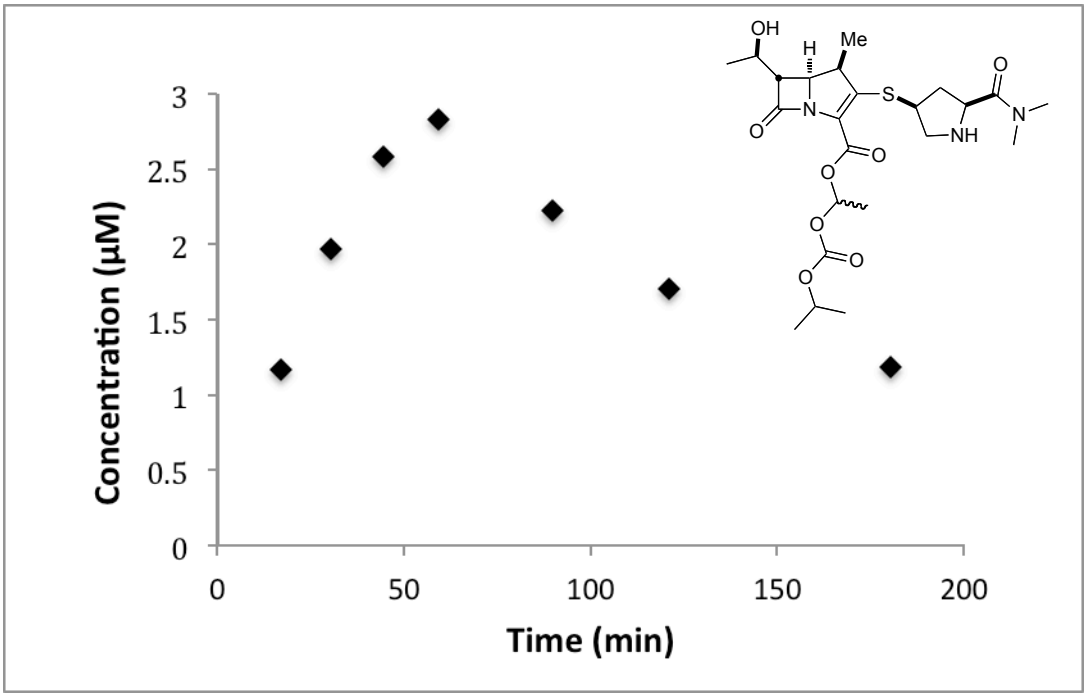


**Figure 27: Concentration vs. time profile for guinea pig D following an oral dose (100 mg/kg) of compound 2, diastereomeric meropenem proxetil**

| Guinea Pig ("Miss") | Dose (mg/kg) | $C_{max}$ (µM) | $T_{max}$ (min) | $AUC_{0-\infty}$ (min*µmol/L) | Bioavailability |
|---|---|---|---|---|---|
| B | 107.5 | 1.5 | 60.4 | 321 | 3.5% |
| C | 114.7 | 1.52 | 45.5 | 103 | 0.7% |
| D | 114 | 2.8 | 59.2 | 510 | 2.8% |
| E | 108 | 1.45 | 45.6 | 59 | 0.4% |
| AVG | 111.1 | 1.8 | 52.7 | 248 | 1.9% |
| S.D. | 3.8 | 0.66 | 8.2 | 209 | 1.5% |

**Table 7: Pharmacokinetic paramters following an oral dose (100 mg/kg) of meropenem proxetil**

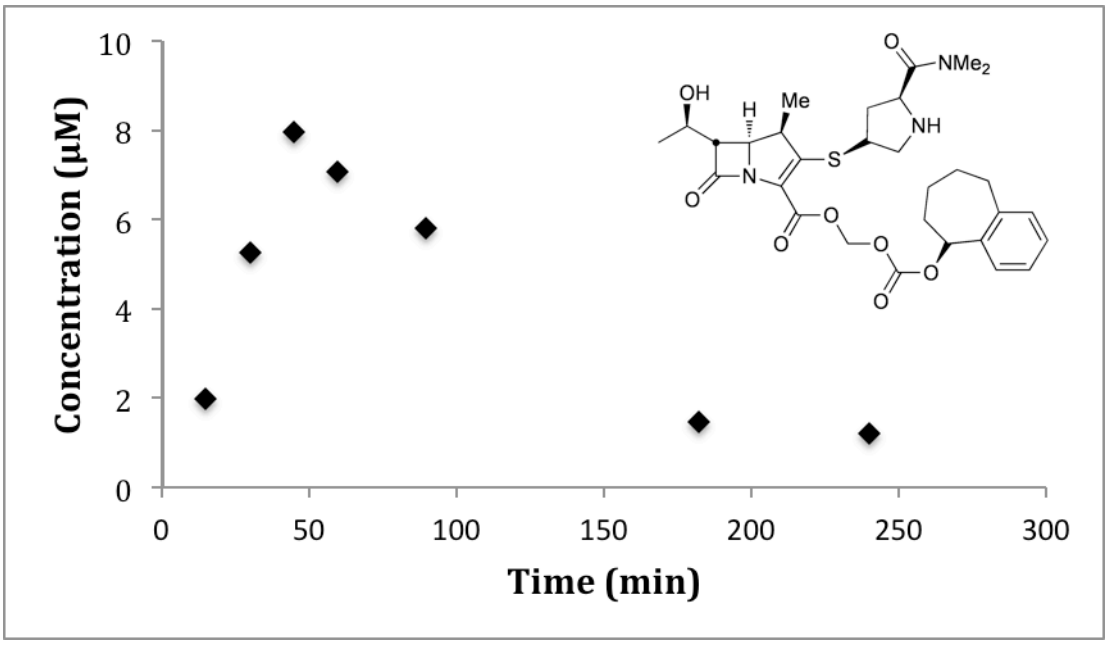


**Figure 28: Concentration vs. time profile for guinea pig B following an oral dose (100 mg/kg) of compound 19, (*S*)-1-benzosuberyloxycarbonyloxymethyl meropenemate**

| Guinea Pig ("Miss") | Dose (mg/kg) | $C_{max}$ (µM) | $T_{max}$ (min) | $AUC_{0-\infty}$ (min*µmol/L) | Bioavailability |
|---|---|---|---|---|---|
| B | 119 | 7.9 | 45.0 | 998 | 9.8 % |
| F | 120 | 4.95 | 44.5 | 554 | 5.9 % |
| F* | 110 | 3.5 | 91.1 | 598 | 3.3 % |
| F*§ | 103 | 14.6 | 60.1 | 1157 | 6.8 % |
| G | 116 | 3.7 | 59.2 | 628 | 5.1 % |
| AVG | 114 | 6.9 | 60.0 | 787.0 | 6.2 % |
| S.D. | 7 | 4.6 | 19 | 272 | 2.4 % |

**Table 8: Pharmacokinetic parameters following an oral dose (100 mg/kg) of compound 19, (*S*)-1-benzosuberyloxycarbonyloxymethyl meropenemate**

* Indicates a dosing of 5 mg/kg lanzoprazole the night prior and two hours before dosing compound **19**

§ Indicates 2% SDS as the dosing vehicle

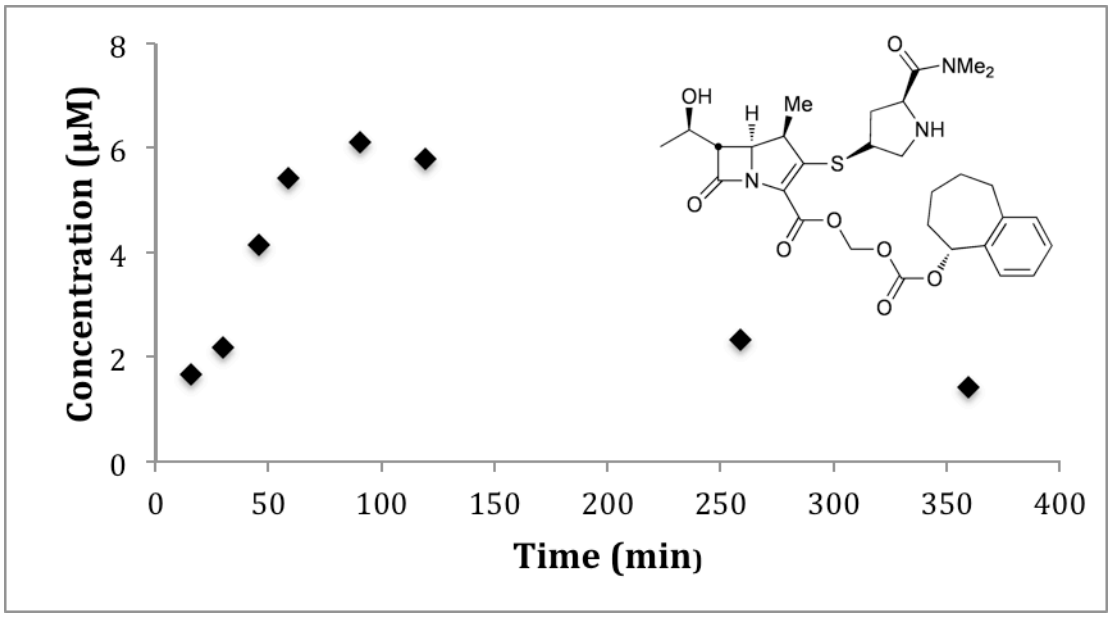


**Figure 29: Concentration vs. time profile for guinea pig C following an oral dose (100 mg/kg) of compound 22, (*R*)-1-Benzosuberyloxycarbonyloxymethyl meropenemate**

| Guinea Pig ("Miss") | Dose (mg/kg) | $C_{max}$ (µM) | $T_{max}$ (min) | $AUC_{0-\infty}$ (min*µmol/L) | Bioavailability |
|---|---|---|---|---|---|
| **B** | 105 | 2.6 | 29 | 155 | 1.7 % |
| **C** | 120 | 6.1 | 90 | 1559 | 9.9 % |
| **D** | 129 | 3.1 | 88 | 294 | 1.4 % |
| **AVG** | 118 | 3.9 | 69 | 670 | 4.4 % |
| **S.D.** | 12.1 | 1.9 | 35 | 774 | 4.8 % |

**Table 9: Pharmacokinetic parameters following an oral dose (100 mg/kg) of compound 22, (*R*)-1-benzosuberyloxycarbonyloxymethyl meropenemate**

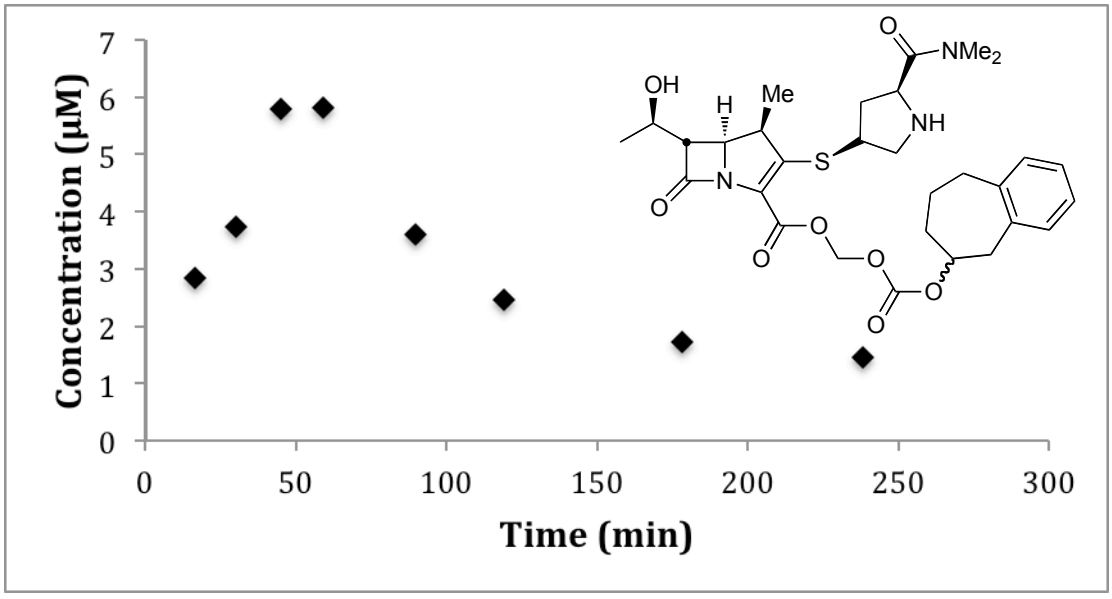


**Figure 30: Concentration vs. time profile for guinea pig D following an oral dose (100 mg/kg) of compound 40, 2-Benzosuberyloxycarbonyloxymethyl meropenemate**

| Guinea Pig ("Miss") | Dose (mg/kg) | $C_{max}$ (µM) | $T_{max}$ (min) | $AUC_{0-\infty}$ (min*µmol/L) | Bioavailability |
|---|---|---|---|---|---|
| D | 114 | 5.5 | 29.7 | 1234 | 6.8 % |
| D | 118 | 5.8 | 45.2 | 935 | 5.0 % |
| **AVG** | 116 | 5.7 | 37.4 | 1084 | 5.9 % |
| **S.D** | 3 | 0.2 | 10.9 | 211 | 1.3 % |

**Table 10: Pharmacokinetic parameters following an oral dose (100 mg/kg) of compund 40, 2-Benzosuberyloxycarbonyloxymethyl meropenemate**

## V. Discussion

Several alkyloxycarbonyloxy prodrugs of meropenem **(1)** were successfully synthesized in an effort to improve the lipophilicity and oral absorption of the parent carbapenem. The alkyloxycarbonyloxy promoieties were chosen as a result of the early studies conducted with simple alkyl esters of penicillin G. Richardson et al.[41] initially described the large species-dependent differences regarding the hydrolysis of the simple methyl and benzyl esters of penicillin G. Ultimately, it was discovered that of the species tested, only mice and rats had the ability to cleave the ester whereas dogs, rabbits, and monkeys showed no parent penicillin in the plasma. A follow up study conducted two years later in 1947 concluded that the plasma of humans and rabbits do not contain a "penicillin esterase or penicillinase" which actually is present in the plasma of mice, rats, and guinea pigs.[42] Over the next several years, the idea of "double ester" (alklyoxycarbonyloxy) promoiteies gave rise to several β-lactam prodrugs, which could be given orally and release the parent antibiotic in the systemic circulation in a variety of species, including humans. The general idea of the "double ester" was pioneered by Jansen and Russel[43] and has ultimately led to the development of current FDA approved oral β-lactams, which include: cefpodoxime proxetil, cefuroxime axetil, and cefditoren pivoxil.

The initial approach to improving the oral bioavailability of meropenem was to synthesize the isopropoxycarbonyloxymethyl (proxetil) ester of meropenem. The original synthesis of this molecule involved the protection of the pyrrolidine nitrogen with *p*-nitrobenzyl chloroformate, followed by carboxylate alkylation with 1-iodoethyl

isopropyl carbonate, and subsequent deprotection of the protecting group by hydrogenolysis or by addition of sodium dithionite in aqueous solution. However, despite multiple attempts of HPLC purification and recrystallization, the product could not be purely isolated or was isolated in poor yields due to degradation or dimerization in aqueous solvents. The idea of direct alklylation (**Scheme 1**) came from Tanaka et al. in which they synthesized the pivoxil ester of meropenem in one step by reacting pivaloyloxymethyl iodide with meropenem and 1.1 equivalents of $K_2CO_3$ in DMF at 4 °C.[23] Following purification by reversed phase flash chromatography and recrystallization, the yield reported was only 23%. The same procedure was exactly repeated except 1-iodoethyl isopropyl carbonate was used at the alkylating agent and the reaction was monitored by a developed HPLC method. Interestingly, 41% conversion was obtained in 60 and 120 minutes and perhaps explains the low yield reported by Tanaka and co-workers.[23] The conversion was subsequently optimized by changing the base to $Cs_2CO_3$. We hypothesize that the $Cs_2CO_3$ less efficiently coordinates with the carboxylate of meropenem compared with the other inorganic bases due to the relatively large size of the cesium atom and thus causes increased nucleophilicity of the carboxylate. Also under these conditions, the pyrrolidine nitrogen is not deprotonated and therefore not nucleophilic enough to attack the iodide reagent. Additionally, a standard purification procedure was developed by normal phase flash chromatography and a solvent system consisting of DCM/MeOH and 1% $NH_4OH$, which yielded beautiful white foams of high purity following evaporation under reduced pressure. Triethylamine was initially utilized to enhance the movement of the product on silica gel; however, the

product became an oily orange residue following purification and the triethylamine was difficult to remove. The same purification strategy was utilized to purify all the synthesized prodrugs with >95% purity without the need of laborious and time-consuming HPLC purification or recrystallization. $^{1}$H NMR, $^{13}$C NMR, and high-resolution time of flight (TOF) mass spectrometry (MS) spectra were obtained on all final compounds. $^{1}$H NMR and $^{13}$C NMR spectra were obtained for all intermediates. (See experimental section)

The aqueous stability of prodrugs **2**, **17-24**, and **37-41** at biologically relevant pH 1.2 (stomach), 6.0 (intestinal), and 7.4 (blood) at 37 °C is reported in **Table 4**. The most stable prodrug at pH 7.4 and 6.0 was the proxetil ester of meropenem (**2**). The prodrugs containing the 1-benzosuberyl, 1-tetralyl, and 1-indanyl promoieties **(17-24)** were all unstable in aqueous solution and resulted in the formation of a racemic alcohol indicative of a $S_N1$ solvolysis mechanism (**Scheme 5)**. The observation of faster hydrolysis occurring as the ring size decrease was an interesting and unexpected observation. The explanation for this phenomenon is still elusive; however, Dr. Dean Tantillo at UC Davis was gracious enough to run some computational calculations regarding benzylic cation stability (personal communication to Dr. Courtney Aldrich). He found that the benzosuberyl cation is less delocalized than the tetralyl cation which in turn is less delocalized than the indanyl cation. The results of the calculation provide evidence that it may be more difficult and less favorable to form the benzosuberyl cation and is perhaps why the 1-benzosuberyloxycarbonyloxymethyl prodrug is the most stable in aqueous solution.

The prodrugs containing the 2-benzosuberyl, 2-tetralyl, and 2-indanyl promoieties (**37-41**) were significantly more stable at physiological pH 7.4 and intestinal pH 6.0 as a result of carbonate attachment at the 2-poistion. In simulated gastric fluid (pH 1.2), all prodrugs degraded quickly and formed the ring-opened parent molecule with the prodrug still intact. The result of this experiment was surprising because one would expect the promoiety to be more labile than the β-lactam ring. In a recent study by Saito et al., the stability of meropenem (carbapenem), cefotaxime (cephalosporin), ceftibuten (cephalosporin), and faropenem (penem) were investigated in simulated gastric fluid, pH 1.2 without enzymes.[44] It was found that meropenem had the shortest half-life compared with the other β-lactams showing 80% degradation in about 30 min. The amount of meropenem, cefotaxime, ceftibuten, and faropenem remaining after incubating for 60 min in simulated gastric fluid was 5, 65, 94, and 70%, respectively. Although the reason for the instability of meropenem was not discussed, it is hypothesized the instability stems from the increased torsional ring strain from the unsaturated double bond within the carbapenem nucleus, thus making carbapenems more unstable compared with other types of β-lactams.

The plasma stability of the most aqueous stable prodrugs was very short implying a rapid release of the parent compounds. Interestingly, the simple benzyl ester derivative had the longest stability in plasma compared to all the other prodrugs. It is a reasonable assumption that steric bulk from the benzyl group slows esterase hydrolysis in guinea pig plasma as described previously. It would be interesting to determine whether human plasma esterases are able to cleave the benzyl prodrug as efficiently as the guinea pig

plasma esterase. From the results of the plasma stability experiments, it is likely that esterases located in both the intestine and liver will cleave the promoieties as efficiently as the plasma esterases, which will prevent oral absorption of the prodrugs.

Bioavailability experiments were conducted with the proxetil ester of meropenem (**2**) as well as the more lipophilic prodrugs **(19, 22, and 40)** in jugular vein catheterized guinea pigs. Guinea pigs were utilized in the bioavailability experiments due to their susceptibility to infection by *Mtb* as well as having similar lung pathology to the human disease.[45-47] In four animals receiving 100 mg/kg of **2**, the bioavailability was calculated to be 2%, indicating poor absorption into the systemic circulation. Despite a significant increase in cLogP, (0.36 for **2**, and 2.5 for **19, 22**, and **40**) the more lipophilic compounds investigated also had relatively poor bioavailability (4-6%) following similar oral doses. The results of this study clearly indicate there is not a direct correlation between bioavailability and the lipophilicity of the prodrugs. The explanation for this finding is mainly due to the stability of the prodrugs within the gastrointestinal tract of the animal. The low pH in the stomach of the guinea pig most likely is cleaving the β-lactam ring before absorption into the intestine can occur. Additionally, if the prodrug happens to avoid degradation in the stomach and actually get absorbed, there is a high likelihood that intestinal esterases will cleave the promoieity releasing meropenem within the enterocyte. In this case, meropenem may be effluxed out of the enterocyte into the intestinal lumen[44] or will remain within the enterocyte due to its natural hydrophilicity . In an attempt to increase the stomach pH before dosing, guinea pigs were treated with 5 mg/kg of a lanzoprazole suspension the night before and two hours prior to the start of the

experiment. There was no significant increase in the calculated bioavailability most likely because the lanzoprazole treatment was not long enough to have a dramatic effect on the stomach pH.

Tanaka et al.[23] reported the bioavailabilities (27 - 29.5%) in rats of bis prodrugs of meropenem with a pivoxil ester attached to the carboxylate and several different alkyloxycarbonloxy groups carbamates attached to the pyrrolidine nitrogen given in a 2% SDS micellular solution. Initially, the simple pivoxil ester prodrug was studied and the bioavailability in the rat was reported to be 19.8%. The differences in bioavailabilities reported in this thesis compared with the results by Tanaka are confounding. One reason for their higher bioavailability may be due to the dosing formulation used, which was 2% SDS. The SDS surfactant can form a micelle around the prodrug and facilitate absorption and protection from the low pH environment. Another reason may be due to the rapid absorption of the lipophilic prodrugs i.e the rate of absorption is faster than the rate of degradation in the stomach. However, when 2% SDS was formulated with compound **19**, no significant increase in bioavailability was achieved compared to the standard buffer/hydroxypropyl-β-cyclodextrin formulation, although the $T_{max}$ was shorter with this formulation.

## VI. Conclusions and Future Directions

Overall, the work presented in chapter 2 of this thesis describes the facile synthesis of meropenem prodrugs with increased lipophilicity. The results of the aqueous and plasma stability experiments highlight the instability of the prodrugs. Caution should be exercised regarding the choice of promoiety to ensure the stability of the prodrug is acceptable for future *in vitro* and *in vivo* investigations. Bioavailability experiments in the guinea pig with select prodrugs did not show improved absorption of meropenem despite prodrugs having cLogP values of 2.5. Prodrug instability within the gastrointestinal tract of the animal leading to incomplete absorption is the likely reason for the reported low bioavailability.

The results of this work have ultimately laid the foundation for the development of an orally bioavailable prodrug of meropenem and several issues from this work remain to be addressed. First and foremost, the carbapenem instability in an acidic environment raises the question if prodrugs are actually the ideal method for delivery of meropenem if the parent molecule is unstable in the stomach. A method to circumvent this issue is to deliver the prodrug in an enteric-coated capsule, with the idea of prodrug release within the intestine. Dr. Raj Suryanarayanan, a professor in the pharmaceutics department at the University of Minnesota, has agreed to collaborate and offer his expertise in designing a pharmaceutics approach to improving the bioavailability of meropenem. Small capsules for delivery to laboratory animals can be purchased from Torpac, Inc and the enteric coating formulation is available from Eudragit® products. Experiments such as determining the kinetics of prodrug release from an enteric-coated capsule at intestinal pH will provide useful information for the intial development of this dosing strategy.

Additionally, it would be interesting to determine the stability of the prodrugs **2, 19, 22, 40, 38, 37, and 42** in the plasma of multiple species. The previous work regarding the species differences in the hydrolysis of the benzyl and methyl esters of penicillin may also apply to meropenem prodrugs and further stability studies are warranted. The benzyl ester of meropenem was the most stable in guinea pig plasma (**Table 5**), and perhaps simple sterically bulky esters may be hydrolyzed more slowly compared to the alkyloxycarbonyloxy promoietes. Simple amide and carbamate prodrugs may also have some utility as they will most likely not be hydrolyzed as quickly as the previously synthesized prodrugs. In accordance with Tanaka et al, the development of bis prodrugs of meropenem may improve the overall absorption. Some hypothesized prodrug structures are shown below:

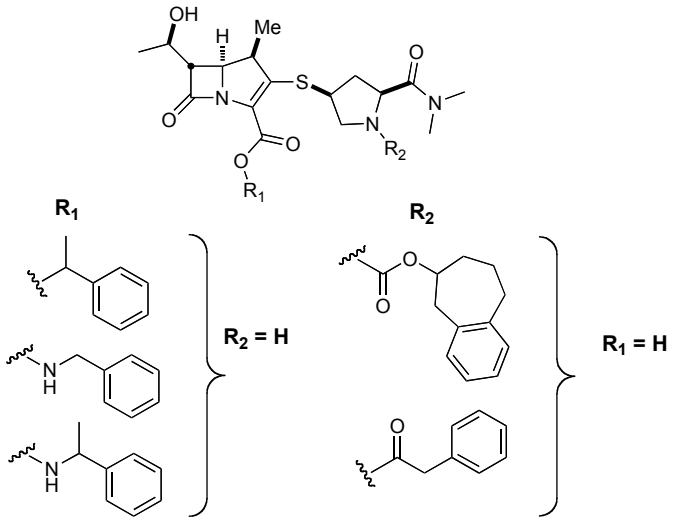


**Figure 31: Proposed structures of new meropenem prodrugs**

In each case, stability and permeability experiments in MDCK or Caco-2 cell systems must be investigated to ascertain a generally understanding of prodrug disposition in the gastrointestinal environment before any bioavailability experiments are undertaken.

## VII. Experimentals

General procedure (**A**) for the enatioselective reduction of ketones (**3-5**)

To a solution of (*R*)-(+)-2-methyl-CBS-oxazaborolidine or (*S*)-(–)-2-methyl-CBS-oxazaborolidine (0.2 equiv) in THF (1 mL/0.21 mmol ketone) at 0 °C was added a 2.0 M solution of borane dimethyl sulfide in THF (1.2 equiv). The mixture was stirred for 15 min, then a solution of ketone (3-5) (1.0 equiv) in THF (1 mL/0.21 mmol ketone) was cannulated dropwise into the reaction mixture. After stirring for 30 min, the reaction was quenched by the addition of MeOH (1 mL/0.75 mmol of $BH_3$•$SMe_2$), then concentrated under reduced pressure to afford colorless oils which solidified overnight at –20 °C. The (*R*)-CBS reagent produced the (*S*)-alcohols (**6-8a**) and the (*S*)-CBS produced the (*R*)-alcohols (**6-8b**).

General procedure (**B**) for the synthesis of chloromethyl carbonates (**9-11**)

To a solution of alcohols (**3-5**) (1.0 equiv) in $CH_2Cl_2$ (0.1 M) at rt was added pyridine (2 equiv.) and the reaction was stirred for 15 min. Next, chloromethyl chloroformate (2.0 equiv) was added drop-wise and the resulting solution was stirred for 30 min at rt. The reaction mixture was washed consecutively with $H_2O$, 1 N aqueous HCl, and saturated aqueous NaCl. The organic layer was dried ($MgSO_4$), filtered, and concentrated under reduced pressure to afford the crude product, which was taken on to the next step without any further purification due to instability on silica gel.

General procedure (**C**) for the synthesis of iodomethylcarbonates (**13-15**)

To a solution of chloromethylcarbonates (**9-12**) (1.0 equiv) and 4Å molecular sieves (0.5 g) in acetone (0.2 M) was added sodium iodide (3.0 equiv). The solution was stirred for 5 hrs in a dark environment at 40 °C. Subsequently, the reaction mixture was filtered and evaporated under reduced pressure to yield a solid orange precipitate, which immediately was dissolved in $Et_2O$ and washed consecutively with 10% $Na_2SO_3$, $dH_2O$, and saturated aqueous NaCl. The organic layer was dried over $MgSO_4$ and concentrated under reduced pressure to afford the crude product. Purification was not required due to the instability of the molecules.

General procedure (**D**) for the synthesis of meropenem prodrugs (**17-24, 37-40**)

A solution of meropenem (100 mg, 1.0 equiv.) and $Cs_2CO_3$ (367 mg, 1.04 mmols 4.0 equiv.) in DMF (1.3 mL) was stirred at 0 °C for 10 minutes. Next, iodomethylcarbonate (**13-15**) (0.6 mmols, 2.3 equiv) was dissolved in DMF (1.3) mL and added dropwise to the reaction mixture. After stirring for 20 min at 0 °C, the reaction mixture was subsequently evaporated to dryness under high pressure. Purification by flash chromatography (10% MeOH-DCM 1% $NH_4OH$) afforded the title compound as white foams.

**(*S*)-1-Indanol (6a).** Synthesized from 1-indanone (1.00 g, 7.57 mmol, 1.0 equiv) by general procedure **A.** Purification by flash chromatography (10% EtOAc–hexanes) afforded the title compound (1.01 g, quant. yield); er = 99:1 (Chiral HPLC, method 1); Analytical data including previously reported values.[ref]

**(*R*)-1-Indanol (6b).** This compound was prepared similarly to (*S*)-1-indanol except (*S*)-(+)-2-methyl-CBS-oxazaborolidine was utilized at the enanatioselective catalyst and afforded the title compound (1.01 g, quant. yield): er = 99:1 (Chiral HPLC, method 1). Analytical data including matched previously reported values.

**(*S*)-1-Tetralol (7a).** Synthesized from 1-tetralone (1.00 g, 6.84 mmol, 1.0 equiv) using general procedure **A.** Purification by flash chromatography (10% EtOAc–hexanes) afforded the title compound (1.12 g, quant. yield); er = 99:1(Chiral HPLC, method 2); Analytical data matched previously reported values.

**(*R*)-1-Tetralol (7b).** This compounds was prepared analogously to (*S*)-1-tetralol, but (*S*)-(+)-2-methyl-CBS oxazaborolidine was employed as the enatioselective catalyst and afforded the title compound (1.02 g, quant. yield) as white/yellow solid: er = 98:2 (Chiral HPLC, method 2). Analytical data matched previously reported values.

**(*S*)-1-Benzosuberol (8a).** Synthesized from 1-benzosuberone (1.00 g, 6.24 mmol, 1.0 equiv) using general procedure A. Purification by flash chromatography (10% EtOAc–hexanes) afforded the title compound (974 mg, 96% yield) as a white solid; er = 98:2 (Chiral HPLC, method 3); Analytical data matched previously reported values.

**(*R*)-1-Benzosuberol (8b).** This compound was prepared analogously to (*S*)-1-benzosuberol, but using (*S*)-(–)-2-methyl-CBS-oxazaborolidine to afford the title compound (1.02 g, 99% yield) as a white solid; er = 99:1 (Chiral HPLC, method 3). Analytical data matched previously reported values.

**2-Indanol (28).** To a solution of 2-indanone (1.0 g, 7.5 mmol, 1.0 equiv.) in MeOH (150 mL) was added $NaBH_4$ (500 mg, 12.21 mmol, 1.7 equiv) portion wise. The reaction was complete within 10 min as evidenced by a spot-to-spot conversion by TLC $R_f$ 0.26 (20% EtOAc-Hexanes 1% Formic Acid). Subsequently, the reaction mixture was diluted with $dH_2O$ (75 mL) and extracted twice $Et_2O$ (100 mL). The organic layer was dried over $MgSO_4$, filtered, and concentrated under reduced pressure to afford the crude product as a brown solid in quantitative yield. The product was utilized in the following step without further purification. Analytical data matched previously reported values.

**(*S*)-2-Tetralol (29a).** Synthesized from 2-tetralone (1.00 g, 6.84 mmol, 1.0 equiv) using general procedure **A.** (1.0g quant. yield); Purification by flash chromatography (20% EtOAc–hexanes) afforded the title compound (1.0g, quant. yield) a colorless oil. $R_f$ 0.12 (20% EtOAc–hexanes); er = 7:3 Chiral HPLC, method 2). $^1$H NMR (600 MHz, $CDCl_3$): δ (ppm) = 1.61 (m, 1H), 1.83 (dtd, *J* = 12.5, 9.3, 5.9 Hz, 1H), 2.07 (m, 1H), 2.78 (dd, *J* = 16.1, 7.9 Hz, 1H), 2.85 (ddd, *J* = 16.2, 9.6, 6.6 Hz, 1H), 2.96 (dt, *J* = 16.8, 6.0 Hz, 1H), 3.10 (dd, *J* = 16.1, 5.0 Hz, 1H), 4.17 (m, 1H), 7.10 (m, 4H); $^{13}$C NMR (150 MHz, $CDCl_3$): δ (ppm) = 27.0, 31.5, 38.4, 67.2, 125.9, 126.0, 128.6, 129.5, 134.2, 135.6; HRMS (APCI+) calcd for $C_{10}H_{12}O$ $[M - OH]^+$ 131.0855, found 131.0857 (error 1.5 ppm).

**(*S*)-2-Tetralol (29b).** This compound was prepared identically to **29a** except (*S*)-(–)-2-methyl-CBS-oxazaborolidine was used to afford the desired compound (1.02 g, 99% yield) as a white solid; er = 7:13 (Chiral HPLC, method 2).

**2-Benzosuberol (30).** Synthesized from 2-benzosuberone by general procedure **A.** Purification by flash chromatography (20% EtOAc–Hexanes) afforded the title compound as a colorless oil (97 mg, 89%) which solidified overnight; $R_f$ 0.42 (20% EtOAc–Hexanes); er = 1:1 (Chiral HPLC, method 3). $^1$H NMR (600 MHz, $CDCl_3$): δ (ppm) = 1.56 (m, 1H), 1.88 (m, 2H), 2.08 (s, 1H), 2.13 (m, 1H), 2.78 (m, 1H), 2.80 (m, 1H), 3.01 (d, *J* = 13.2 Hz, 1H), 3.09 (dd, *J* = 13.2, 9.0 Hz, 1H), 3.82 (t, *J* = 7.9 Hz, 1H), 7.12 (dd, *J* = 9.6, 4.2 Hz, 1H), 7.16 (t, *J* = 4.4 Hz, 2H), 7.19 (dd, *J* = 8.4, 4.2 Hz, 1H); $^{13}$C NMR (150 MHz, $CDCl_3$): δ (ppm) = 24.4, 35.5, 40.6, 44.7, 69.3, 126.2, 126.6, 128.8,

130.5, 136.5, 143.4; HRMS (APCI+) calcd for $C_{11}H_{14}O$ [M - OH]$^+$ 145.1012, found 145.1013 (error 0.7 ppm).

**(*S*)-1-Indanol chloromethylcarbonate (9a).** Synthesized from (*S*)-1-indanol (998 mg, 7.43 mmol, 1.0 equiv) according to general procedure **B** and afforded a yellow oil (1.6 g, 98% yield), which was directly taken onto the next step without further purification due to instability on silica gel. $R_f$ 0.77 (20% EtOAc–Hexanes)

**(*R*)-1-Indanyl chloromethylcarbonate (9b).** This compound was prepared identically to (*S*)-1-indanol chloromethyl carbonate; however, (*R*)-1-indanol was the initial substrate and afforded the title compound as a yellow oil (1.6 g, 97% yield).

**(*S*)-1-Tetralyl chloromethylcarbonate (10a).** Synthesized from (*S*)-1-tetralol (1.12g, 7.6 mmol, 1.0 equiv) according to general procedure **B.** Purification by flash chromatography (1% EtOAc–hexanes) afforded the title compound (1.68 g, 92%) as a yellow oil. $R_f$ = 0.58 (20% EtOAc–hexanes); $^1$H NMR (600 MHz, $CDCl_3$) δ 1.82–1.89 (m, 1H), 1.96–2.07 (m, 2H), 2.14–2.20 (m, 1H), 2.73–2.79 (m, 1H), 2.85–2.91 (m, 1H), 5.74 (d, $J$ = 6.0 Hz, 1H), 5.77 (d, $J$ = 6.0 Hz, 1H), 5.92 (s, 1H), 7.14 (d, $J$ = 6.6 Hz, 1H), 7.18–7.20 (m, 1H), 7.24–7.29 (m, 1H), 7.36 (d, $J$ = 7.8 Hz, 1H) $^{13}$C NMR (150 MHZ, $CDCl_3$) δ 18.3, 28.7, 28.8, 72.2, 75.8, 126.2, 128.7, 129.2, 129.7, 132.9, 137.9, 153.2.

**(*R*)-1-Tetralyl chloromethylcarbonate (10b).** This compound was prepared similarly to (*S)*-1-tetralol chloromethylcarbonate, but (*R*)-1-tetralol was used and afforded the title compound (1.4 g, 94% yield) as a yellow oil.

**(*S*)-1-Benzosuberyl chloromethylcarbonate (11a).** Synthesized from (*S*)-1-benzosuberol (973 mg, 6.0 mmol, 1.0 equiv) according to general procedure **B**. Purification by flash chromatography (1% EtOAc–hexanes) afforded the title compound (1.40 g, 94% yield) as a colorless oil: $R_f$ = 0.14 (1% EtOAc–hexanes); $^1$H NMR (600 MHz, $CDCl_3$)δ(ppm) = 1.62–1.77 (m, 2H), 1.84–1.93 (m, 1H), 1.94–2.01 (m, 1H), 2.03–2.13 (m, 2H), 2.75 (dd, *J* = 10.2, 4.2 Hz, 1H), 3.01 (dd, *J* = 11.4, 1.8 Hz, 1H), 5.72 (d, *J* = 6.6 Hz, 1H), 5,79 (d, *J* = 6.6 Hz, 1H), 5.87 (d, *J* = 8.4 Hz, 1H), 7.14 (t, d = 6.6 Hz, 1H), 7.18–7.23 (m, 1H), 7.32 (d, *J* = 6.6 Hz, 2H) $^{13}$C NMR (150 MHZ, $CDCl_3$) δ 26.9, 27.5, 33.1, 35.6, 72.2, 81.7, 126.1 (C2), 128.1, 129.9, 138.7, 141.4, 152.7.

**(*R*)-1-Benzosuberyl chloromethylcarbonate (11b).** This compound was prepared similarly to (*S*)-1-benzosuberol chloromethylcarbonate, but (*R*)-1-benzosuberol was utilized to afford the title compound (1.2 g, 76% yield) as a colorless oil.

**(*S*)-1-Benzosuberyl chloroethylcarbonate (12).** Synthesized from (*S*)-1-benzosuberol (1.13 g, 6.99 mmol, 1.0 equiv) according to general procedure **B** except chloroethyl chloroformate was used as the alkylating agent. Purification by flash chromatography (10% EtOAc–hexanes) afforded the title compound (1.60 g, 85%) as a colorless oil: $R_f$ =

0.48 and 0.43 (diastereomers) (10% EtOAc–hexanes); $^{1}$H NMR (600 MHz, $CDCl_3$) δ(ppm) = 1.61 (m, 0.5H), 1.69 (m, 1H), 1.73 (m, 0.5 H), 1.84 (d, *J* = 5.9 Hz, 1.5H), 1.86 (d, *J* =5.9 Hz, 1.5H), 1.87 (m, 1H), 1.97 (m, 1.5H), 2.06 (m, 1.5H), 2.75 (m, 1H), 3.00 (m, 1H), 5.84 (d, *J* = 9.6 Hz, 0.5H), 5.86 (d, J = 9.6 Hz, 0.5H), 6.43 (dd, *J* = 12.0, 6.0 Hz, 0.5H), 6.47 (dd, *J* = 12.0, 6.0 Hz, 0.5H), 7.13 (m, 1H), 7.19 (m, 2H), 7.32 (m, 1H); $^{13}$C NMR (150 MHZ, $CDCl_3$) δ (ppm) = 25.0, 25.10, 25.18, 25.14, 26.8, 27.1, 27.45, 27.55, 33.0, 33.3, 35.57, 35.58, 81.2, 81.5, 84.55, 84.60, 84.7, 84.9, 126.1, 126.2, 128.0, 128.1, 129.8, 129.9, 138.8, 138.9, 152.2, 152.3.

**2-Indanyl chloromethylcarbonate (31).** Synthesized from 2-indanol (971 mg, 7.2 mmol, 1.0 equiv) according to general procdure **B**. Purification by flash chromatography (10% EtOAc/hexanes 1% Formic Acid) afforded the title compound (1.53 g, 94%) as a white solid. $R_f$ = 0.57 (10% EtOAc/hexanes, 1% Formic Acid); $^{1}$H NMR (600 MHz, $CDCl_3$)δ(ppm) = 3.14 (s, br., 1H), (3.17 (s, br., 1H), 3.37 (d, *J* = 6.6 Hz, 1H), 3.40, (d, *J* = 6.6 Hz, 1H), 5.54 (s, br., 1H), 5.74 (s, 2H), 7.21 – 7.23 (m, 2H), 7.25 – 7.28 (m, 2H); $^{13}$C NMR (150 MHZ, $CDCl_3$) δ 39.3, 39.6, 72.1, 80.5, 124.6 (2C), 126.9 (2C), 139.6, 140.8, 153.1.

**(*S*)-2-Tetralyl chloromethylcarbonate (32a).** Synthesized from (*S*)-2-tetralol (1.0 g 6.8 mmol, 1.0 equiv.) according to general procedure **B**. Purification by flash chromatography by a gradient of hexanes to 20% EtOAc in hexanes, resulting in 1.14 g (4.7 mmol, 70% over two steps) of a colorless solid. $R_f$ 0.39 (20% EtOAc–hexanes); $^{1}$H

NMR (600 MHz, $CDCl_3$): δ (ppm) = 2.06 (m, 1H), 2.14 (m, 1H), 2.87 (dt, *J* = 16.8, 7.2 Hz, 1H), 2.97 (t, *J* = 6.0 Hz, 1H), 2.99 (dd, *J* = 16.2, 6.6 Hz, 1H), 3.20 (dd, *J* = 16.7, 5.0 Hz, 1H), 5.18 (m, 1H), 5.73 (d, *J* = 6.6 Hz, 1H), 5.75 (d, *J* = 6.6 Hz, 1H), 7.08 (m, 1H), 7.11 (m, 1H), 7.15 (m, 2H); $^{13}C$ NMR (150 MHz, $CDCl_3$): δ (ppm) = 26.2, 27.6, 34.3, 72.1, 75.3, 126.1, 126.3, 128.6, 129.3, 132.7, 135.1, 152.9.

**(*R*)-2-Tetralyl chloromethylcarbonate (32b).** Synthesized from (*R*)-2-tetralol (1.0 g 6.8 mmol, 1.0 equiv.) according to general procedure **B**. Purification by flash chromatography with a gradient of hexanes to 20% EtOAc in hexanes, resulting in 1.14 g (4.7 mmol, 70% over two steps) of a colorless solid. $R_f$ 0.39 (20% EtOAc–hexanes); Analytical data identical to reported above.

**2-Benzosuberyl chloromethylcarbonate (33).** Synthesized from (*S*)-2-benzosuberol (62 mg,0.38 mmol, 1 equiv) according to general procedure **B**. The residue was filtrated over a pad of silica gel with 20% EtOAc–hexanes, resulting in 90 mg (0.35 mmol, 92%) of a colorless solid: $R_f$ 0.42 (20% EtOAc–hexanes); $^1H$ NMR (600 MHz, $CDCl_3$): δ (ppm) = 1.57 (m, 1H), 1.98 (m, 2H), 2.24 (m, 1H), 2.80 (t, *J* = 4.2 Hz, 2H), 3.07 (d, *J* = 13.5 Hz, 1H), 3.25 (dd, *J* = 13.8, 10.3 Hz, 1H), 4.76 (t, *J* = 9.4 Hz, 1H), 5.72 (s, 2H), 7.12 (d, *J* = 7.0 Hz, 1H), 7.17 (m, 3H); $^{13}C$ NMR (150 MHz, $CDCl_3$): δ (ppm) = 24.3, 35.2, 36.7, 41.0, 72.0, 77.6, 126.5, 127.1, 128.9, 130.4, 135.1, 142.9, 152.5.

**(*S*)-1-Indanyl iodomethylcarbonate (13a).** Synthesized from (*S*)-1-indanol chloromethyl carbonate (1.6 g, 7.19 mmol, 1.0 equiv.) according to general procedure **C,** which afforded the pressure to afforded the title compound as a yellow oil (1.73 g, 76% yield). $R_f$ 0.61 (hex:EtOAc 4:1); $^1$H NMR (600 MHz, $CDCl_3$): δ (ppm) = 2.25 (m, 1H), 2.51 (m, 1H), 2.89 (ddd, *J* = 16.1, 8.5, 3.5 Hz, 1H), 3.15 (m, 1H), 5.71 (d, *J* = 6.0 Hz, 1H), 5.75 (d, *J* = 6.0 Hz, 1H), 6.15 (dd, *J* = 6.7, 2.6 Hz, 1H), 7.24 (m, 1H), 7.28 (d, *J* = 7.2 Hz, 1H), 7.32 (t, *J* = 7.2 Hz, 1H), 7.49 (d, *J* = 7.6 Hz, 1H); $^{13}$C NMR (150 MHz, $CDCl_3$) δ (ppm) = 30.1, 32.1, 72.1, 83.6, 124.9, 125.8, 126.8, 129.6, 139.5, 144.7, 153.3

**(*R*)-1-Indanyl iodomethylcarbonate (13b).** This compound was prepared identically to (*S*)-1-indanol iodomethyl carbonate; however, (*R*)-1-indanol chloromethyl carbonate was the initial substrate and afforded the title compound as a yellow oil (1.72 g, 75% yield).

***(S*)-1-Tetralyl iodomethylcarbonate (14a).** Synthesized from (*S)*-1-tetralol chloromethyl carbonate (1.6 g, 6.7 mmol, 1.0 equiv.) according to general procedure **C**, which afforded the title compound as a yellow oil (1.8 g, 85% yield): $R_f$ 0.64 (hex:EtOAc 4:1); $^1$H NMR (600 MHz, $CDCl_3$) δ 1.74–1.81 (m, 1H), 1.87–1.99 (m, 2H), 2.06–2.11 (m, 1H), 2.64–2.74 (m, 1H), 2.77–2.83 (m, 1H), 5.84 (s, br., 1H), 5.87–5.91 (m, 2H), 7.06 (d, 1H, *J* = 6.6 Hz), 7.10–7.14 (m, 1H), 7.16–7.20 (m, 1H), 7.28 (d, 1H, *J* = 7.8 Hz); $^{13}$C NMR (150 MHZ, $CDCl_3$) δ 18.4, 28.7, 28.9, 34.1, 75.9, 126.2, 128.7, 129.2, 129.7, 132.9, 137.9, 153.0.

**(*R*)-1-Tetralyl iodomethylcarbonate (14b).** This compound was prepared analogously to (*S*)-1-tetralol iodomethyl carbonate, but (*R*)-1-tetralol chloromethyl carbonate was used as the initial substrate and afforded the title compound (1.5 g, 70% yield) as a yellow oil.

**(*S*)-1-Benzosuberyl iodomethylcarbonate (15a).** Synthesized from (*S*)-1-benzosuberyl chloromethylcarbonate (1.4 g, 5.5 mmol, 1.0 equiv) according to procedure **C**, which afforded the title compound as a pale yellow oil (1.8 g, 95% yield): $R_f$ 0.53 (hex:EtOAc 4:1); $^1$H NMR (600 MHz, $CDCl_3$) δ 1.62–1.77 (m, 2H), 1.84–1.92 (m, 1H), 1.94–2.01 (m, 1H), 2.02–2.12 (m, 2H), 2.72–2.79 (m, 1H), 2.97–3.04 (m, 1H), 5.86 (d, *J* = 8.4 Hz, 1H), 5.95 (d, *J* = 4.8 Hz, 1H), 5.99 (d, *J* = 4.8 Hz, 1H), 7.14 (d, *J* = 6.0 Hz, 1H), 7.17–7.24 (m, 2H), 7.31 (d, *J* = 6.0 Hz, 1H) $^{13}$C NMR (150 MHZ, $CDCl_3$) δ 26.7, 27.3, 32.9, 33.9, 35.4, 81.5, 125.9 (C2), 127.9, 129.7, 138.5, 141.1, 152.8.

***(R)*-1-Benzosuberyl iodomethylcarbonate (15b).** This compound was prepared similarly to (*S*)-1-benzosuberol iodomethylcarbonate, but (*R*)-1-benzosuberol chloromethylcarbonate was initially used to afford the title compound (1.5 g, 93% yield) as a pale yellow oil.

***(R)*-1-Benzosuberyl iodoethylcarbonate (16).** Synthesized from (*S*)-1-benzosubero chloroethylcarbonate (1.57 g, 5.84 mmol, 1.0 equiv) according to procedure **C.** This reaction only went 30% to conversion by $^{1}$HMR and the crude product was directly taken on to the next step

**2-Indanyl iodomethylcarbonate (34).** Synthesized from chloromethyl-2-indanocarbonate (1.50 g, 6.65 mmol, 1.0 equiv) according to general procedure **C**, which afforded the title compound as a white solid with a yellow hue (1.47 g, 70%). $R_f$ 0.52 (hex:EtOAc 4:1); $^{1}$H NMR (600 MHz, $CDCl_3$) δ 3.12 (s, br, 1H), 3.15 (s, br, 1H), 3.36 (d, $J$ = 6.6 Hz, 1H), 3.39 (d, $J$ = 6.6 Hz, 1H), 5.53 (s, br, 1H), 5.95 (s, 2H), 7.20 – 7.22 (m, 2H), 7.24 – 7.27 (m, 2H); ) $^{13}$C NMR (150 MHZ, $CDCl_3$) δ (ppm) = 33.9, 39.4, 80.5, 124.6, 127.0, 139.6, 152.9.

**(*S*)-2-Tetralyl iodomethylcarbonate (35a).** Synthesized from (*S*)-2-tetralol chloro methylcarbonate (1.14 g, 4.74 mmol) according to general procedure **C**, which furnished the title compound as a colorless solid (3.28 mmol, 69%). $R_f$ 0.53 (hex:EtOAc 4:1); $^{1}$H NMR (600 MHz, $CDCl_3$): δ (ppm) = 2.10 (m, 1H), 2.16 (m, 1H), 2.90 (dt, $J$ = 16.8, 7.2 Hz, 1H), 2.98 (t, $J$ = 6.6 Hz, 1H), 3.02 (dd, $J$ = 16.8, 7.8 Hz, 1H), 3.23 (dd, $J$ = 16.4, 4.7 Hz, 1H), 5.13 (m, 1H), 5.96 (d, $J$ = 4.8 Hz, 1H), 5.98 (d, $J$ = 4.8 Hz, 1H), 7.13 (m, 1H), 7.15 (m, 1H), 7.19 (m, 2H); $^{13}$C NMR (150 MHz, $CDCl_3$): δ (ppm) = 25.9, 27.3, 34.0, 34.2, 75.0, 125.8, 126.0, 128.3, 129.0, 132.4, 134.7, 152.3.

**(*R*)-2-Tetralyl iodomethylcarbonate (35b).** Synthesized from (*R*)-2-tetralol chloro methylcarbonate (1.14 g, 4.74 mmol) according to general procedure **C**, which provided the title compound as a colorless solid (3.28 mmol, 69%). $R_f$ 0.53 (hex:EtOAc 4:1);

**2-Benzosuberyl iodomethylcarbonate (36).** Synthesized from (*S*)-2-benzosuberol iodomethylcarbonate according to general procedure **C**, affording the title (0.57 g, 1.7 mmol, 77%) as a colorless solid: $R_f$ 0.55 (20% EtOAc–hexanes); $^1$H NMR (600 MHz, $CDCl_3$): δ (ppm) = 1.57 (m, 1H), 1.96 (m, 2H), 2.22 (m, 1H), 2.79 (t, *J* = 5.4 Hz, 2H), 3.05 (d, *J* = 14.1 Hz, 1H), 3.24 (dd, *J* = 14.1, 10.0 Hz, 1H), 4.75 (t, *J* = 9.4 Hz, 1H), 5.94 (s, 2H), 7.10 (d, *J* = 7.0 Hz, 1H), 7.16 (m, 3H); $^{13}$C NMR (150 MHz, $CDCl_3$): δ (ppm) = 24.3, 34.0, 35.2, 36.8, 41.0, 77.6, 126.5, 127.1, 128.9, 130.5, 135.1, 142.9, 152.3.

**Isopropoxycarbonyloxymethyl meropenemate (2).**

A solution of meropenem (100 mg, 0.26 mmols, 1.0 equiv.) and $Cs_2CO_3$ (367 mg, 1.04 mmols 4.0 equiv.) in DMF (0.5 mL) was stirred at 0 °C for 10 minutes. Next, 1-iodoethyl isopropyl carbonate[ref] (87 mg, 0.34 mmols, 1.3 equiv) was added dropwise and the reaction mixture was allowed to stir for 30 min at 0 °C. The reaction mixture was subsequently evaporated to dryness under high pressure. Purification by flash chromatography (10% MeOH-DCM 1% $NH_4OH$) afforded the title compound (75.4 mg, 64% yield) as an off-white foam: $R_f$ = 0.23 and 0.25 (10% MeOH-DCM 1% $NH_4OH$); $^1$H NMR (600 MHz, $CDCl_3$) δ (ppm) = 1.26 (d, *J* = 7.2 Hz, 3H), 1.28 (t, *J* = 5.9 Hz, 3H), 1.29 (d, *J* = 6.0 Hz, 3H), 1.32 (d, *J* = 6.0 Hz, 3H), 1.55 (dd, *J* = 13.5, 5.3 Hz, 3H), 1.60

(m, 1H), 2.44 (m, 2H), 2.60 (dt, $J$ = 13.6, 8.1 Hz, 1H), 2.95 (s, 3H), 2.99 (s, 3H), 3.06 (td, $J$ = 11.3, 4.4 Hz, 1H), 3.24 (d, $J$ = 6.5 Hz, 1H), 3.24 (m, 1H), 3.42 (m, 1H), 3.74 (m, 1H), 3.99 (m, 1H), 4.23 (m, 2H), 4.88 (dt, $J$ = 12.3, 6.2 Hz, 1H), 6.83 (ddd, $J$ = 10.8, 5.4, 2.4Hz, 1H); $^{13}$C NMR (150 MHZ, $CDCl_3$) δ (ppm) = 17.3, 17.4, 19.9, 20.0, 21.9, 21.97, 22.00, 22.04, 22.1, 36.1, 36.5, 36.6, 37.0, 43.9, 44.0, 44.56, 44.63, 56.07, 56.12, 56.59, 56.65, 58.70, 58.72, 60.41, 60.45, 66.07, 66.12, 73.28, 73.31, 91.9, 92.3, 124.9, 125.0, 152.3, 152.4, 152.9, 153.0, 159.2, 159.3, 172.0, 172.1, 173.1, 173.2; HRMS (ESI+) calcd for $C_{23}H_{35}N_3O_8S$ $[M + H]^+$ 514.2218, found 514.2219 (error 0.2 ppm).

***(S)*-1-Indanyloxycarbonyloxymethyl meropenemate (17).**

Synthesized according to general procedure **D**, which afforded the title compound (112 mg, 75% yield) as a white solid: $R_f$ = 0.19 (10% MeOH-DCM 1% $NH_4OH$); $^1$H NMR (600 MHz, $CDCl_3$) δ (ppm) = (d, $J$ = 7.0 Hz, 3H), 1.29 (d, $J$ = 5.9 Hz, 3H), 1.59 (m, 1H), 2.20 (m, 1H), 2.48 (td, $J$ = 15.0, 7.2 Hz, 1H), 2.71 (dt, $J$ = 13.2, 7.8 Hz, 1H), 2.87 (m, 1H), 2.92 (s, 3H), 2.97 (s, 3H), 3.10 (m, 2H), 3.24 (dd, $J$ = 6.6, 1.8 Hz, 1H), 3.49 (dd, $J$ = 11.4, 5.6 Hz, 1H), 3.57 (m, 1H), 3.83 (m, 1H), 4.05 (m, 2H), 4.19 (t, $J$ = 6.6 Hz, 1H), 4.27 (t, $J$ = 8.2 Hz, 1H), 4.35 (d, $J$ = 9.4 Hz, 1H), 5.79 (d, $J$ = 5.9 Hz, 1H), 5.90 (d, $J$ = 5.3 Hz, 1H), 6.11 (dd, $J$ = 6.5, 2.9 Hz, 1H), 7.21 (t, $J$ = 6.9 Hz, 1H), 7.29 (m, 2H), 7.47 (d, $J$ = 7.6 Hz, 1H);δ$^{13}$C NMR (150 MHZ, $CDCl_3$) δ (ppm) = 17.5, 22.0, 30.6, 32.5, 36.0, 36.2, 37.1, 43.2, 44.6, 55.5, 56.9, 58.5, 60.5, 66.1, 82.7, 83.7, 124.6, 125.3, 126.3, 127.2, 129.9, 140.3, 145.3, 153.2, 154.2, 159.9, 171.1, 173.5; HRMS (ESI+) calcd for $C_{28}H_{35}N_3O_8S$ $[M + H]^+$ 574.2218, found 574.2224 (error 1.0 ppm)

**(*R*)-1-Indanyloxycarbonyloxymethyl meropenemate (20).**

This compound was prepared similarly to (*S*)-1-inadnol meropenem, but (*R*)-1-indanol iodomethylcarbonate was used to afford the title compound (108mg , 72% yield) as a white foam. $R_f$ = 0.24 (10% MeOH-DCM 1% $NH_4OH$); $^1$H NMR (600 MHz, $CDCl_3$) δ (ppm) = 1.22 (d, *J* = 7.0 Hz, 3H), 1.29 (d, *J* = 5.9 Hz, 3H), 1.59 (dt, *J* = 13.8, 7.2 Hz, 1H), 2.21 (m, 1H), 2.48 (m, 1H), 2.71 (dt, *J* = 13.2, 8.1 Hz, 1H), 2.85 (m, 1H), 2.91 (s, 3H), 2.97 (s, 3H), 3.09 (m, 2H), 3.23 (dd, *J* = 6.0, 2.4 Hz, 1H), 3.46 (dd, *J* = 11.4, 5.6 Hz, 1H), 3.56 (m, 1H), 3.82 (m, 1H), 3.98 (m, 2H), 4.19 (m, 1H), 4.25 (t, *J* = 8.2 Hz, 1H), 4.34 (dd, *J* = 9.1, 1.5 Hz, 1H), 5.82 (d, *J* = 5.9 Hz, 1H), 5.88 (d, *J* = 5.9 Hz, 1H), 6.10 (dd, *J* = 6.5, 2.9 Hz, 1H), 7.21 (t, *J* = 6.9 Hz, 1H), 7.28 (m, 2H), 7.46 (d, *J* = 7.6 Hz, 1H); $\delta^{13}$C NMR (150 MHZ, $CDCl_3$) δ (ppm) = 17.4, 22.0, 30.6, 32.6, 36.1, 36.2, 37.1, 43.3, 44.6, 55.6, 56.9, 58.5, 60.5, 66.1, 82.7, 83.7, 124.6, 125.4, 126.2, 127.2, 129.9, 140.3, 145.4, 153.3, 154.2, 159.9, 171.2, 173.5; HRMS (ESI+) calcd for $C_{28}H_{35}N_3O_8S$ $[M + H]^+$ 574.2218, found 574.2221 (error 0.5 ppm).

***(S)*-1-Tetralyloxycarbonyloxymethyl meropenemate (18).**

Synthesized according to general procedure **D**, which afforded the title compound (87 mg, 57% yield) as a white solid: $R_f$ = 0.35 (10% MeOH-DCM 1% $NH_4OH$); $^1$H NMR (600 MHz, $CDCl_3$) δ (ppm) = 1.24 (d, *J* = 7.6 Hz, 3H), 1.27 (d, *J* = 6.5 Hz, 3H), 1.54 (dt, *J* = 13.6, 7.0 Hz, 1H), 1.80 (m, 1H), 1.93 (m, 1H), 2.01 (td, *J* = 11.4, 2.4 Hz, 1H), 2.13 (m, 1H), 2.58 (dt, *J* = 13.8, 8.4 Hz, 1H), 2.72 (ddd, *J* = 16.8, 9.0, 6.0 Hz, 1H), 2.84 (m, 1H), 2.92 (s, 3H), 2.96 (s, 3H), 3.05 (dd, *J* = 11.7, 3.5 Hz, 1H), 3.06 (m, 2H), 3.20 (dd, *J*

= 12.0, 5.6 Hz, 1H), 3.23 (dd, *J* = 6.6, 1.8 Hz, 1H), 3.42 (m, 1H), 3.73 (m, 1H), 3.93 (t, *J* = 8.2 Hz, 1H), 4.19 (m, 1H), 4.24 (d, *J* = 9.4 Hz, 1H), 5.80 (d, *J* = 5.9 Hz, 1H), 5.85 (t, *J* = 4.2 Hz, 1H), 5.92 (d, *J* = 5.3 Hz, 1H), 7.11 (d, *J* = 7.0 Hz, 1H), 7.17 (t, *J* = 7.5 Hz, 1H), 7.22 (t, *J* = 7.2 Hz, 1H), 7.37 (d, *J* = 7.6 Hz, 1H); $^{13}$C NMR (150 MHZ, $CDCl_3$) δ (ppm) = 17.3, 19.0, 22.1, 29.2, 29.3, 36.1, 36.6, 36.9, 44.2, 44.6, 56.1, 56.6, 58.7, 60.4, 65.8, 75.8, 82.6, 124.4, 126.6, 129.0, 129.5, 130.2, 133.8, 138.6, 153.7, 154.2, 159.7, 172.2, 173.5; HRMS (ESI+) calcd for $C_{29}H_{38}N_3O_8S$ $[M + H]^+$ 588.2374, found 588.2379 (error 0.9 ppm).

***(R)*-1-Tetralyloxycarbonyloxymethyl meropenemate (21).**

This compound was prepared similarly to (*S*)-1-tetralol meropenem, but (*R*)-1-tetralol iodomethylcarbonate was used to afford the title compound (124mg , 82% yield) as a white solid foam. $R_f$ = 0.29 (10% MeOH-DCM 1% $NH_4OH$) $^1$H NMR (600 MHz, $CDCl_3$) δ (ppm) = 1.23 (d, J = 7.0 Hz, 3H), 1.28 (d, J = 6.5 Hz, 3H), 1.55 (dt, J = 13.6, 7.0 Hz, 1H), 1.80 (m, 1H), 1.93 (m, 1H), 2.00 (m, 1H), 2.13 (m, 1H), 2.63 (dt, *J* = 13.8, 8.4 Hz, 1H), 2.72 (ddd, *J* = 16.8, 9.0, 6.0 Hz, 1H), 2.84 (m, 1H), 2.92 (s, 3H), 2.96 (s, 3H), 3.05 (dd, J = 12.0, 3.8 Hz, 1H), 3.22 (dd, *J* = 6.6, 2.4 Hz, 1H), 3.28 (dd, *J* = 11.7, 5.9 Hz, 1H), 3.46 (m, 4H), 3.76 (m, 1H), 4.03 (t, *J* = 8.2 Hz, 1H), 4.18 (m, 1H), 4.27 (dd, *J* = 9.4, 1.2 Hz, 1H), 5.81 (d, *J* = 5.9 Hz, 1H), 5.85 (m, 1H), 5.91 (d, *J* = 5.9 Hz, 1H), 7.11 (d, *J* = 7.6 Hz, 1H), 7.16 (t, *J* = 7.5 Hz, 1H), 7.22 (t, *J* = 7.2 Hz, 1H), 7.35 (d, *J* = 7.6 Hz, 1H); $^{13}$C NMR (150 MHZ, $CDCl_3$) δ (ppm) = 17.4, 19.0, 22.0, 29.2, 36.1, 36.4, 36.9, 43.9, 44.6, 56.0, 56.7, 58.6, 60.5, 66.0, 75.9, 82.7, 124.5, 126.5, 129.0, 129.6, 130.2,

133.8, 138.7, 153.6, 154.1, 159.8, 171.9, 173.5; HRMS (ESI+) calcd for $C_{29}H_{38}N_3O_8S$ [M + H]$^+$ 588.2374, found 588.2378 (error 0.7 ppm).

***(S)*-1-Benzosuberyloxycarbonyloxymethyl meropenemate (19).**

Synthesized according to general procedure **D**, which afforded the title compound (131 mg, 84% yield) as a white foam: $R_f$ = 0.32 (10% MeOH-DCM 1% $NH_4OH$); $^1$H NMR (600 MHz, $CDCl_3$) δ (ppm) = 1.25 (d, *J* = 7.0 Hz, 3H), 1.30 (d, *J* = 6.5 Hz, 3H), 1.58 (dt, *J* = 13.6, 7.0 Hz, 2H), 1.68 (m, 1H), 1.83 (m, 1H), 1.96 (m, 1H), 2.01 (m, 2H), 2.62 (m, 1H), 2.73 (dd, *J* = 13.8, 9.6 Hz, 1H), 2.94 (s, 3H), 2.95 (m, 1H), 2.98 (s, 3H), 3.04 (dd, *J* = 11.7, 4.1 Hz, 1H), 3.20 (m, 2H), 3.23 (d, *J* = 6.5 Hz, 1H), 3.30 (dd, *J* = 11.4, 5.6 Hz, 1H), 3.47 (m, 1H), 3.75 (m, 1H), 4.06 (t, *J* = 7.5 Hz, 1H), 4.21 (m, 1H), 4.28 (d, *J* = 9.4 Hz, 1H), 5.80 (m, 2H), 5.89 (d, J = 5.9 Hz, 1H), 7.11 (d, J = 7.6 Hz, 1H), 7.16 (m, 2H), 7.29 (m, 1H); $^{13}$C NMR (150 MHZ, $CDCl_3$) δ (ppm) = 17.4, 22.0, 27.5, 28.1, 33.7, 36.0, 36.1, 36.3, 37.0, 43.7, 44.6, 55.8, 56.8, 58.5, 60.4, 65.9, 81.6, 82.8, 124.4, 126.5, 128.4, 130.3, 139.7, 141.8, 153.6, 153.7, 159.8, 171.7, 173.6; HRMS (ESI+) calcd for $C_{30}H_{39}N_3O_8S$ [M + H]$^+$ 602.2531, found 602.2537 (error 1.0 ppm).

***(R)*-1-Benzosuberyloxycarbonyloxymethyl meropenemate (22).**

This compound was prepared similarly to (*S*)-1-benzosuberol meropenem, but (*R*)-1-benzosuberol iodomethylcarbonate was used to afford the title compound (123 mg, 79% yield) as a white solid foam. $R_f$ = 0.24 (10% MeOH-DCM 1% $NH_4OH$) $^1$H NMR (600 MHz, $CDCl_3$) δ (ppm) = 1.23 (d, *J* = 7.0 Hz, 3H), 1.27 (d, *J* = 5.9 Hz, 3H), 1.55 (m,

2H), 1.66 (m, 1H), 1.83 (m, 1H), 1.93 (m, 1H), 2.00 (m, 2H), 2.66 (m, 1H), 2.72 (dd, *J* = 13.8, 9.6 Hz, 1H), 2.92 (s, 3H), 2.97 (s, 3H), 3.05 (dd, *J* = 12.0, 4.4 Hz, 1H), 3.22 (d, *J* = 5.3 Hz, 1H), 3.35 (dd, *J* = 11.4, 5.6 Hz, 1H), 3.52 (m, 1H), 3.78 (m, 1H), 3.89 (m, 3H), 4.12 (t, *J* = 8.2 Hz, 1H), 4.17 (t, *J* = 6.0 Hz, 1H), 4.30 (d, *J* = 8.8 Hz, 1H), 5.80 (d, *J* = 8.2 Hz, 1H), 5.85 (s, 2H), 7.10 (d, *J* = 6.5 Hz, 1H), 7.15 (m, 2H), 7.28 (d, *J* = 7.0 Hz, 1H); $^{13}$C NMR (150 MHZ, $CDCl_3$) δ (ppm) = 17.4, 22.0, 27.4, 28.1, 33.6, 36.0, 36.1, 36.3, 37.0, 43.6, 44.6, 55.8, 56.8, 58.5, 60.4, 66.0, 81.7, 82.6, 124.4, 126.5, 128.4, 130.3, 139.6, 142.0, 153.6, 153.7, 159.8, 171.7, 173.6; HRMS (ESI+) calcd for $C_{30}H_{39}N_3O_8S$ $[M + H]^+$ 602.2531, found 602.2529 (error 0.3 ppm).

***(S)*-1-Benzosuberyloxycarbonyloxyethyl meropenemate (23).**

Synthesized according to general procedure **D,** which afforded the title compound (69 mg, 43% yield). $R_f$ = 0.29 and 0.32 (10% MeOH-DCM 1% $NH_4OH$) $^1$H NMR (600 MHz, $CDCl_3$) δ= 1.22 (d, J = 7.0 Hz, 1.5H), 1.25 (d, J = 7.0 Hz, 1.5H), 12.7 (d, J = 7.2 Hz, 1.5H), 1.29 (d, J = 7.2 Hz, 1.5H), 1.53 (m, 1H), 1.54 (d, J = 5.3 Hz, 1.5H), 1.60 (d, J = 5.3 Hz, 1.5H), 1.70 (m, 1H), 1.83 (m, 1H), 1.97 (m, 2H), 2.01 (m, 1H), 2.56 (m, 1H), 2.73 (m, 2H), 2.79 (m, 2H), 2.93 (d, J = 4.1 Hz, 3H), 2.95 (m, 0.5H), 2.96 (d, J = 5.3 Hz, 3H), 3.03 (td, J = 11.4, 4.2 Hz, 1H), 3.06 (m, 0.5H), 3.17 (dt, J = 6.0, 5.4 Hz, 1H), 3.21 (ddd, J = 15.6, 6.0, 2.4 Hz, 1H), 3.38 (m, 1H), 3.72 (m, 1H), 3.91 (m, 1H), 4.18 (m, 1H), 4.21 (td, J = 9.6, 2.4 Hz, 1H), 5.78 (m, 1H), 6.84 (m, 1H), 7.10 (m, 1H), 7.16 (m, 2H), 7.28 (m, 1H); $^{13}$C NMR (150 MHZ, $CDCl_3$) δ= 17.3, 19.9, 20.0, 22.1, 27.7, 28.17, 28.23, 33.8, 33.9, 36.06, 36.11, 36.7, 36.8, 36.9, 44.27, 44.29, 44.6, 44.7, 56.3, 56.4, 56.51,

56.53, 58.9, 60.3, 60.4, 66.1, 81.2, 81.3, 92.1, 92.5, 124.7, 124.9, 126.5, 126.7, 128.3, 128.4, 130.3, 152.5, 152.6, 152.8, 153.0, 159.1, 159.2, 172.2, 172.3, 173.0, 173.1; HRMS (ESI+) calcd for $C_{31}H_{41}N_3O_8S$ $[M + H]^+$ 616.2687, found 616.2691 (error 0.7 ppm).

**_(S)_-1-Benzosuberyloxycarbonyloxymethyl _N_-(acetyl)meropenemate (24).**

A solution of meropenem (100 mg, 1.0 equiv.) and $Cs_2CO_3$ (367 mg, 1.04 mmols 4.0 equiv.) in DMF (1.3 mL) was stirred at 0 °C for 10 minutes. Next, acetic anhydride (30 mg, 0.29 mmol, 1.1 equiv) was added and the reaction mixture was stirred for 1 hour until starting material was consumed by TLC. Subsequently, (*S*)-1-benzosuberol iodomethylcarbonate (200 mg, 1.73 mmols, 1.57 equiv) was dissolved in DMF (1.0 mL) and added dropwise to the reaction mixture. After 1 hr of stirring, the contents were evaporated and purified by flash chromatography (10% MeOH–DCM 1%$NH_4OH$). $R_f$ 0.25 (10% MeOH–DCM 1%$NH_4OH$) $^1$H NMR (600 MHz, $CD_2Cl_2$): δ (ppm) = 1.25 (d, *J* = 7.0 Hz, 3H), 1.28 (d, *J* = 5.9 Hz, 3H), 1.60 (m, 1H), 1.68 (m, 1H), 1.80 (s, 1H), 1.84 (m, 2H), 1.96 (m, 1H), 2.01 (s, 3H), 2.01 (m, 1H), 2.67 (dt, *J* = 14.4, 7.8 Hz, 1H), 2.72 (dd, *J* = 13.5, 10.6 Hz, 1H), 2.90 (s, 3H), 2.96 (t, *J* = 11.7 Hz, 1H), 3.07 (s, 3H), 3.20 (m, 1H), 3.24 (dd, *J* = 6.5, 2.3 Hz, 1H), 3.42 (m, 1H), 3.51 (t, *J* = 10.0 Hz, 1H), 3.70 (m, 1H), 3.98 (dd, *J* = 10.0, 7.6 Hz, 1H), 4.17 (m, 1H), 4.25 (dd, *J* = 9.0, 1.8 Hz, 1H), 4.78 (t, *J* = 8.2 Hz, 1H), 5.79 (d, *J* = 6.5 Hz, 1H), 5.82 (d, *J* = 5.9 Hz, 1H), 5.89 (d, *J* = 5.9 Hz, 1H), 7.11 (m, 1H), 7.16 (m, 2H), 7.28 (m, 1H); $^{13}$C NMR (150 MHZ, $CDCl_3$) δ= 17.5, 22.1, 22.7, 27.5, 28.1, 33.7, 35.5, 36.0, 36.3, 37.4, 41.6, 44.6, 56.1, 56.2, 56.6, 58.1, 60.7, 66.1, 81.7, 82.8, 125.2, 126.6, 128.4, 130.3, 139.7, 142.0, 151.4, 153.6, 159.7, 168.9, 171.3,

173.6; HRMS (ESI+) calcd for $C_{32}H_{42}N_3O_9S$ $[M + H]^+$ 644.2636, found 644.2633 (error 0.5 ppm).

**2-Indanyloxycarbonyloxymethyl meropenemate (37).**

Synthesized according to general procedure **D**, which afforded the title compound (107 mg 0.187 mmol, 71%) of an off-white foam; $R_f$ 0.26 (10% MeOH–DCM 1%$NH_4OH$); $^1H$ NMR (600 MHz, $CD_2Cl_2$): δ (ppm) = 1.25 (d, $J$ = 7.6 Hz, 3H), 1.29 (d, $J$ = 5.9 Hz, 3H), 1.55 (dt, $J$ = 13.5, 6.7 Hz, 1H), 2.58 (dt, $J$ = 14.4, 7.2 Hz, 1H), 2.94 (s, 3H), 2.96 (m, 1H), 2.97 (s, 3H), 3.06 (m, 2H), 3.13 (m, 2H), 3.19 (dd, $J$ = 11.7, 5.3 Hz, 1H), 3.24 (d, $J$ = 5.9 Hz, 1H), 3.33 (m, 2H), 3.41 (m, 1H), 3.74 (m, 1H), 3.92 (t, $J$ = 7.9 Hz, 1H), 4.20 (t, $J$ = 6.2 Hz, 1H), 4.24 (d, $J$ = 9.4 Hz, 1H), 5.47 (m, 1H), 5.79 (d, $J$ = 5.9 Hz, 1H), 5.88 (d, $J$ = 5.3 Hz, 1H), 7.17 (m, 2H), 7.24 (m, 2H); $^{13}C$ NMR (150 MHz, $CD_2Cl_2$): δ (ppm) = 17.3, 22.1, 36.1, 36.7, 36.9, 39.8, 44.3, 44.7, 56.3, 56.6, 58.8, 60.4, 65.9, 80.7, 82.5, 124.4, 125.1, 127.3, 140.5, 153.8, 154.1, 159.7, 172.2, 173.4; HRMS (ESI+) calcd for $C_{28}H_{35}N_3O_8S$ $[M + H]^+$ 574.2218, found 574.2214 (error 0.7 ppm).

**(*S*)-2-Tetralyloxycarbonyloxymethyl meropenemate (38).**

Synthesized according to general procedure **D**, which afforded the title compound **(**127 mg 0.216 mmol, 82%) of an off-white foam; $R_f$ 0.25 and 0.30 (10% MeOH–DCM 1%$NH_4OH$)); $^1H$ NMR (600 MHz, $CD_2Cl_2$): δ (ppm) = 1.25 (d, $J$ = 7.0 Hz, 3H), 1.28 (d, $J$ = 6.5 Hz, 3H), 1.55 (dt, $J$ = 13.5, 6.7 Hz, 1H), 2.03 (m, 1H), 2.10 (m, 1H), 2.61 (dt, $J$ = 13.8, 8.1 Hz, 1H), 2.84 (m, 1H), 2.93 (s, 3H), 2.95 (m, 1H), 2.97 (s, 3H), 3.06 (dd, $J$ =

11.7, 2.9 Hz, 1H), 3.19 (m, 3H), 3.44 (m, 1H), 3.54 (m, 2H), 3.75 (m, 1H), 3.95 (t, *J* = 7.9 Hz, 1H), 4.18 (t, *J* = 6.0 Hz, 1H), 4.25 (d, *J* = 9.4 Hz, 1H), 5.13 (m, 1H), 5.80 (t, *J* = 5.3 Hz, 1H), 5.89 (t, *J* = 4.7 Hz, 1H), 7.10 (m, 4H); $^{13}$C NMR (150 MHz, $CD_2Cl_2$): δ (ppm) = 17.3, 22.1, 26.6, 28.0, 34.7, 36.0, 36.6, 36.8, 44.1, 44.6, 54.4, 56.1, 56.5, 58.6, 60.4, 65.7, 75.3, 82.5, 124.3, 126.3, 126.5; HRMS (ESI+) calcd for $C_{29}H_{38}N_3O_8S$ [M + H]$^+$ 588.2374, found 588.2369 (error 0.9 ppm).

**(*R*)-2-Tetralyloxycarbonyloxymethyl meropenemate (39).**

Synthesized according to general procedure **D**, which afforded the title compound **(**127 mg 0.216 mmol, 82%) of an off-white foam; $R_f$ 0.25 and 0.30 (10% MeOH–DCM 1%$NH_4OH$)); $^1$H NMR (600 MHz, $CD_2Cl_2$): δ (ppm) = 1.25 (d, *J* = 7.0 Hz, 3H), 1.28 (d, *J* = 6.5 Hz, 3H), 1.55 (dt, *J* = 13.5, 6.7 Hz, 1H), 2.03 (m, 1H), 2.10 (m, 1H), 2.61 (dt, *J* = 13.8, 8.1 Hz, 1H), 2.84 (m, 1H), 2.93 (s, 3H), 2.95 (m, 1H), 2.97 (s, 3H), 3.06 (dd, *J* = 11.7, 2.9 Hz, 1H), 3.19 (m, 3H), 3.44 (m, 1H), 3.54 (m, 2H), 3.75 (m, 1H), 3.95 (t, *J* = 7.9 Hz, 1H), 4.18 (t, *J* = 6.0 Hz, 1H), 4.25 (d, *J* = 9.4 Hz, 1H), 5.13 (m, 1H), 5.80 (t, *J* = 5.3 Hz, 1H), 5.89 (t, *J* = 4.7 Hz, 1H), 7.10 (m, 4H); $^{13}$C NMR (150 MHz, $CD_2Cl_2$): δ (ppm) = 17.3, 22.1, 26.6, 28.0, 34.7, 36.0, 36.6, 36.8, 44.1, 44.6, 54.4, 56.1, 56.5, 58.6, 60.4, 65.7, 75.3, 82.5, 124.3, 126.3, 126.5; HRMS (ESI+) calcd for $C_{29}H_{38}N_3O_8S$ [M + H]$^+$ 588.2374, found 588.2369 (error 0.9 ppm).

**2-Benzosuberyloxycarbonyloxymethyl meropenemate (40).**

Synthesized according to general procedure **D**, which afforded the title compound (110 mg, 65%) of an off-white foam: $R_f$ 0.25 and 0.27 (10% DCM–MeOH 1% $NH_4OH$); $^1H$ NMR (600 MHz, $CD_2Cl_2$): δ (ppm) = 1.26 (d, *J* = 7.0 Hz, 3H), 1.28 (dd, *J* = 6.2, 2.6 Hz, 3H), 1.54 (m, 2H), 1.93 (m, 2H), 2.18 (m, 1H), 2.59 (dt, *J* = 13.5, 8.2 Hz, 1H), 2.77 (m, 2H), 2.94 (s, 3H), 2.97 (s, 3H), 3.06 (m, 4H), 3.19 (m, 2H), 3.24 (dd, *J* = 6.5, 1.8 Hz, 1H), 3.41 (dt, *J* = 16.2, 7.5 Hz, 1H), 3.74 (m, 1H), 3.92 (t, *J* = 7.9 Hz, 1H), 4.20 (pent, *J* = 6.5, 1.8 Hz, 1H), 4.24 (dd, *J* = 9.1, 2.1 Hz, 1H), 4.68 (t, *J* = 8.5 Hz, 1H), 5.78 (dd, *J* = 7.0, 5.9 Hz, 1H), 5.87 (dd, *J* = 8.2, 5.9 Hz, 1H), 7.13 (m, 4H); $^{13}C$ NMR (150 MHz, $CD_2Cl_2$): δ (ppm) = 17.4, 22.1, 25.1, 35.7, 36.1, 36.7, 36.9, 37.3, 41.6, 44.2, 44.7, 56.3, 56.7, 58.8, 60.4, 66.0, 77.7, 82.5, 124.5, 126.9, 127.4, 129.4, 130.9, 136.3, 143.8, 153.6, 153.7, 159.8, 172.2, 173.4; HRMS (ESI+) calcd for $C_{30}H_{39}N_3O_8S$ $[M + H]^+$ 602.2531, found 602.2530 (error 0.2 ppm).

***N*-(*p*-nitrobenzyl)meropenem (41)**

To a suspension of meropenem (1.0 g, 2.28 mmol, 1.0 equiv.) and $NaHCO_3$ (210 mg, 2.5 mmols, 1.1 equiv.) in $H_2O$ (10 mL) at 0 °C, was added dropwise a solution *p*-nitrobenzyl chloroformate (540.7 mg, 2.5 mmols, 1.1 equiv.) in THF (10 mL). The reaction was allowed to stir for 10 minutes and 95.6% conversion was identified by HPLC. The solvent was initially evaporated under reduced pressure followed by high pressure to yield a crude white solid that was taken onto the next step without further purification.

**Benzyl (*N*-(*p*-nitrobenzyl)) meropenemate (42).**

A solution of **41** (500 mg, 0.89 mmol, 1.0 equiv.) in DMF (10 mL) and $Cs_2CO_3$ (580 mg, 1.8 mmol, 2.0 equiv) was allowed to stir for 10 min at rt before adding benzyl iodide (427.4 mg, 1.96 mmol, 2.2 equiv). The mixture was allowed to stir for 50 minutes and conversion was monitored by TLC. Subsequently, the reaction mixture was diluted with EtOAc (30 mL) and washed consecutively with 10 mL of 10% $Na_2SO_3$, $dH_2O$, and brine. The organic layer was collected, dried over $MgSO_4$ and concentrated under reduced pressure to yield a liquid. The liquid was purified by silica gel flash chromatography (5% MeOH-DCM) to afford the title compound as an off-white solid (63%). $R_f$ = 0.28 (5% MeOH-DCM); $^1$H NMR (600 MHz, $CD_2Cl_2$): δ (ppm) = 1.34 – 1.35 (m, 3H); 1.4 (d, *J* = 5.9 Hz, 3H); 1.93 – 1.99 (m, 1H); 2.78 – 2.85 (m, 1H); 2.99 (s, 1.5H); 3.03 (s, 3H); 3.15 (s, 1.5H); 3.35 (s, 1H); 3.44 – 3.51 (m, 2H); 3.54 (t, *J* = 10 Hz, 1H); 3.71 – 3.79 (m, 1H); 4.2 (dt, *J* = 8.4, 28.2 Hz, 1H); 4.30 – 4.32 (m, 2H); 4.79 – 4.83 (m, 1H); 5.14 (d, *J* = 14.1 Hz, 1H); 5.28 – 5.32 (m, 2H); 5.37 – 5.43 (m, 2H); 7.42 (d, *J* = 7.0 Hz, 1H); 7.46 (t, = 7.3 Hz, 1H); 7.54 (d, *J* = 7.0 Hz, 1H); 7.63 (d, *J* = 8.2 Hz, 1H); 8.3 (t, *J* = 7.1 Hz, 1H); (missing 1 proton); $^{13}$C NMR (150 MHz, $CD_2Cl_2$): δ (ppm) = 16.8, 21.5, 21.6, 35.2, 35.7, 35.8, 36.5, 36.7, 39.9, 40.7, 43.8, 54.4, 54.9, 55.8, 55.84, 55.87, 56.3, 59.9, 65.6, 66.8, 123.4, 123.5, 127.8, 127.9, 128.0, 128.4, 144.1, 170.4

**Benzyl meropenemate (43)**

Benzyl (*N*-(*p*-nitrobenzyl)) meropenemate (150 mg, 0.23 mmol, 1.0 equiv.) was initially dissolved in a mixture of MeCN/EtOH/$H_2O$ (1:1:1) at rt, followed by the addition of $Na_2S_2O_4$ (320 mg, 1.8 mmol, 8.0 equiv). The mixture was allowed to stir for 10 min and HPLC analysis indicated full conversion of starting material. The reaction mixture was then evaporated to dryness followed by silica gel flash chromatography (20% MeOH/DCM 1$ $NH_4OH$) to yield 24 mg of a white solid (22%). $^1$H NMR (600 MHz, $CD_2Cl_2$): δ (ppm) = 1.25 (d, *J* = 7.0 Hz, 3H), 1.30 (d, *J* = 7.0 Hz, 3H); 1.55 (dt, *J* = 13.6, 7.0 Hz, 1H); 2.59 (dt, *J* = 13.5, 8.2 Hz, 1H); 2.96 (s, 3H); 2.97 (s, 3H); 3.06 (dd, *J* = 12.0, 3.8 Hz, 1H); 3.19-3.24 (m, 2H); 3.39 – 3.41 (m, 1H); 3. 70 – 3.74 (m, 1H); 3.98 (t, *J* = 8.2 Hz, 1H); 4.18 – 4.23 (m, 2H); 5.22 (d, *J* = 9.6 Hz, 1H); 5.31 (d, *J* = 12.6 Hz, 1H); 7.31 - 7.33 (m, 1H); 7.38 (t, *J* = 7.6, 2H); 7.47 (d, *J* = 7.6, 2H); $^{13}$C NMR (150 MHz, $CD_2Cl_2$): δ (ppm) = 17.3, 22.1, 36.1, 36.6, 36.9, 44.1, 44.3, 56.1, 56.6, 58.9, 60.3, 66.2, 67.3, 125.8, 128.6, 128.7, 128.9, 136.4, 150.3, 161.2, 172.1, 173.3

## VII: References


1. 2011 WHO Global Report of Tuberculosis.

2. Koul, A.; Arnoult, E.; Lounis, N.; Guillemont, J.; Andries, K. The challenge of new drug discovery for tuberculosis. *Nature* 469, 483-90.

3. Prevention, C. f. D. C. a. Emergence of *Mycobacterium tuberculosis* with extensive resistance to second-line drugs-worldwide, 2000-2004. *MMWR Morb Wkly Rep* **2006**, 301-305.

4. Banerjee, R.; Schecter, G. F.; Flood, J.; Porco, T. C. Extensively drug-resistant tuberculosis: new strains, new challenges. *Expert Rev Anti Infect Ther* **2008,** 6, 713-24.

5. Velayati, A. A.; Farnia, P.; Masjedi, M. R.; Ibrahim, T. A.; Tabarsi, P.; Haroun, R. Z.; Kuan, H. O.; Ghanavi, J.; Varahram, M. Totally drug-resistant tuberculosis strains: evidence of adaptation at the cellular level. *Eur Respir J* **2009,** 34, 1202-3.

6. Velayati, A. A.; Masjedi, M. R.; Farnia, P.; Tabarsi, P.; Ghanavi, J.; Ziazarifi, A. H.; Hoffner, S. E. Emergence of new forms of totally drug-resistant tuberculosis bacilli: super extensively drug-resistant tuberculosis or totally drug-resistant strains in iran. *Chest* **2009,** 136, 420-5.

7. Goffin, C.; Ghuysen, J. M. Multimodular penicillin-binding proteins: an enigmatic family of orthologs and paralogs. *Microbiol Mol Biol Rev* **1998,** 62, 1079-93.

8. Jarlier, V.; Nikaido, H. Mycobacterial cell wall: structure and role in natural resistance to antibiotics. *FEMS Microbiol Lett* **1994,** 123, 11-8.

9. Goffin, C.; Ghuysen, J. M. Biochemistry and comparative genomics of SxxK superfamily acyltransferases offer a clue to the mycobacterial paradox: presence of penicillin-susceptible target proteins versus lack of efficiency of penicillin as therapeutic agent. *Microbiol Mol Biol Rev* **2002,** 66, 702-38, table of contents.

10. Chambers, H. F.; Moreau, D.; Yajko, D.; Miick, C.; Wagner, C.; Hackbarth, C.; Kocagoz, S.; Rosenberg, E.; Hadley, W. K.; Nikaido, H. Can penicillins and other beta-lactam antibiotics be used to treat tuberculosis? *Antimicrob Agents Chemother* **1995,** 39, 2620-4.

11. Flores, A. R.; Parsons, L. M.; Pavelka, M. S., Jr. Genetic analysis of the beta-lactamases of Mycobacterium tuberculosis and Mycobacterium smegmatis and susceptibility to beta-lactam antibiotics. *Microbiology* **2005,** 151, 521-32.

12. Cynamon, M. H.; Palmer, G. S. In vitro activity of amoxicillin in combination with clavulanic acid against Mycobacterium tuberculosis. *Antimicrob Agents Chemother* **1983,** 24, 429-31.

13. Chambers, H. F.; Kocagoz, T.; Sipit, T.; Turner, J.; Hopewell, P. C. Activity of amoxicillin/clavulanate in patients with tuberculosis. *Clin Infect Dis* **1998,** 26, 874-7.

14. Sorg, T. B.; Cynamon, M. H. Comparison of four beta-lactamase inhibitors in combination with ampicillin against Mycobacterium tuberculosis. *J Antimicrob Chemother* **1987,** 19, 59-64.

15. Wong, C. S.; Palmer, G. S.; Cynamon, M. H. In-vitro susceptibility of Mycobacterium tuberculosis, Mycobacterium bovis and Mycobacterium kansasii to amoxycillin and ticarcillin in combination with clavulanic acid. *J Antimicrob Chemother* **1988,** 22, 863-6.

16. Mitnick, C. D.; Shin, S. S.; Seung, K. J.; Rich, M. L.; Atwood, S. S.; Furin, J. J.; Fitzmaurice, G. M.; Alcantara Viru, F. A.; Appleton, S. C.; Bayona, J. N.; Bonilla, C. A.; Chalco, K.; Choi, S.; Franke, M. F.; Fraser, H. S.; Guerra, D.; Hurtado, R. M.; Jazayeri, D.; Joseph, K.; Llaro, K.; Mestanza, L.; Mukherjee, J. S.; Munoz, M.; Palacios, E.; Sanchez, E.; Sloutsky, A.; Becerra, M. C. Comprehensive treatment of extensively drug-resistant tuberculosis. *N Engl J Med* **2008,** 359, 563-74.

17. Nadler, J. P.; Berger, J.; Nord, J. A.; Cofsky, R.; Saxena, M. Amoxicillin-clavulanic acid for treating drug-resistant Mycobacterium tuberculosis. *Chest* **1991,** 99, 1025-6.

18. Hugonnet, J. E.; Blanchard, J. S. Irreversible inhibition of the Mycobacterium tuberculosis beta-lactamase by clavulanate. *Biochemistry* **2007,** 46, 11998-2004.

19. Hugonnet, J. E.; Tremblay, L. W.; Boshoff, H. I.; Barry, C. E., 3rd; Blanchard, J. S. Meropenem-clavulanate is effective against extensively drug-resistant Mycobacterium tuberculosis. *Science* **2009,** 323, 1215-8.

20. Dauby, N.; Muylle, I.; Mouchet, F.; Sergysels, R.; Payen, M. C. Meropenem/clavulanate and linezolid treatment for extensively drug-resistant tuberculosis. *Pediatr Infect Dis J* 30, 812-3.

21. Payen, M. C.; De Wit, S.; Martin, C.; Sergysels, R.; Muylle, I.; Van Laethem, Y.; Clumeck, N. Clinical use of the meropenem-clavulanate combination for extensively drug-resistant tuberculosis. *Int J Tuberc Lung Dis* 16, 558-60.

22. Mouton, J. W.; van den Anker, J. N. Meropenem clinical pharmacokinetics. *Clin Pharmacokinet* **1995,** 28, 275-86.

23. Tanaka, S.; Matsui, H.; Kasai, M.; Kunishiro, K.; Kakeya, N.; Shirahase, H. Novel prodrugs of meropenem with two lipophilic promoieties: synthesis and pharmacokinetics. *J Antibiot (Tokyo)* 64, 233-42.
24. Takeuchi, Y.; Sunagawa, M.; Isobe, Y.; Hamazume, Y.; Noguchi, T. Stability of a 1 beta-methylcarbapenem antibiotic, meropenem (SM-7338) in aqueous solution. *Chem Pharm Bull (Tokyo)* **1995,** 43, 689-92.

25. Daehne, W.; Frederiksen, E.; Gundersen, E.; Lund, F.; Morch, P.; Petersen, H. J.; Roholt, K.; Tybring, L.; Godtfredsen, W. O. Acyloxymethyl esters of ampicillin. *J Med Chem* **1970,** 13, 607-12.

26. Toshio Kumagai, S. T., Takao Abe, Muneo Hikida. Current Status of Oral Carbapenem Development. *Curr. Med. Chem. - Anti-Infective Agents* **2002,** 1, 1-14.

27. Kijima, K.; Morita, J.; Suzuki, K.; Aoki, M.; Kato, K.; Hayashi, H.; Shibasaki, S.; Kurosawa, T. [Pharmacokinetics of tebipenem pivoxil, a novel oral carbapenem antibiotic, in experimental animals]. *Jpn J Antibiot* **2009,** 62, 214-40.

28. Arrigoni-Martelli, E.; Caso, V. Carnitine protects mitochondria and removes toxic acyls from xenobiotics. *Drugs Exp Clin Res* **2001,** 27, 27-49.

29. Broderick, T. L. Hypocarnitinaemia induced by sodium pivalate in the rat is associated with left ventricular dysfunction and impaired energy metabolism. *Drugs R D* **2006,** 7, 153-61.

30. Doberenz, J.; Hirche, F.; Keller, U.; Eder, K. Pivalate lowers litter sizes and weights in female rats independent of its effect on carnitine status. *Reprod Toxicol* **2007,** 24, 83-8.

31. Ricciolini, R.; Scalibastri, M.; Carminati, P.; Arduini, A. The effect of pivalate treatment of pregnant rats on body mass and insulin levels in the adult offspring. *Life Sci* **2001,** 69, 1733-8.

32. Abrahamsson, K.; Eriksson, B. O.; Holme, E.; Jodal, U.; Jonsson, A.; Lindstedt, S.
Pivalic acid-induced carnitine deficiency and physical exercise in humans. *Metabolism* **1996,** 45, 1501-7.

33. Makino, Y.; Sugiura, T.; Ito, T.; Sugiyama, N.; Koyama, N. Carnitine-associated encephalopathy caused by long-term treatment with an antibiotic containing pivalic acid. *Pediatrics* **2007,** 120, e739-41.

34. Bichlmaier, I.; Siiskonen, A.; Kurkela, M.; Finel, M.; Yli-Kauhaluoma, J. Chiral distinction between the enantiomers of bicyclic alcohols by UDP-glucuronosyltransferases 2B7 and 2B17. *Biol Chem* **2006,** 387, 407-16.

35. US Pharmacopeia Test Solution for Simulated Gastric Fluid. http://www.pharmacopeia.cn/v29240/usp29nf24s0_ris1s126.html

36. Bandgar, B. P.; Sarangdhar, R. J.; Khan, F.; Mookkan, J.; Shetty, P.; Singh, G. Synthesis and biological evaluation of orally active hypolipidemic agents. *J Med Chem* 54, 5915-26.

37. Corey, E. J., Helal, C.j. Reduction of Carbonyl Compounds with Chiral Oxazaborolidine Catalysts: A New Paradigm for Enantioselective Catalysis and a Powerful New Synthetic Method. *Angew Chem Int Ed* **1998**, 1986-2012.

38. Phan, D. H.; Kou, K. G.; Dong, V. M. Enantioselective desymmetrization of cyclopropenes by hydroacylation. *J Am Chem Soc* 132, 16354-5.

39. Li, L.; Cai, P.; Guo, Q.; Xue, S. Et2Zn-mediated rearrangement of bromohydrins. *J Org Chem* **2008,** 73, 3516-22.

40. Stoeckel, K.; Hofheinz, W.; Laneury, J. P.; Duchene, P.; Shedlofsky, S.; Blouin, R. A. Stability of cephalosporin prodrug esters in human intestinal juice: implications for oral bioavailability. *Antimicrob Agents Chemother* **1998,** 42, 2602-6.

41. Richardson, A. P.; Walker, H. A.; et al. Metabolism of methyl and benzyl esters of penicillin by different species. *Proc Soc Exp Biol Med* **1945,** 60, 272-6.

42. Ungar, J. The in vivo activity of penicillin esters. *Br J Exp Pathol* **1947,** 28, 88-93.

43. Jansen, A. B.; Russell, T. J. Some Novel Penicillin Derivatives. *J Chem Soc* **1965,** 65, 2127-32.

44. Saito Toshihide, S. R., Ujiie Kaori, Oda Masako, Saitoh, Hiroshi. Possible Factors Involved in Oral Inactivity of Meropenem, a Carbapenem Antibiotic. *Pharmacology & Pharmacy* **2012**, 201-206.

45. Dai, G.; Phalen, S.; McMurray, D. N. Nutritional modulation of host responses to mycobacteria. *Front Biosci* **1998,** 3, e110-22.

46. McMurray, D. N. Disease model: pulmonary tuberculosis. *Trends Mol Med* **2001,** 7, 1357.

47. Smith, D. W.; Balasubramanian, V.; Wiegeshaus, E. A guinea pig model of experimental airborne tuberculosis for evaluation of the response to chemotherapy: the effect on bacilli in the initial phase of treatment. *Tubercle* **1991,** 72, 223-31.

## VIII. Appendix 1: NMR Spectra

$^{1}$H NMR
Compound **2**

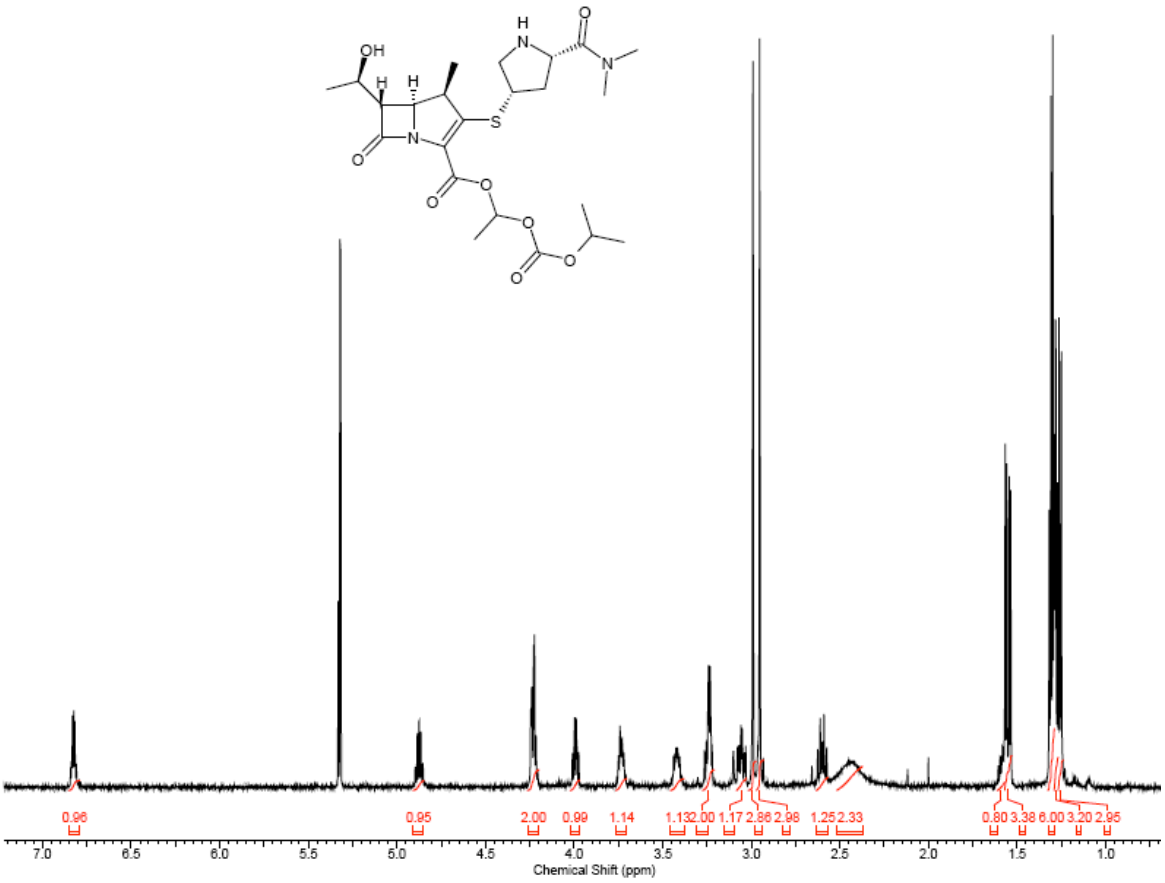

$^{13}$C NMR
Compound **2**

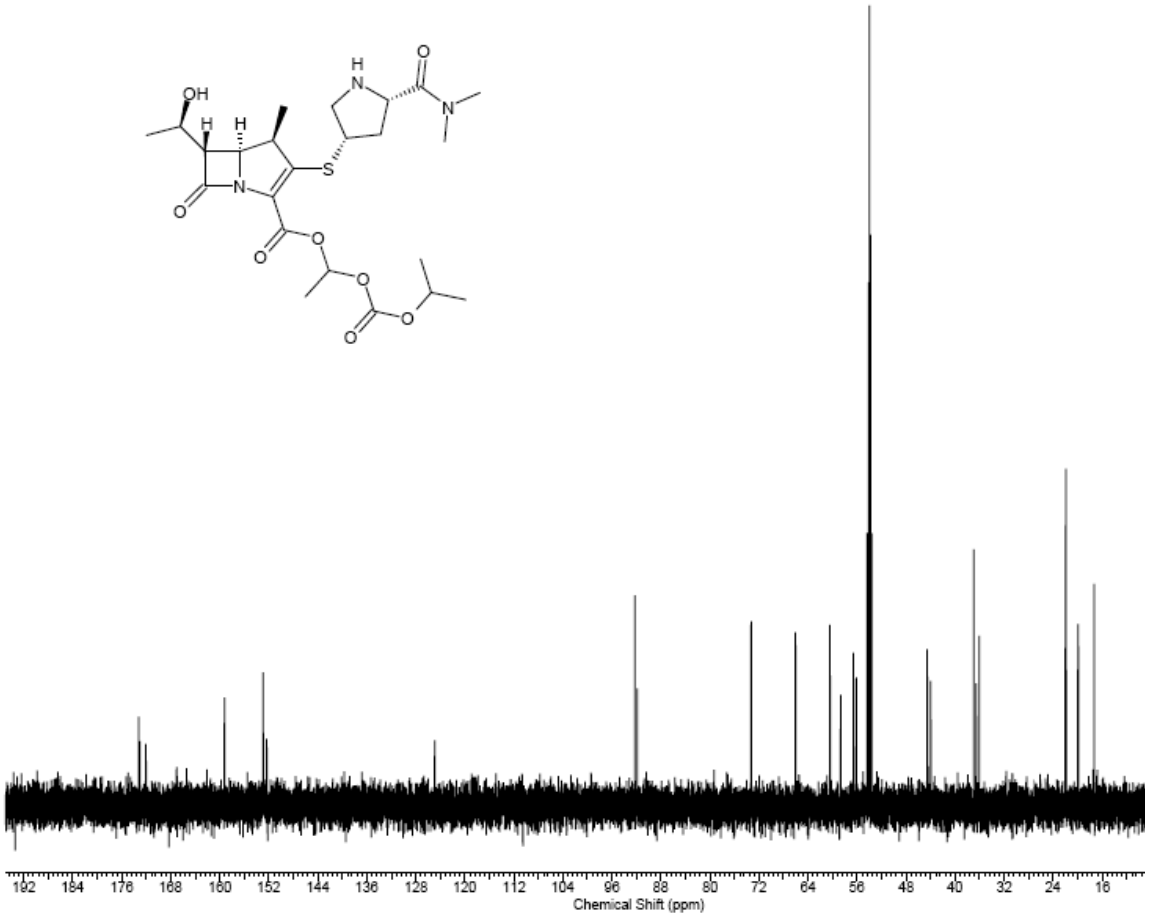

$^{1}$H NMR
Compound **9a**

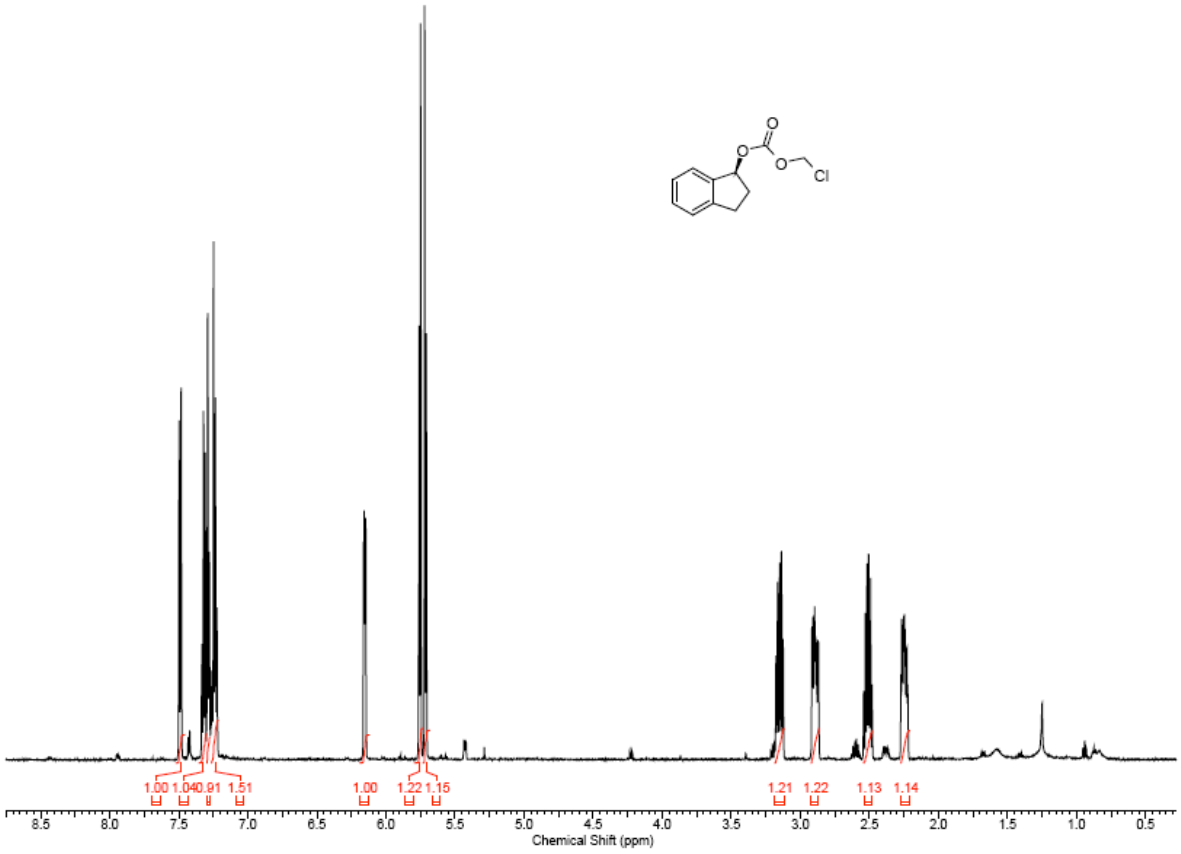

$^{13}$C NMR
Compound **9a**

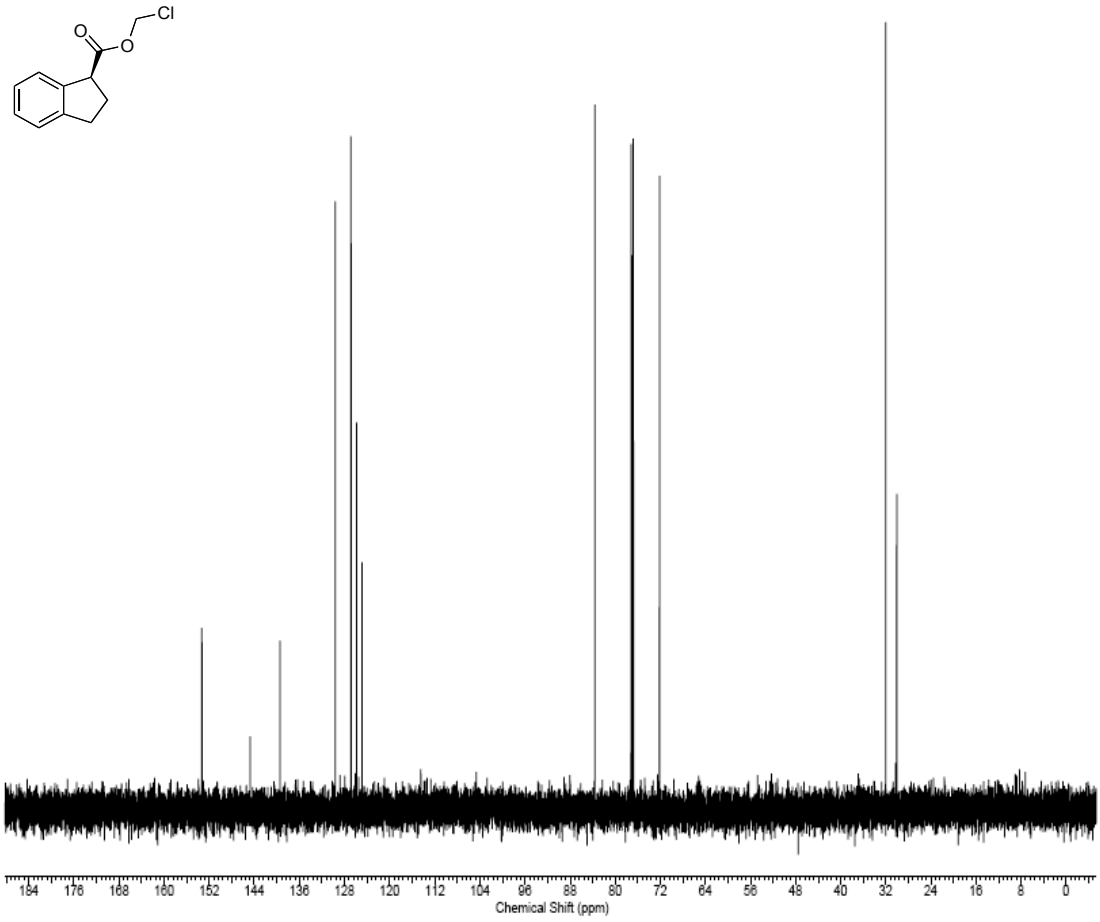

$^{1}$H NMR
Compound **10a**

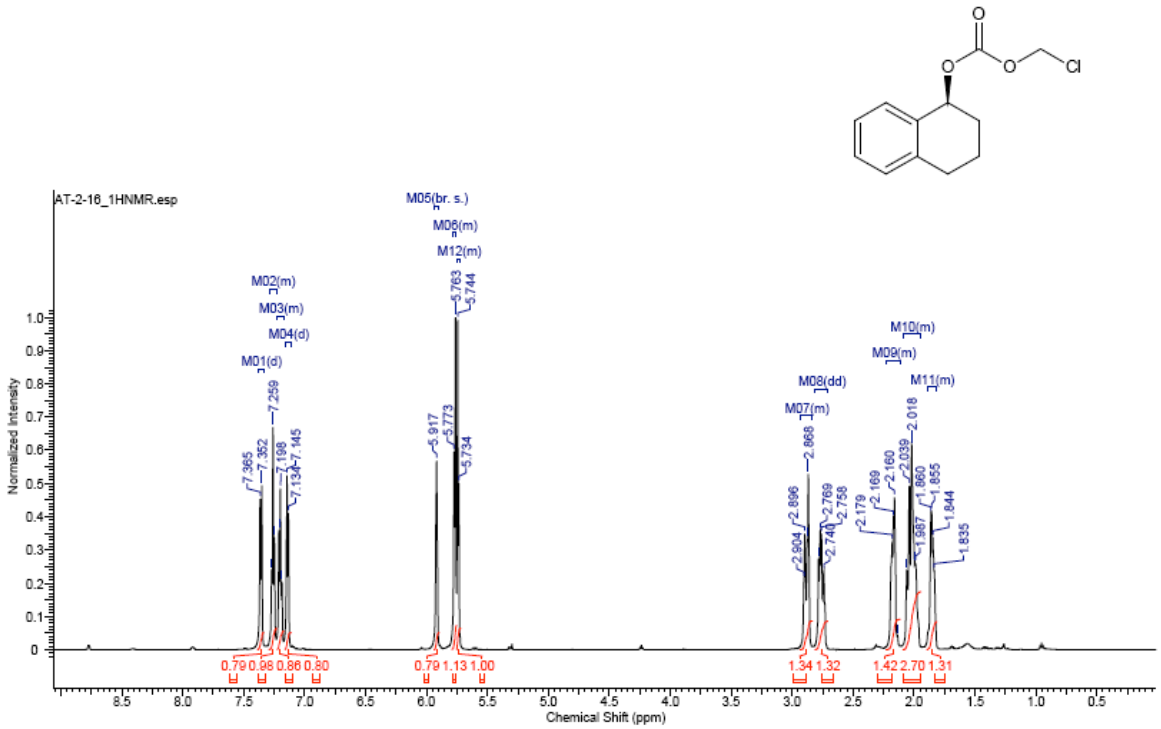

$^{13}$C NMR
Compound **10a**

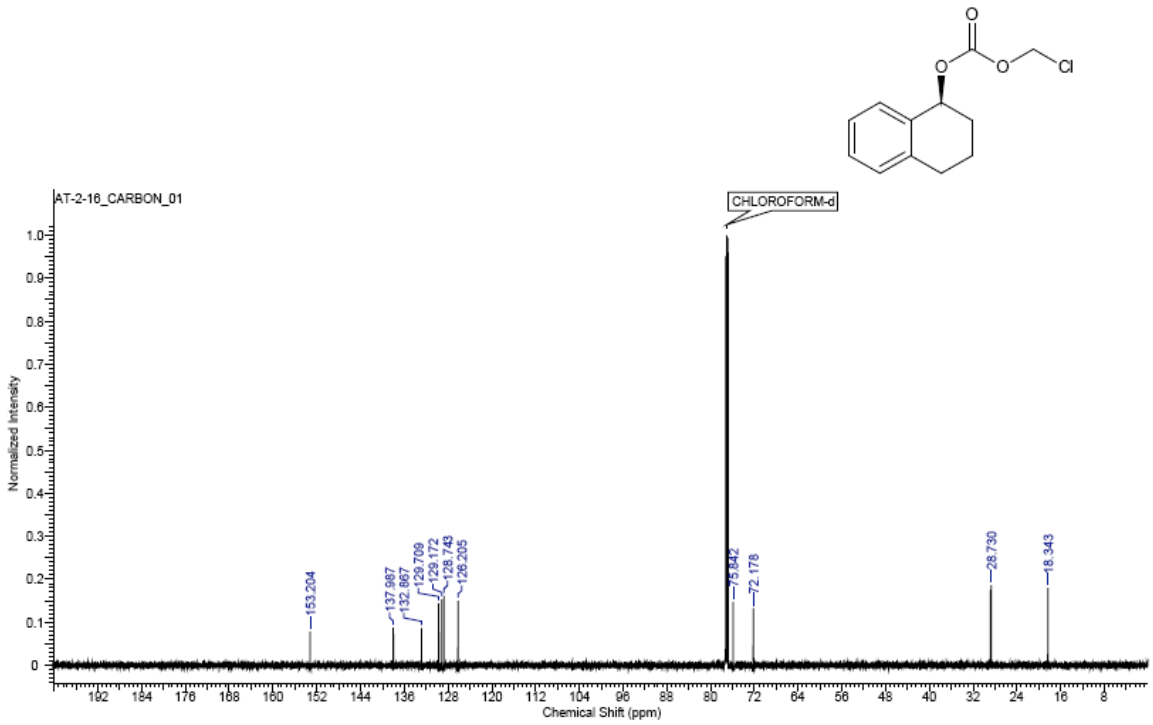

$^{1}$H NMR
Compound **11a**

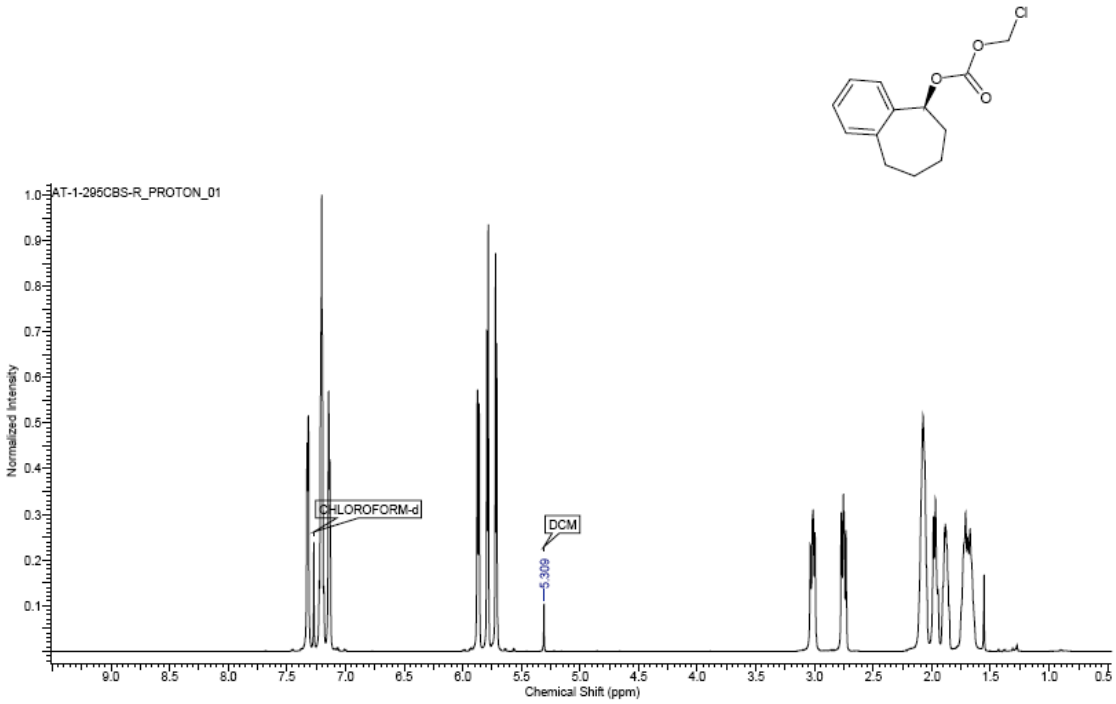

$^{13}$C NMR
Compound **11a**

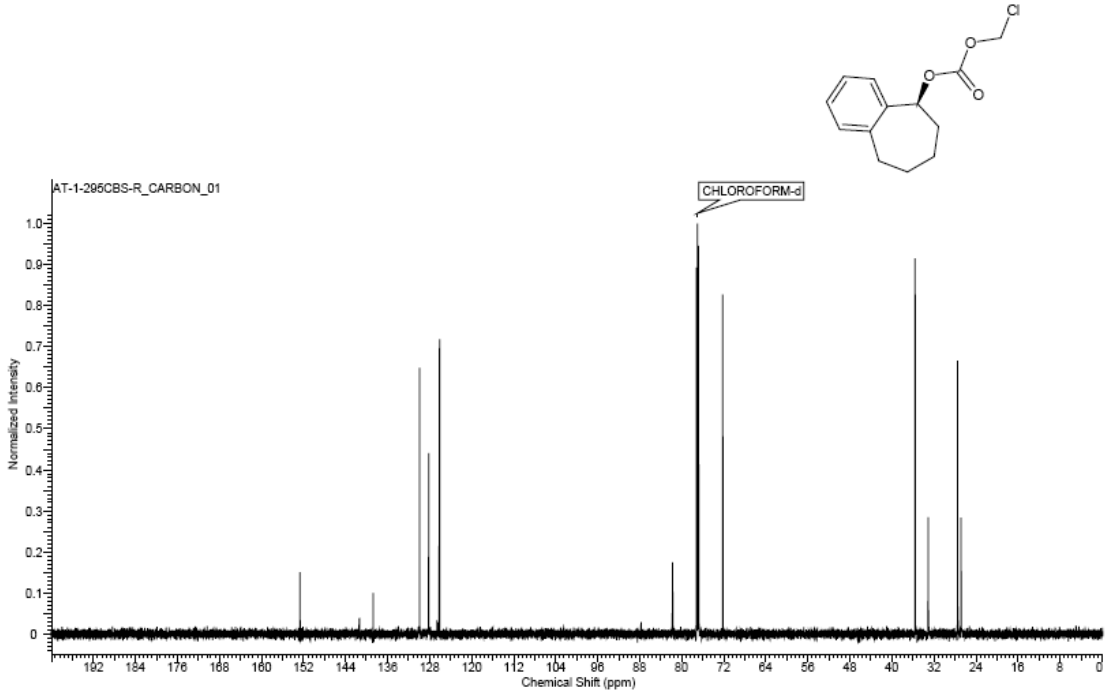

$^{1}$H NMR
Compound **12**

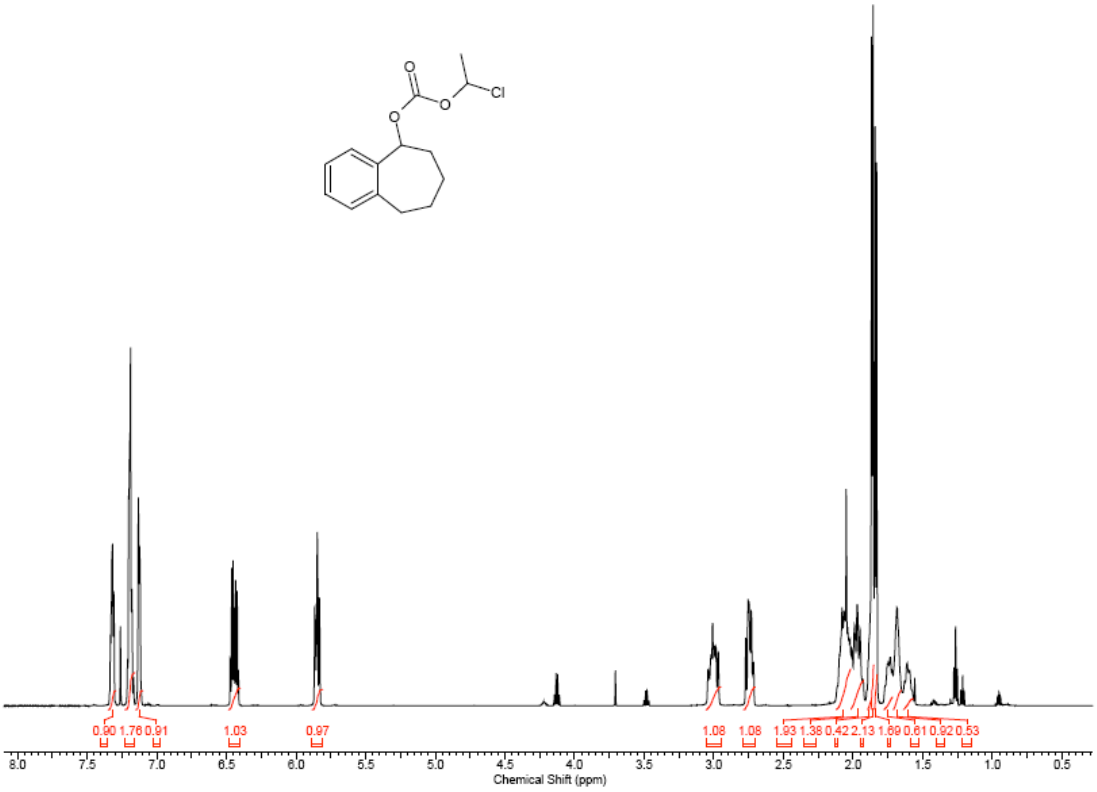

$^{1}$H NMR
Compound **14a**

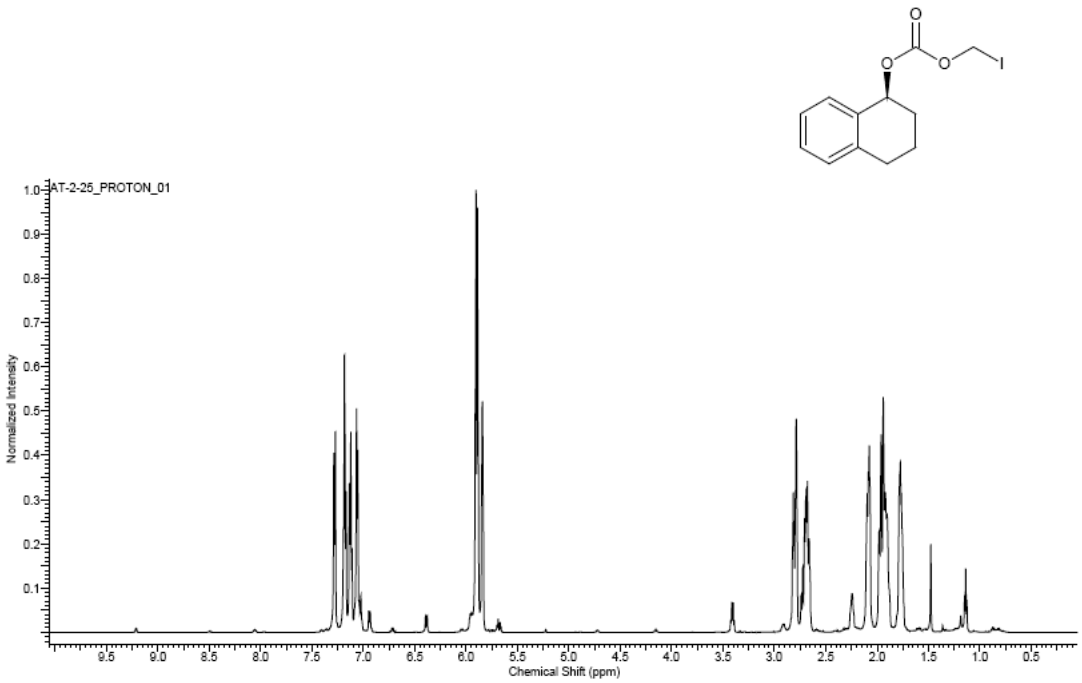

$^{13}$C NMR
Compound **14a**

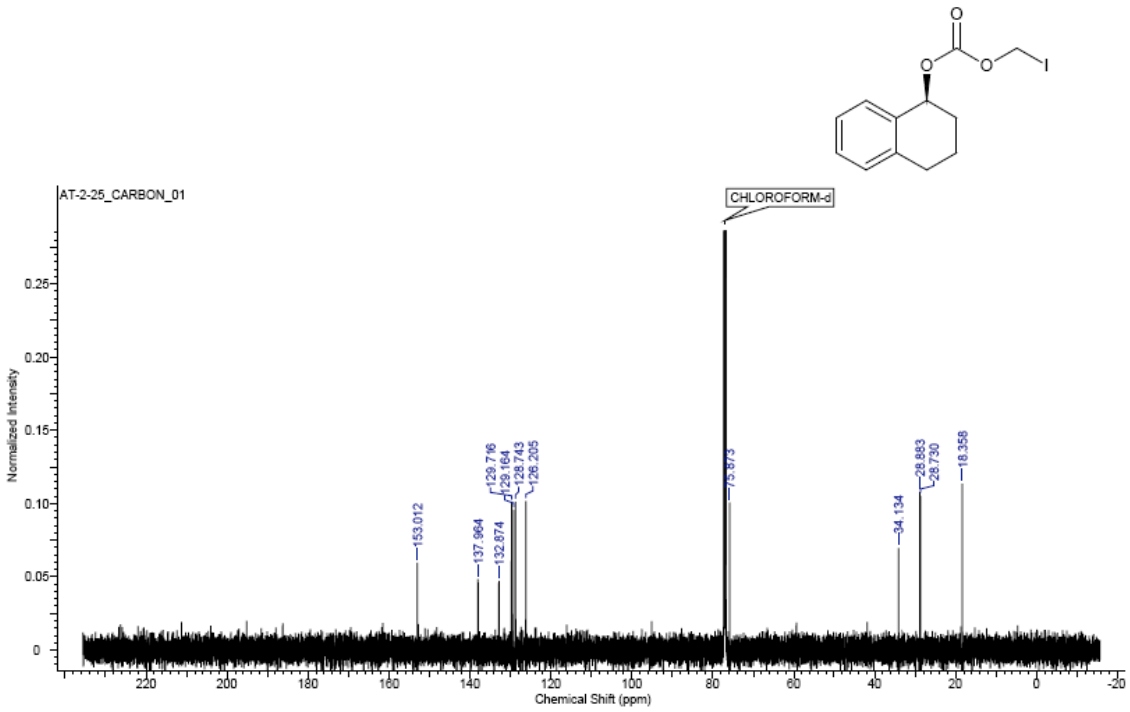

$^{1}$H NMR
Compound **15a**

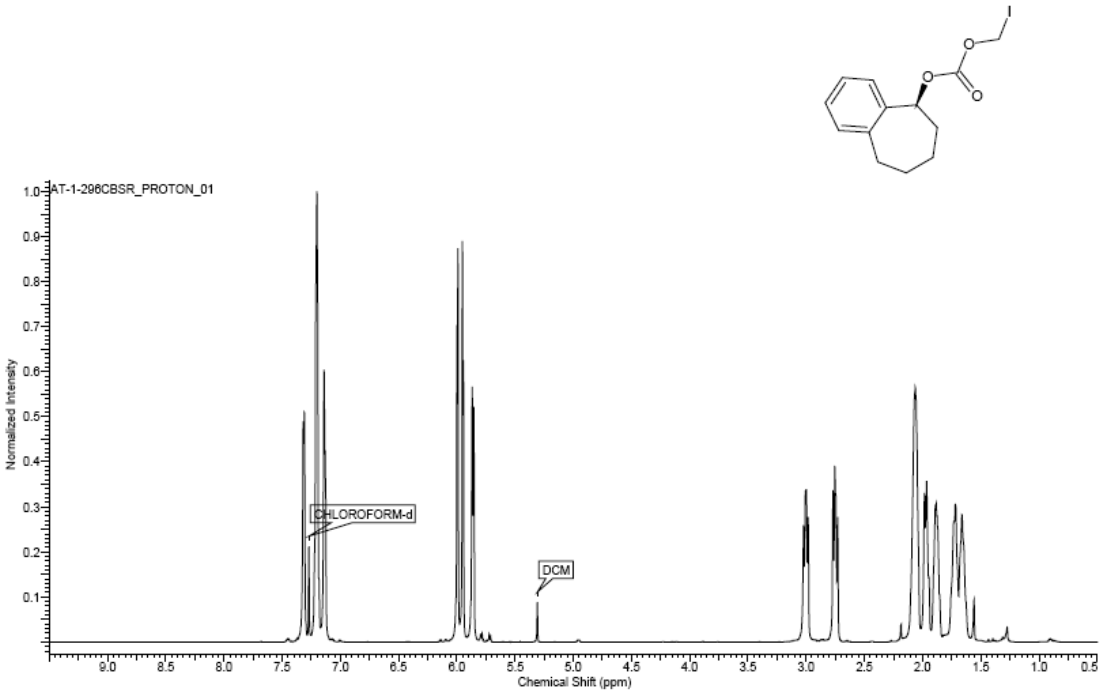

$^{13}$C NMR
Compound **15a**

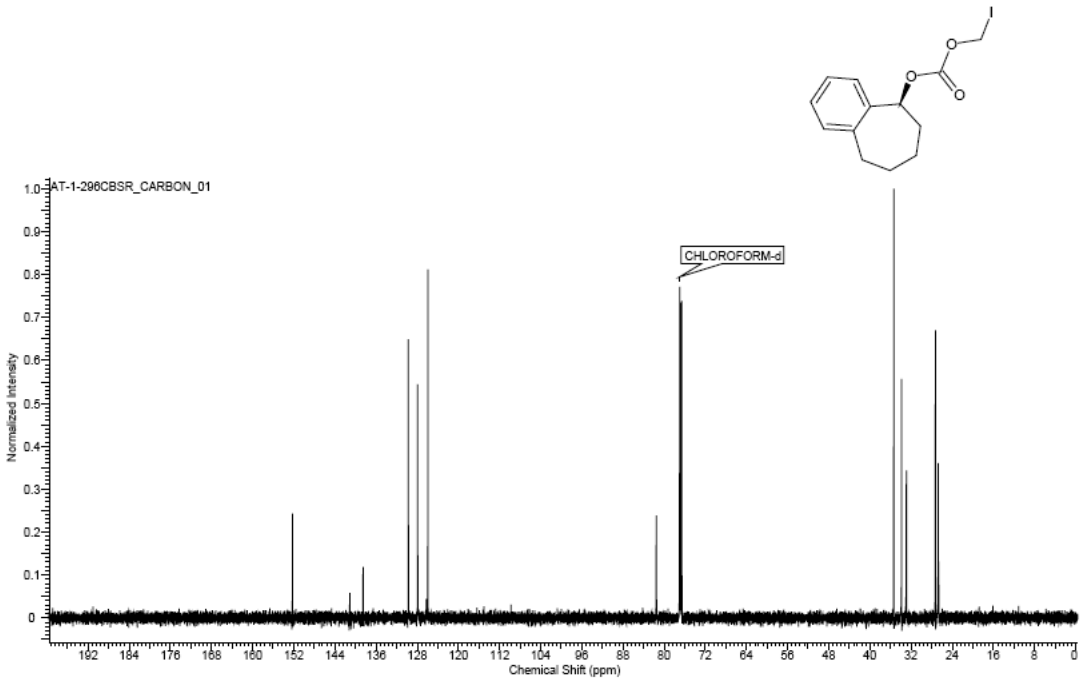

$^{1}$H NMR
Compound **17**

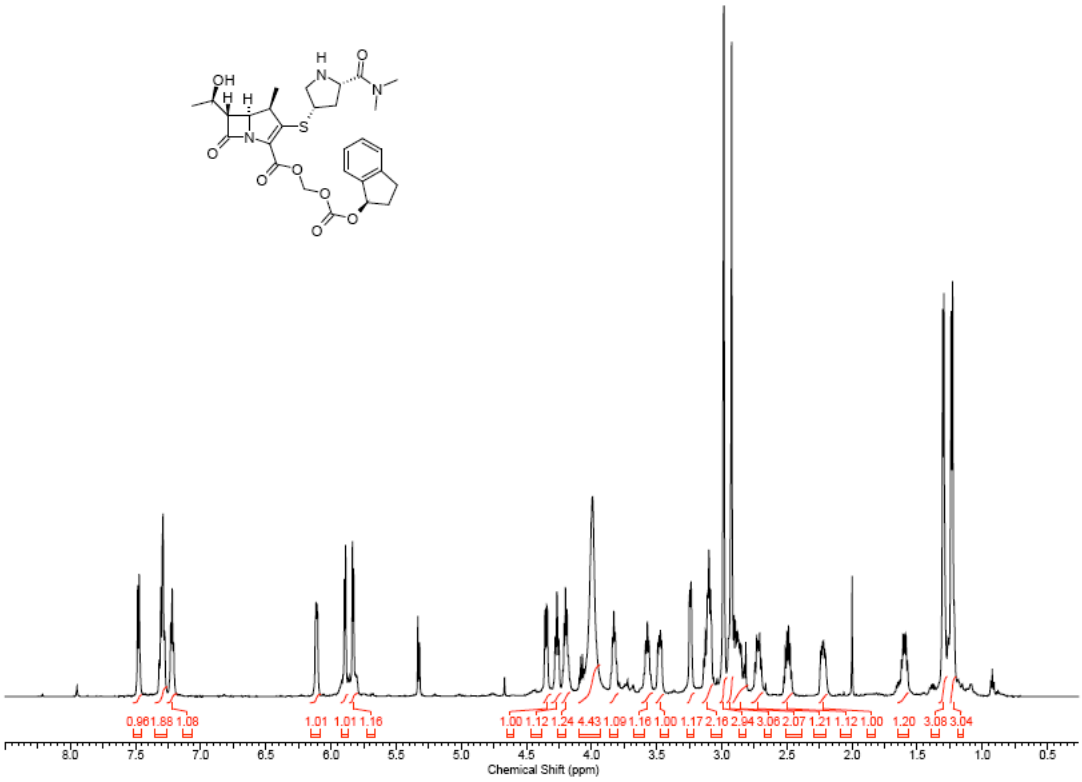

$^{13}$C NMR
Compound **17**

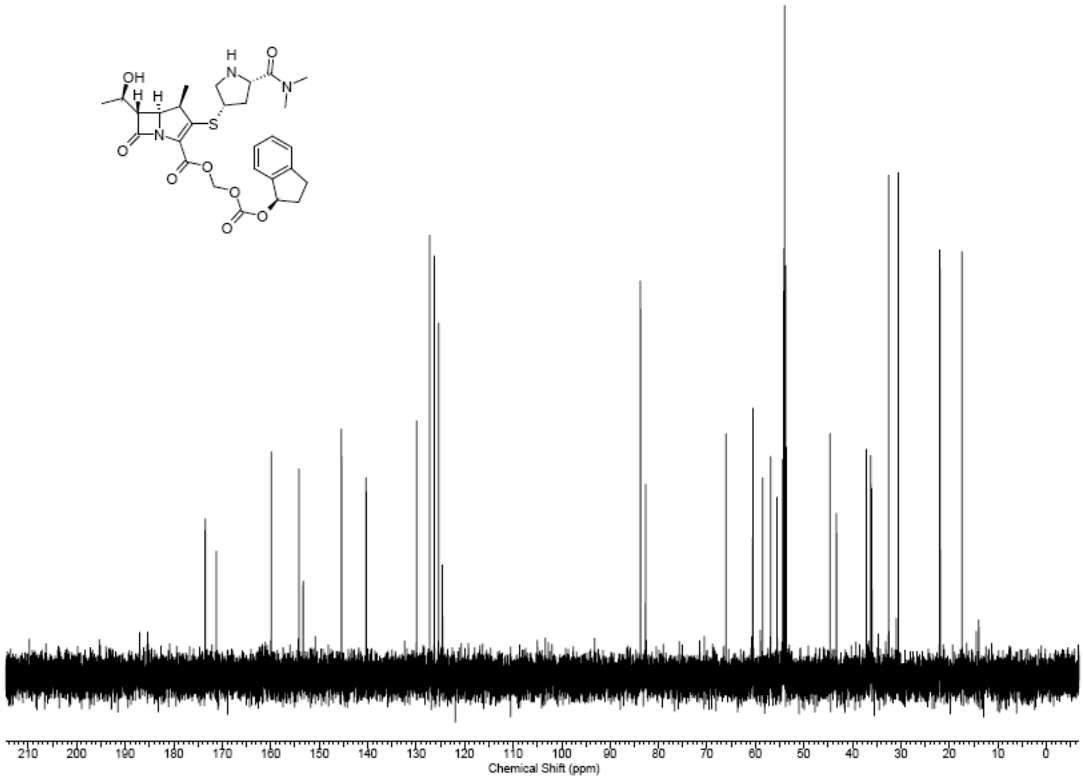

$^{1}$H NMR
Compound **18**

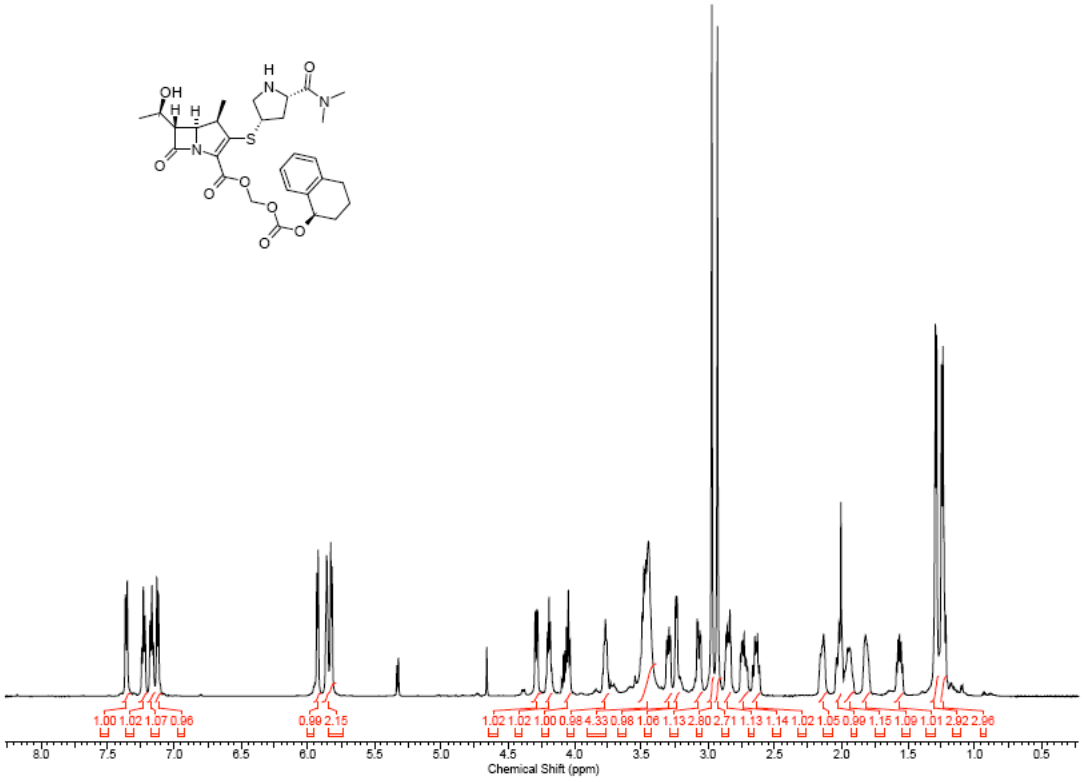

$^{13}$C NMR
Compound **18**

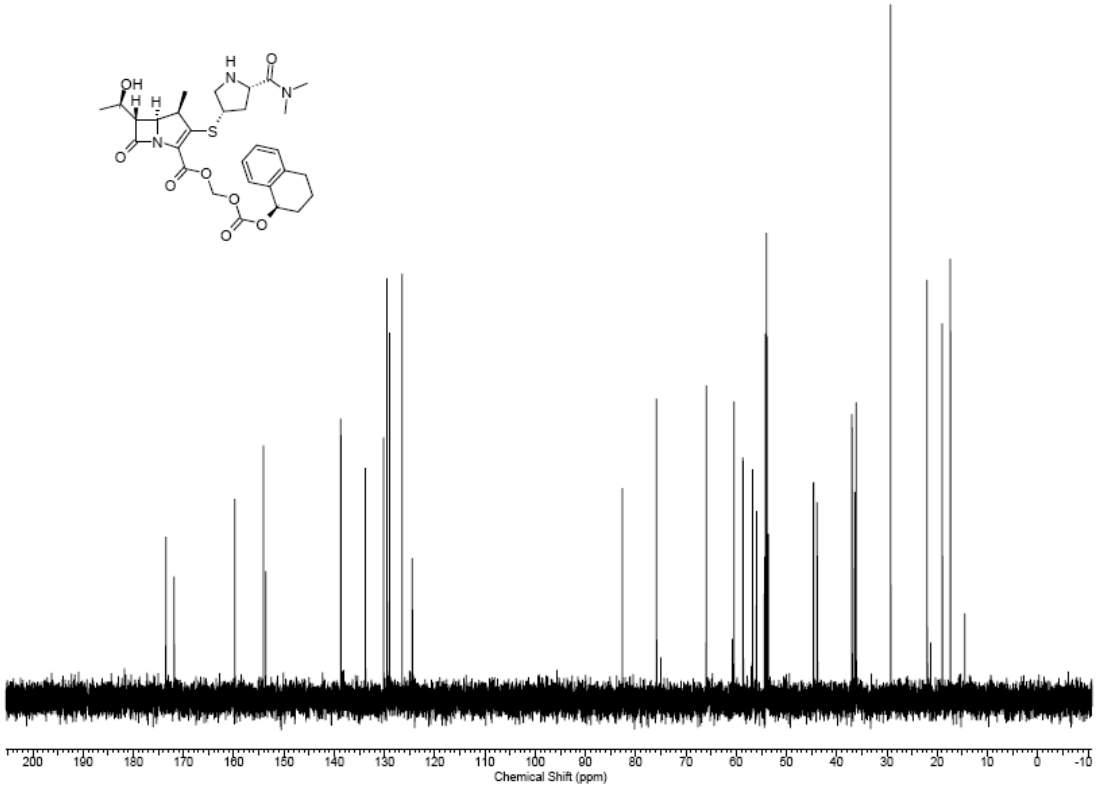

$^{1}$H NMR
Compound **19**

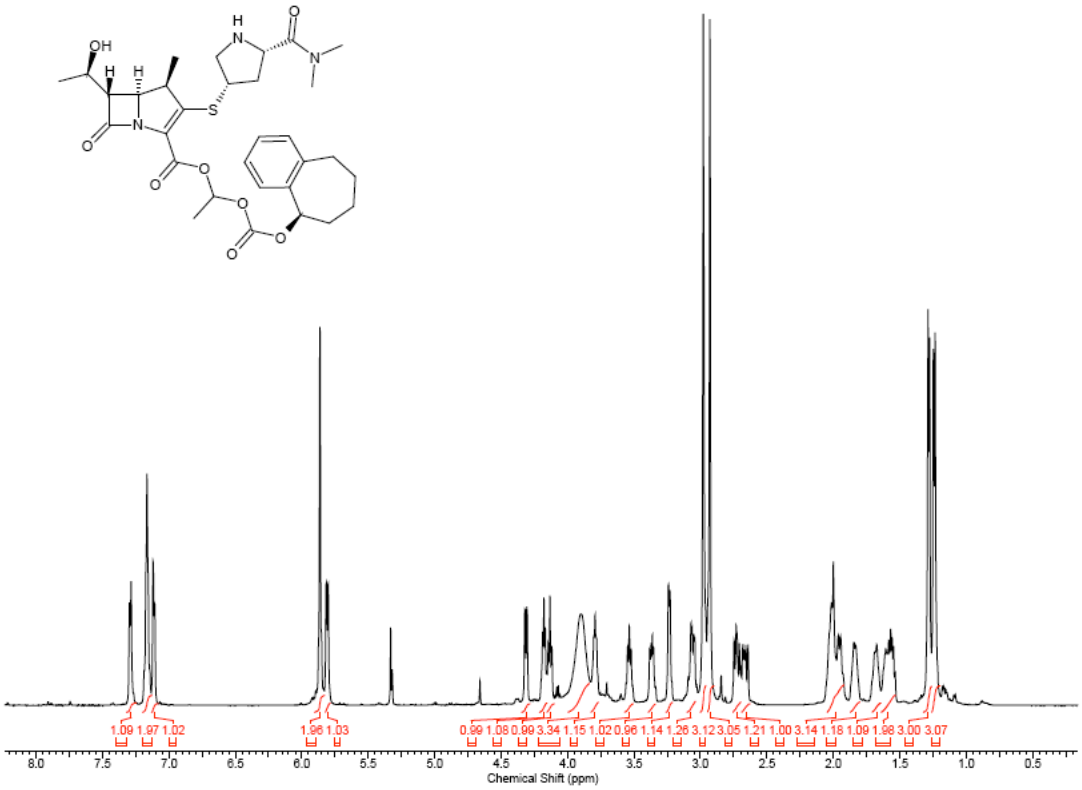

$^{13}$C NMR
Compound **19**

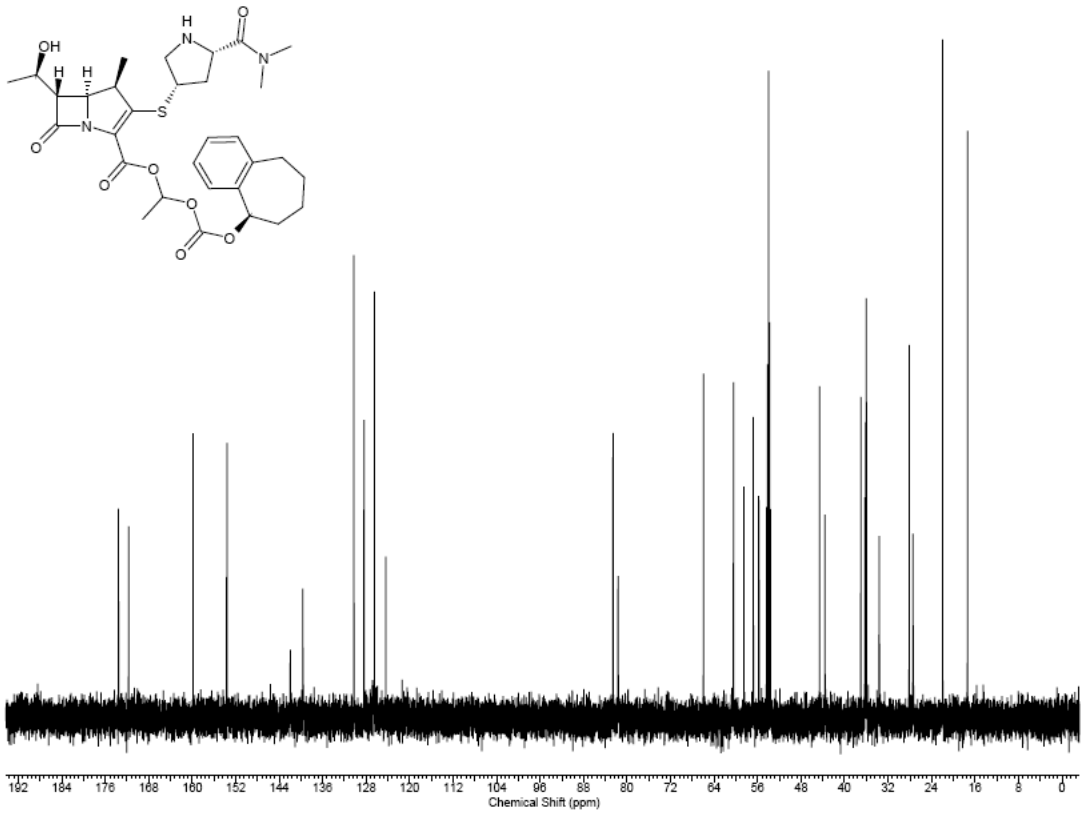

$^{1}$H NMR
Compound **20**

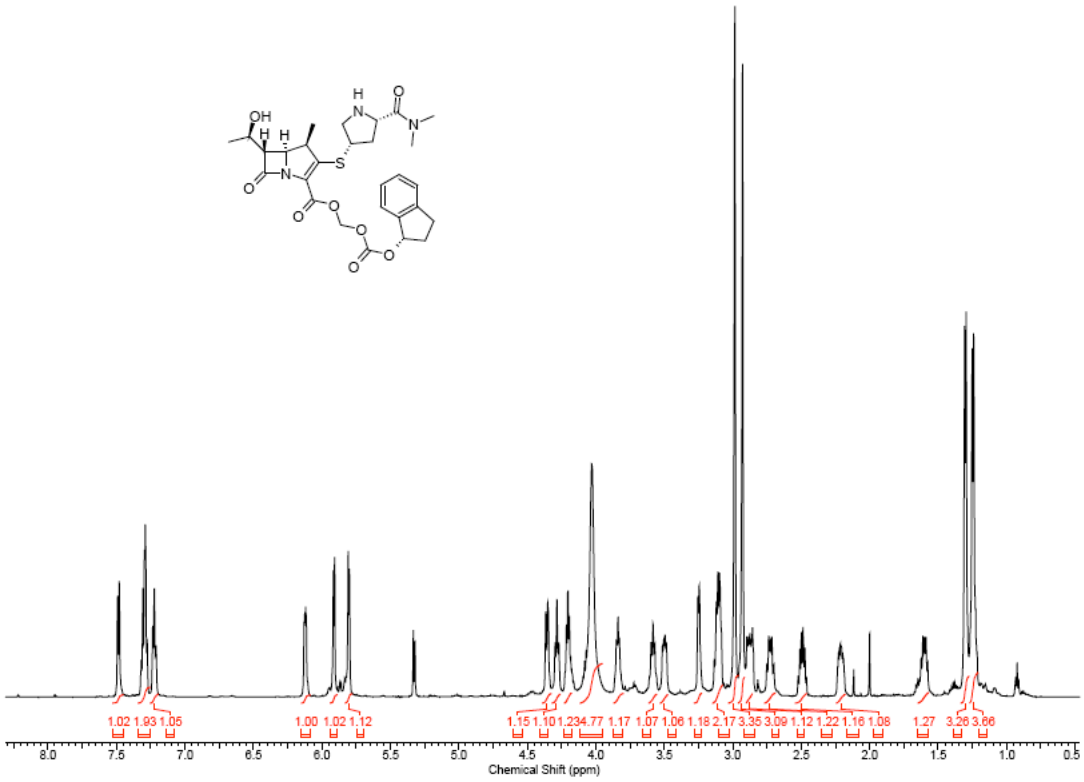

$^{13}$C NMR
Compound **20**

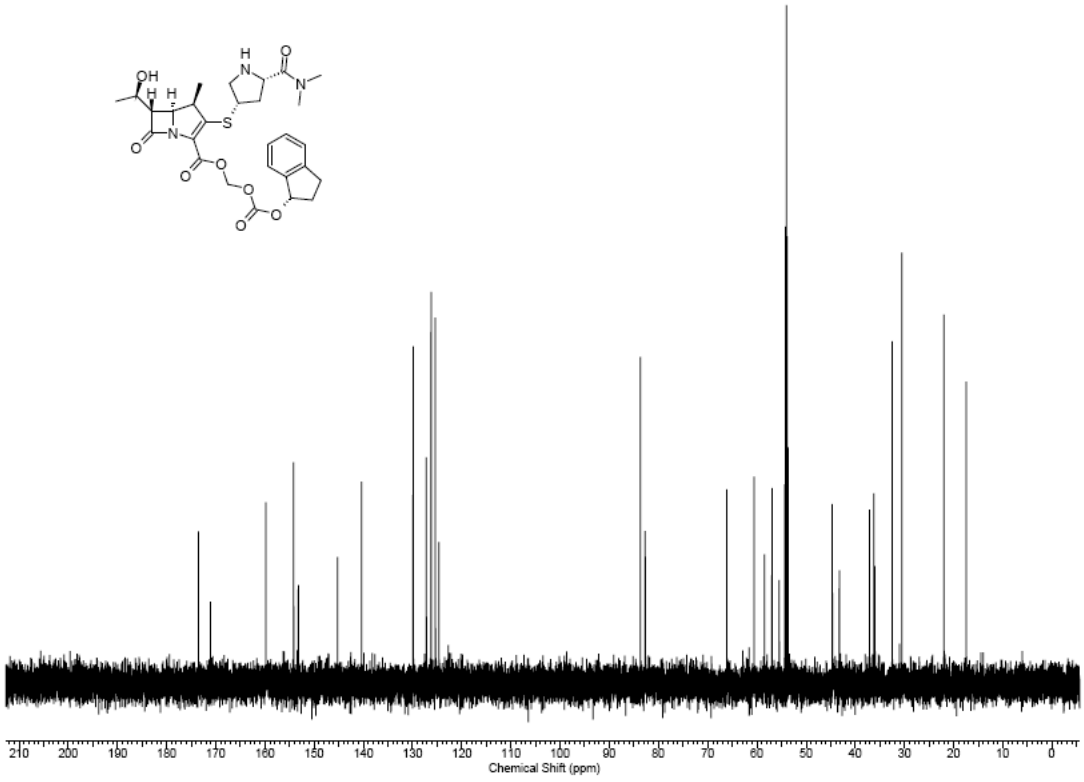

$^{1}$H NMR
Compound **21**

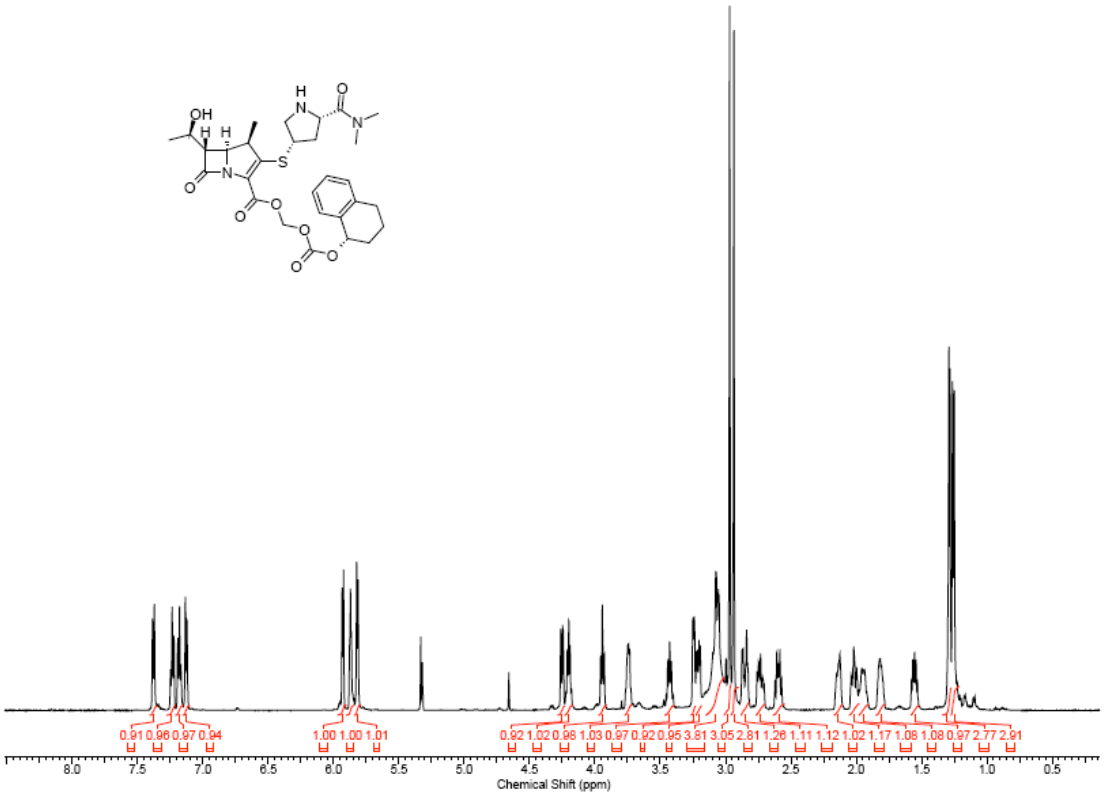

$^{13}$C NMR
Compound **21**

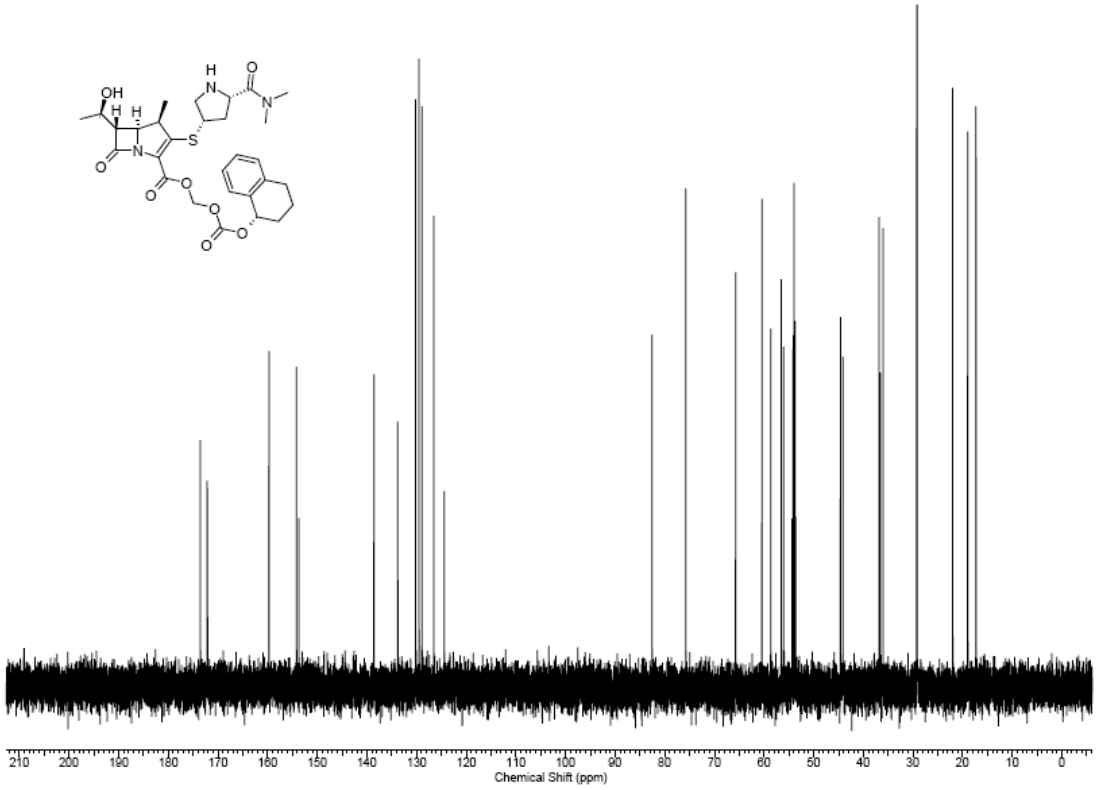

$^{1}$H NMR
Compound **22**

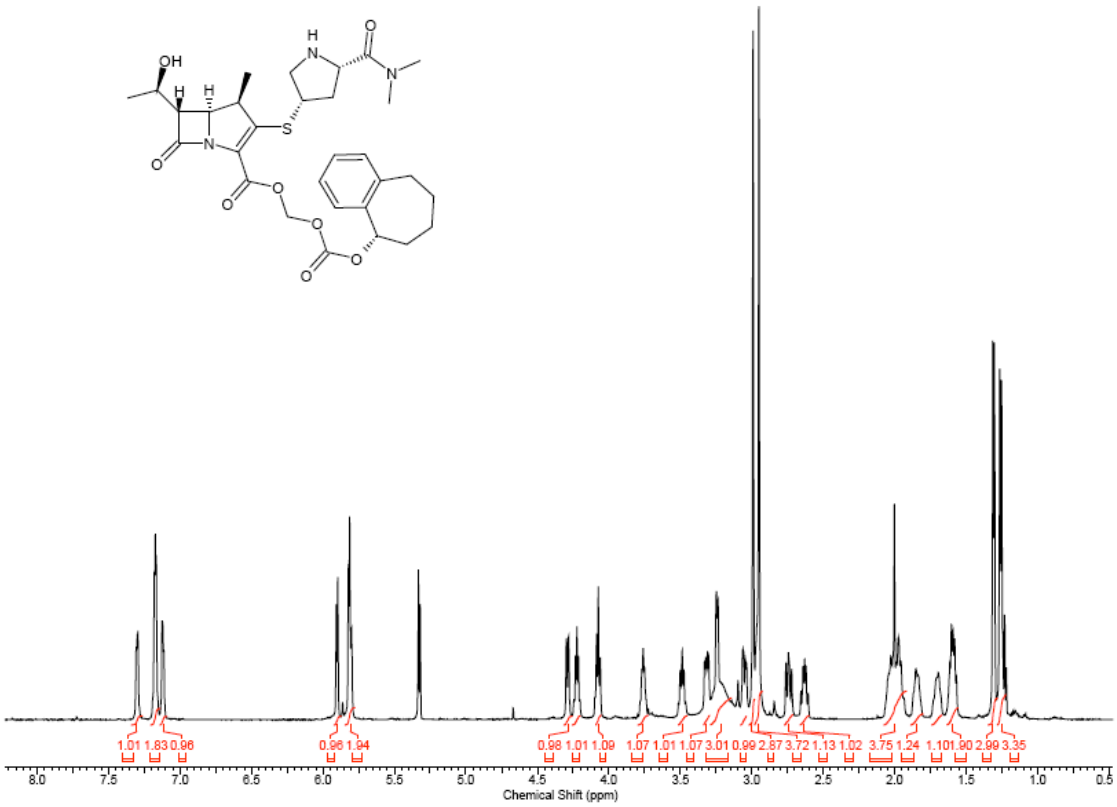

$^{13}$C NMR
Compound **22**

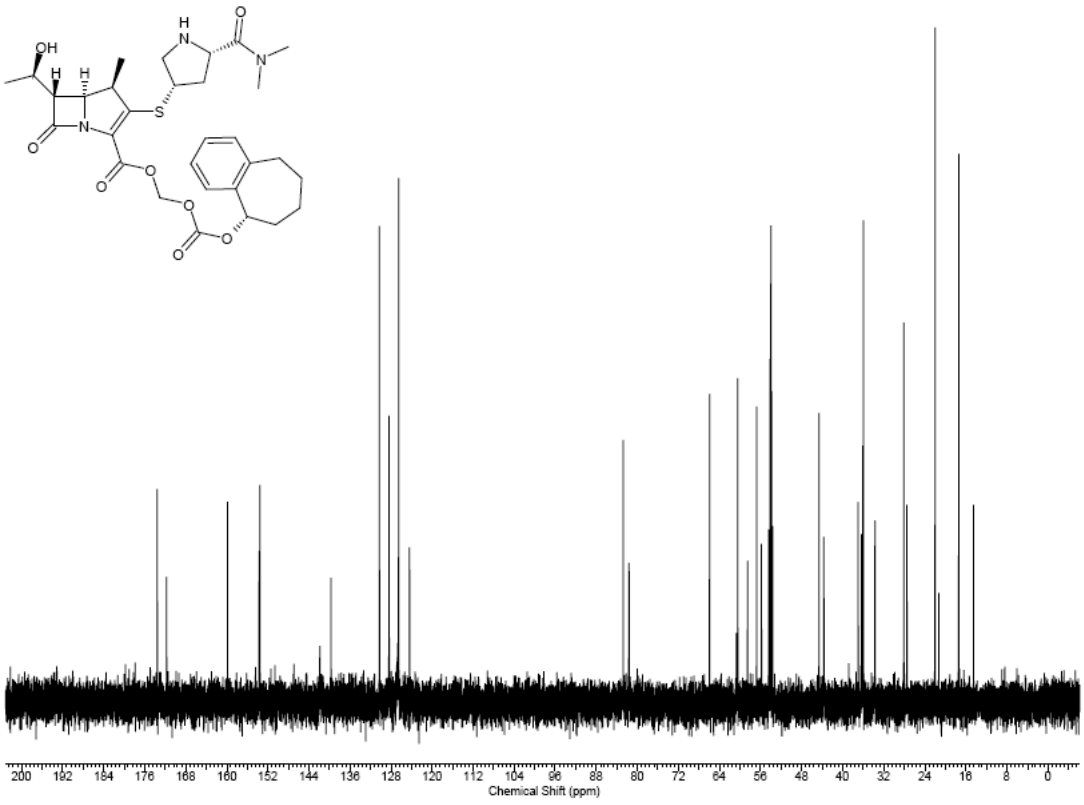

$^{13}$C NMR
Compound **23**

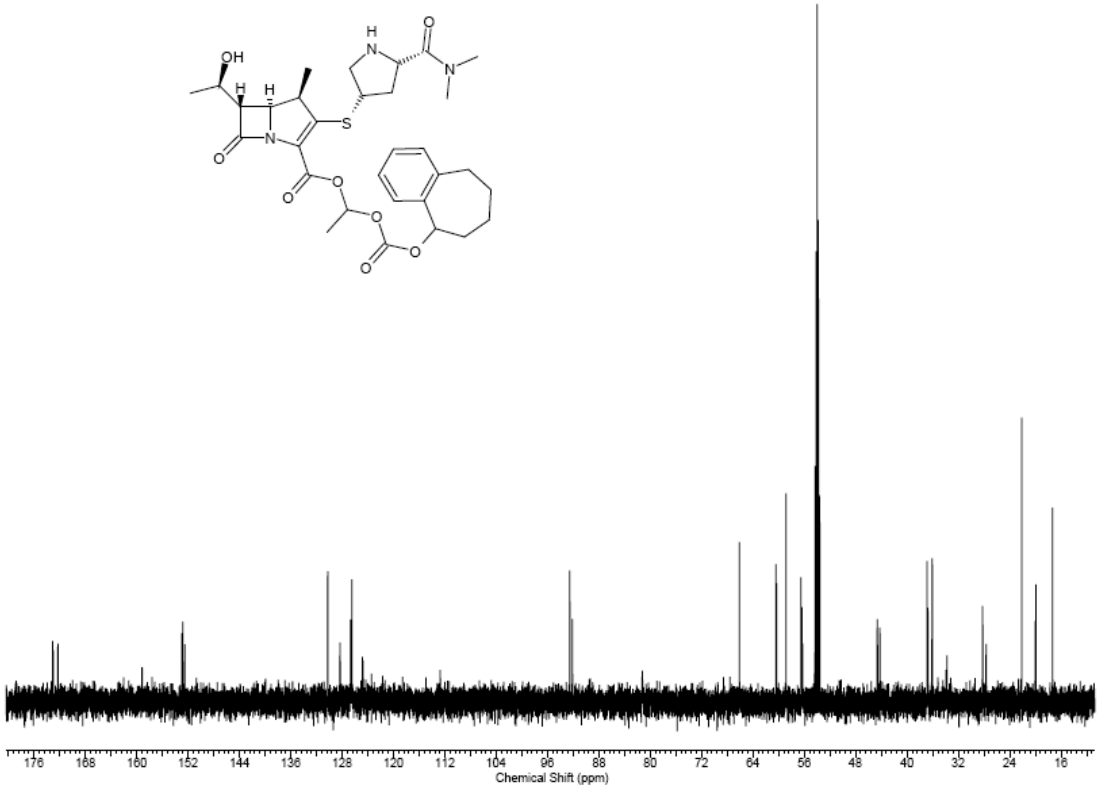

$^{1}$H NMR
Compound **29**

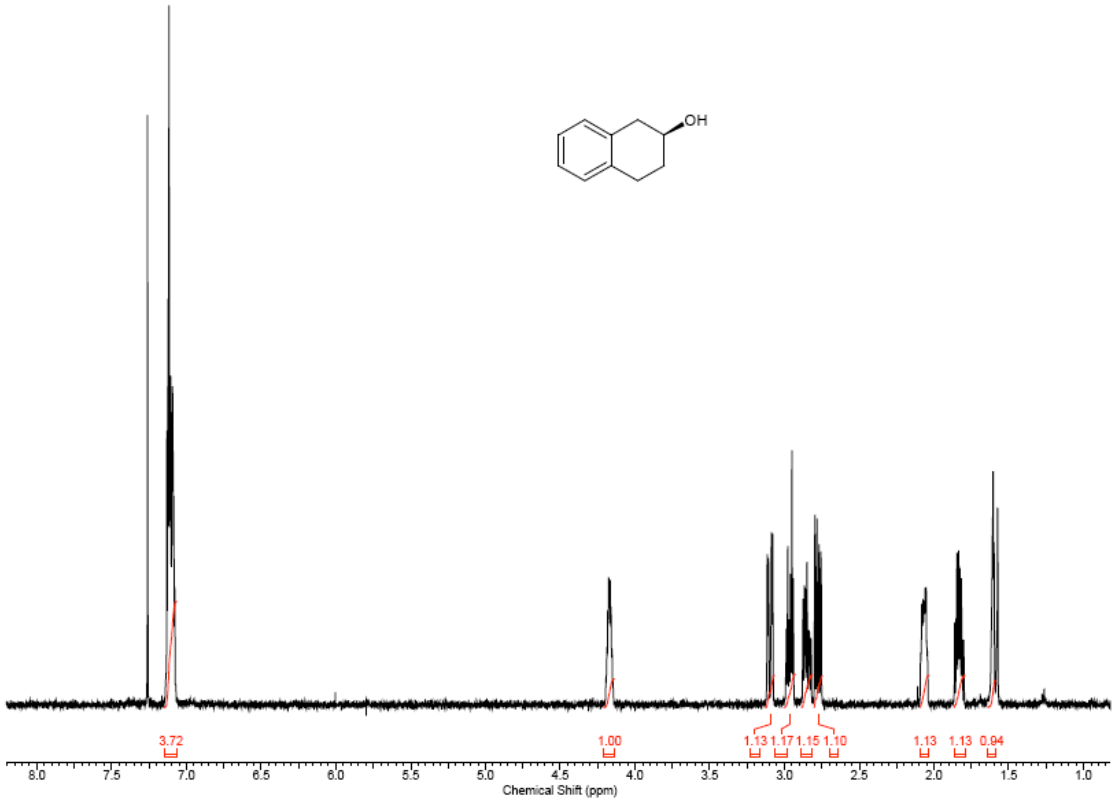

$^{13}$C NMR
Compound **29**

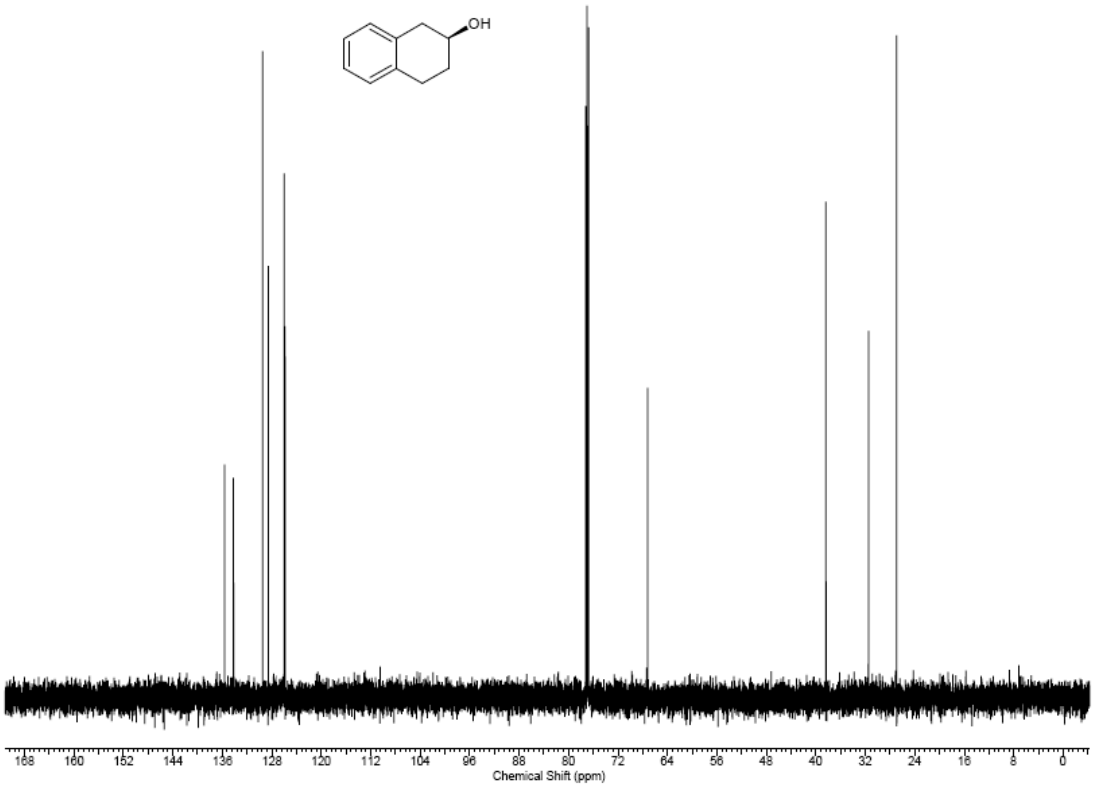

$^{1}$H NMR
Compound **30**

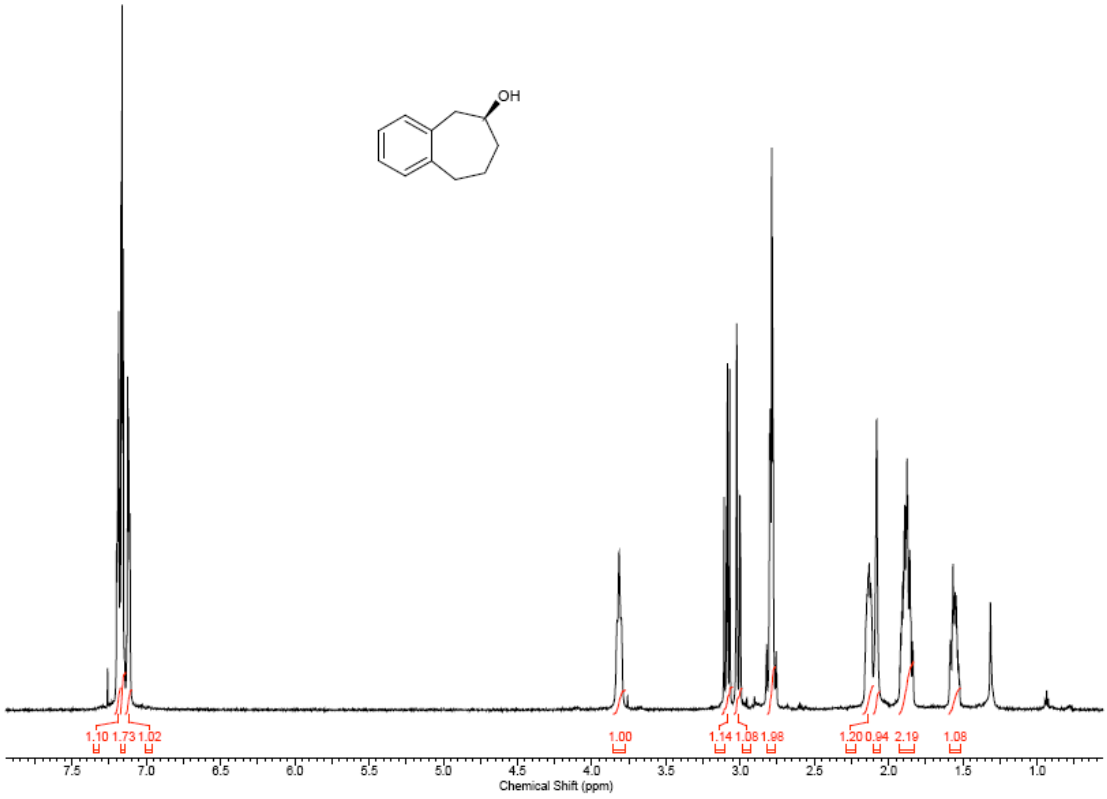

$^{13}$C NMR
Compound **30**

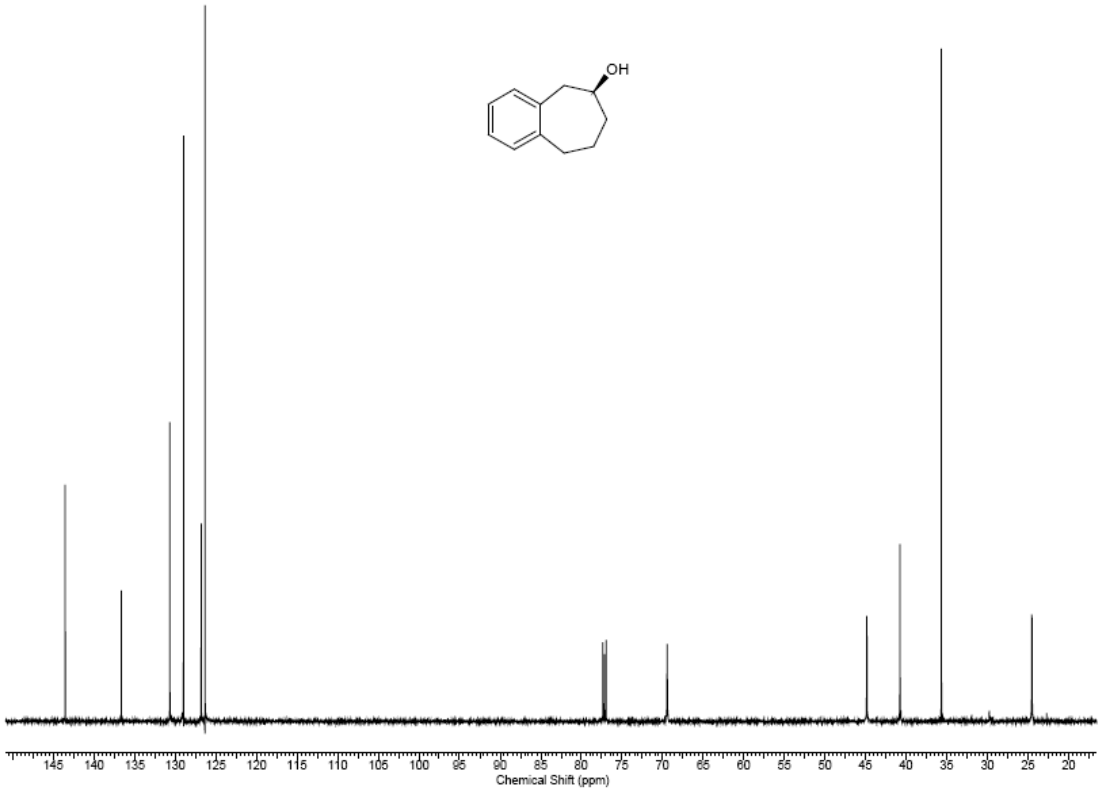

$^{1}$H NMR
Compound **31**

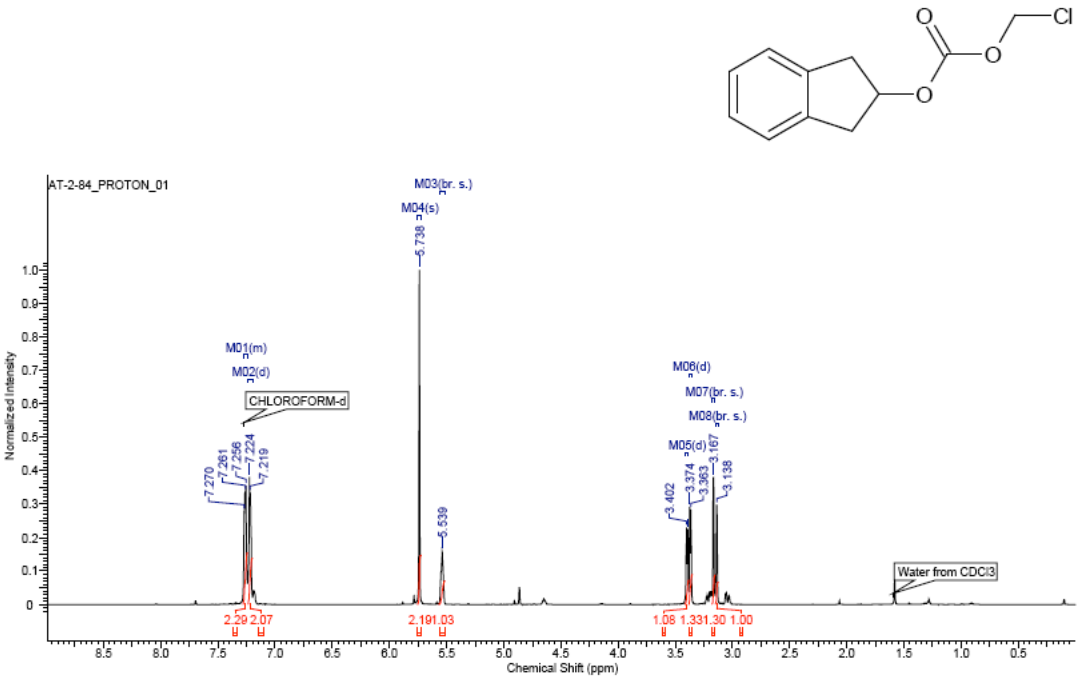

$^{13}$C NMR
Compound **31**

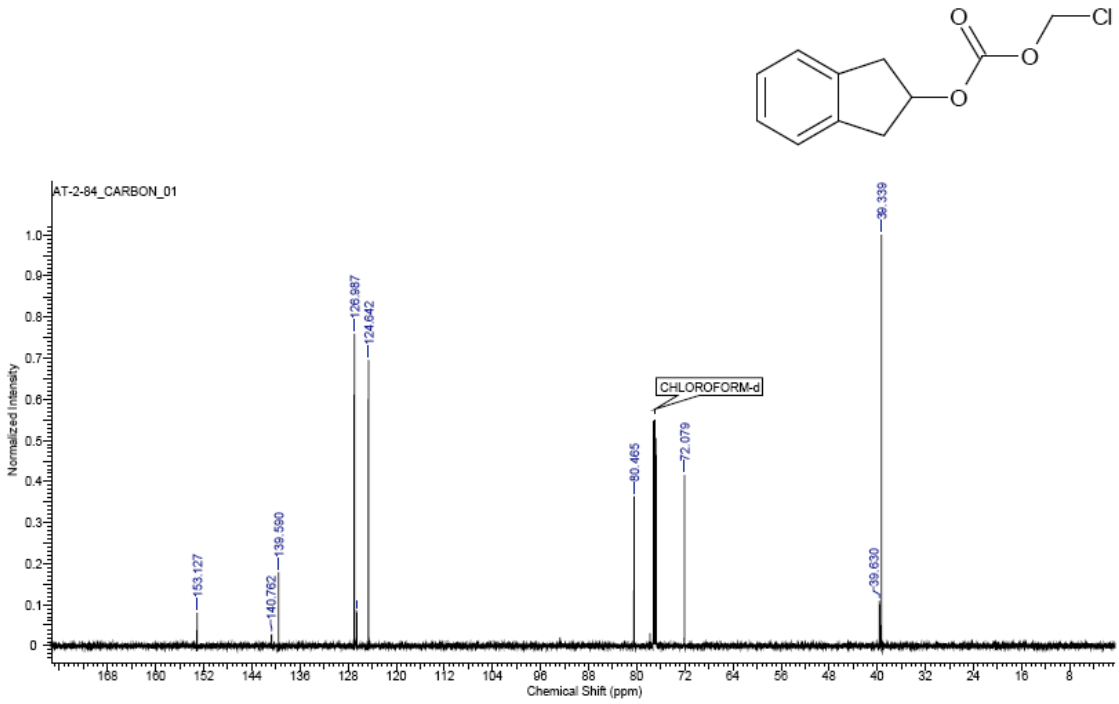

$^{1}$H NMR
Compound **32**

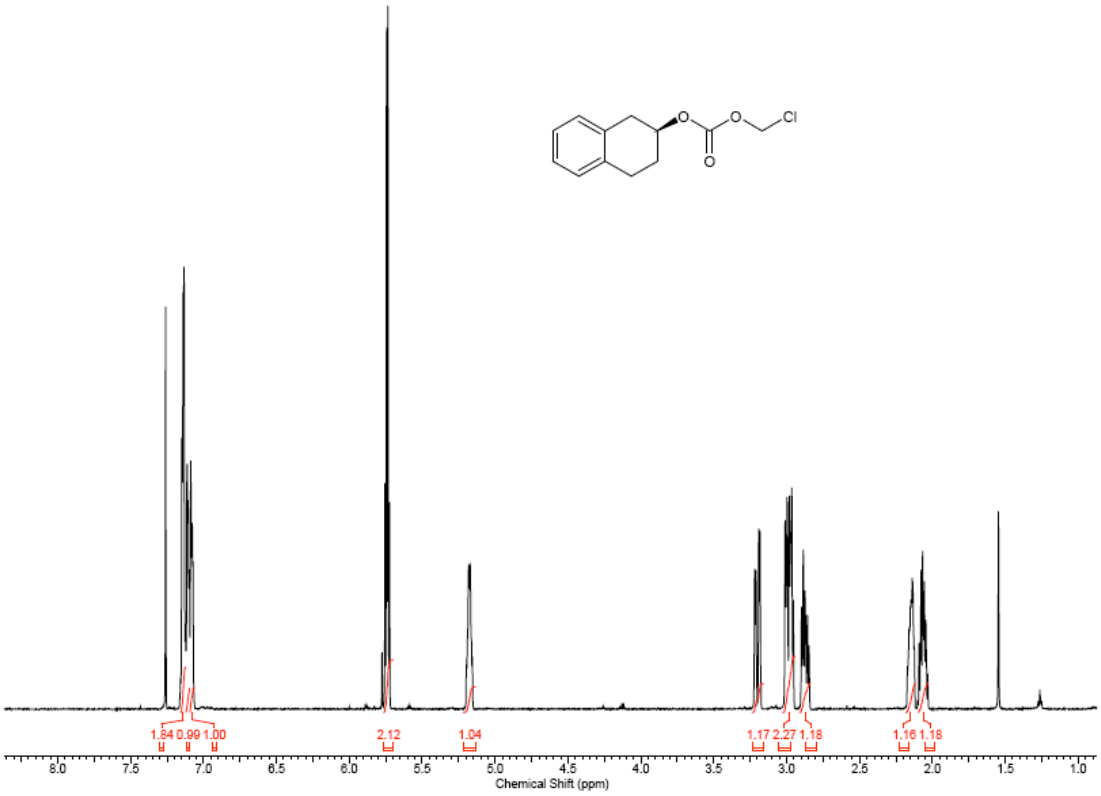

$^{1}$H NMR
Compound **33**

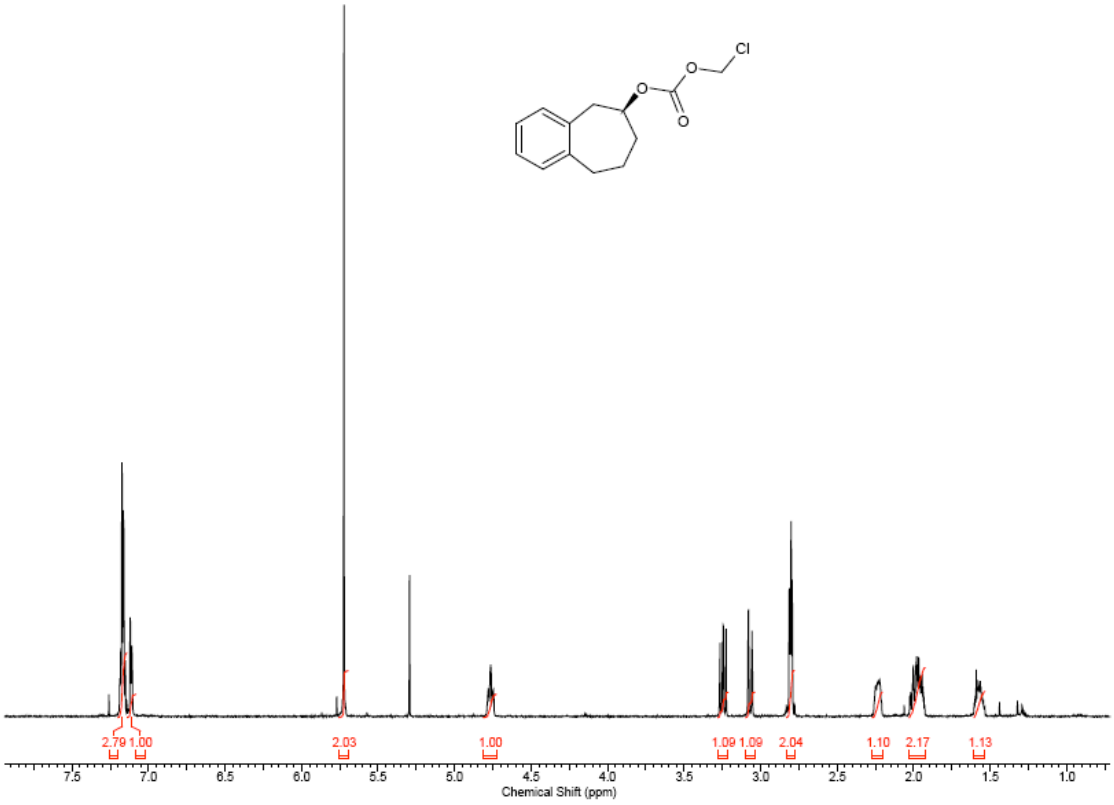

$^{13}$C NMR
Compound **33**

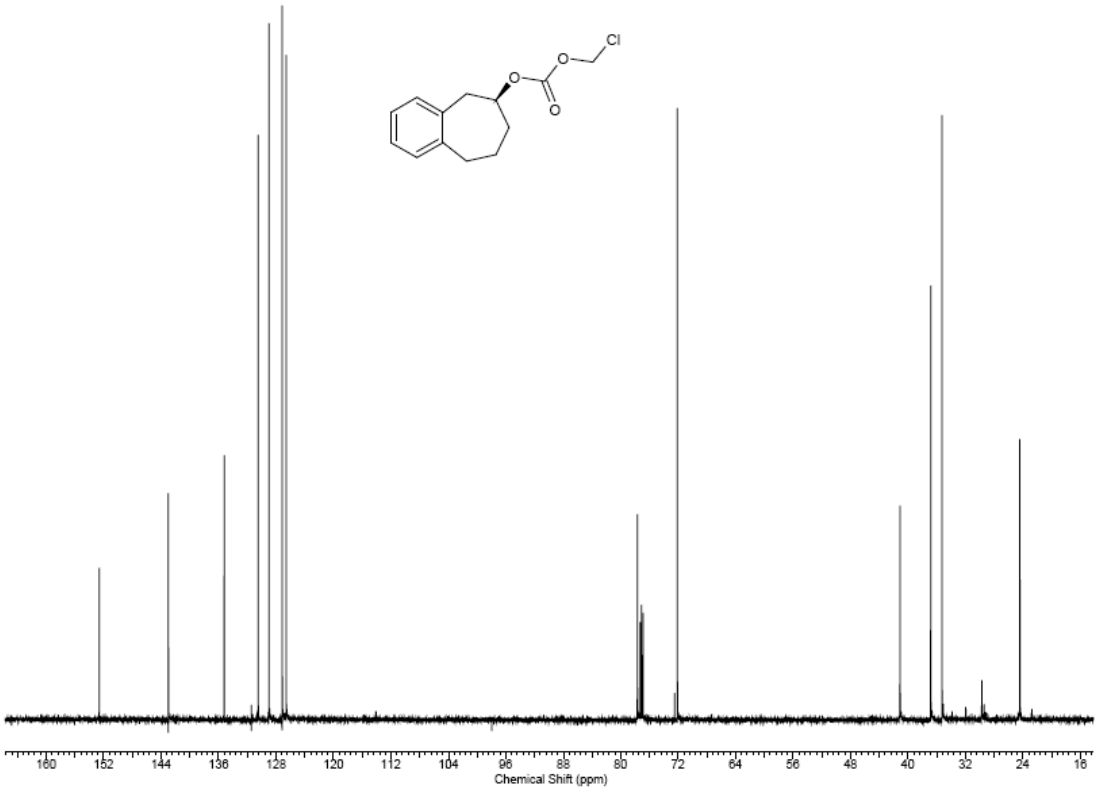

$^{1}$H NMR
Compound **34**

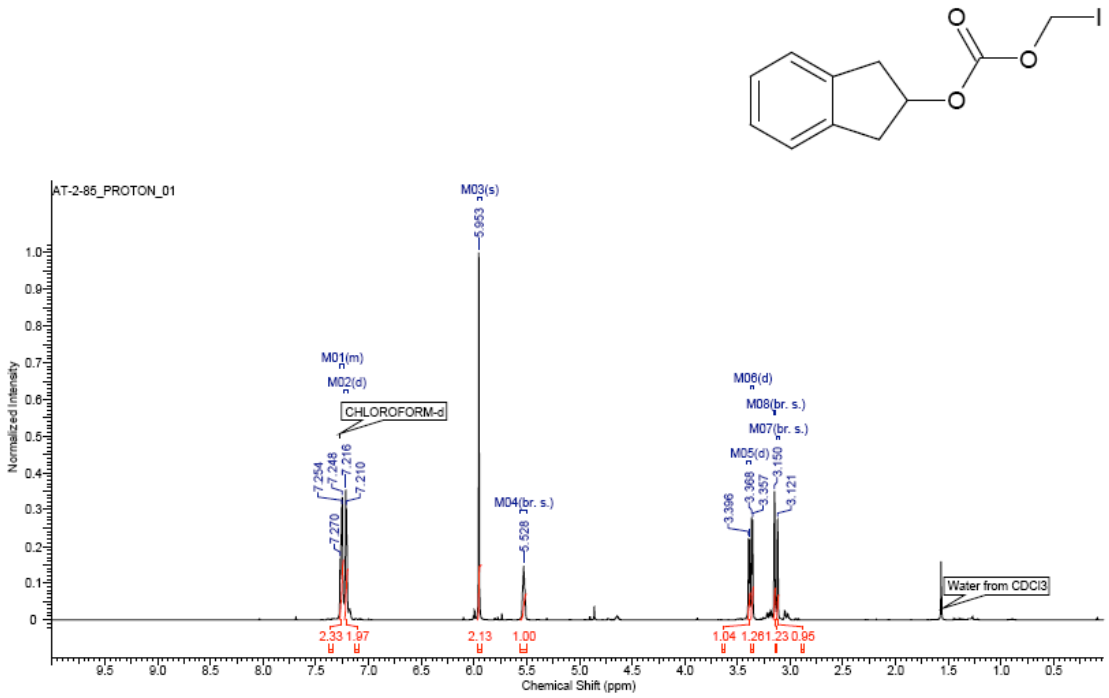

$^{13}$C NMR
Compound **34**

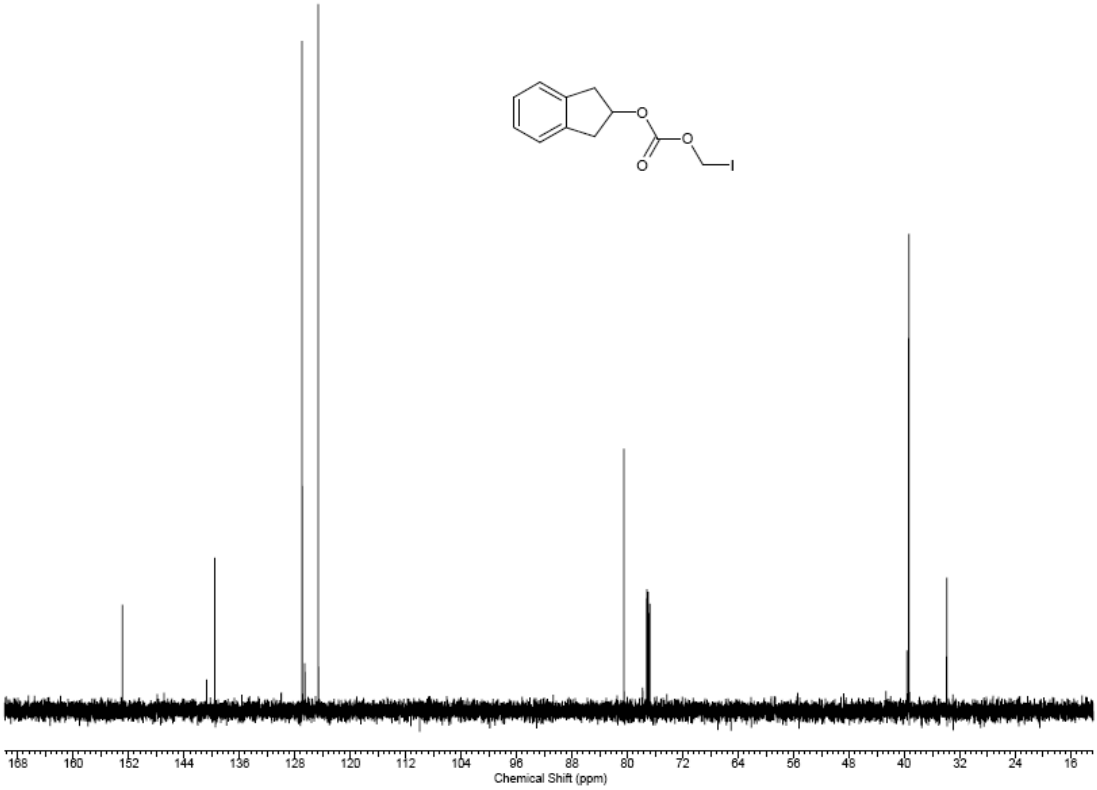

$^{1}$H NMR
Compound **35**

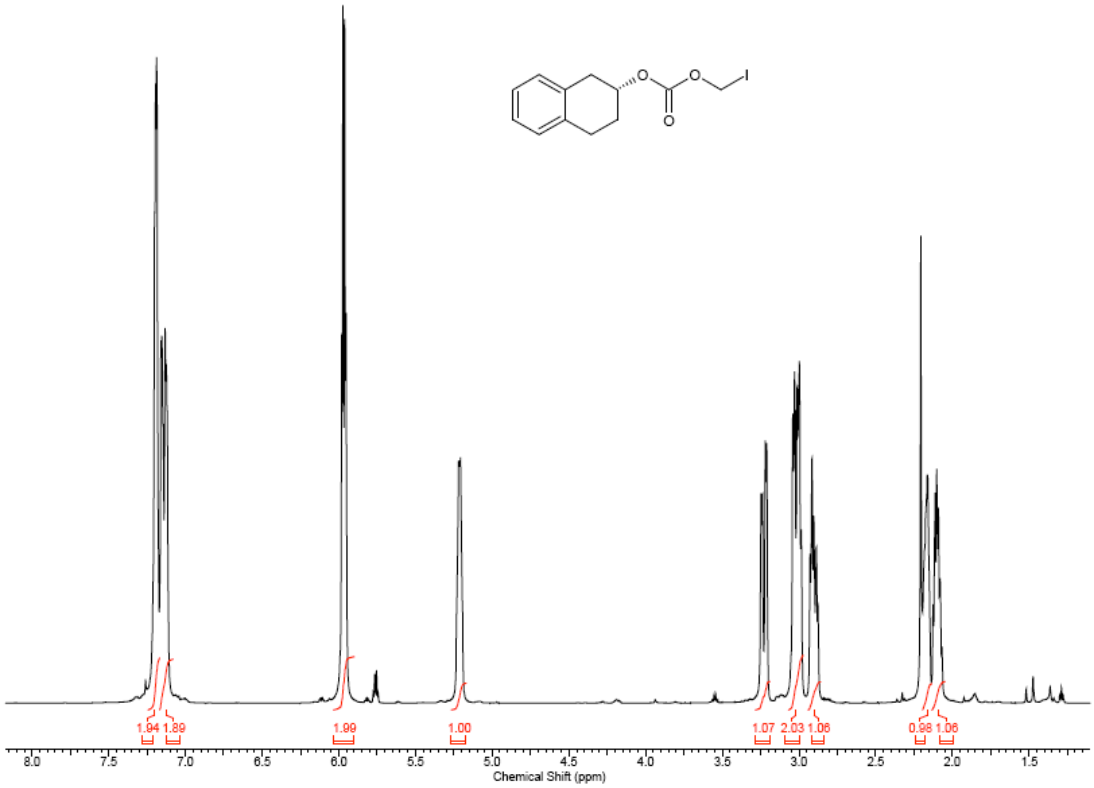

$^{13}$C NMR
Compound **35**

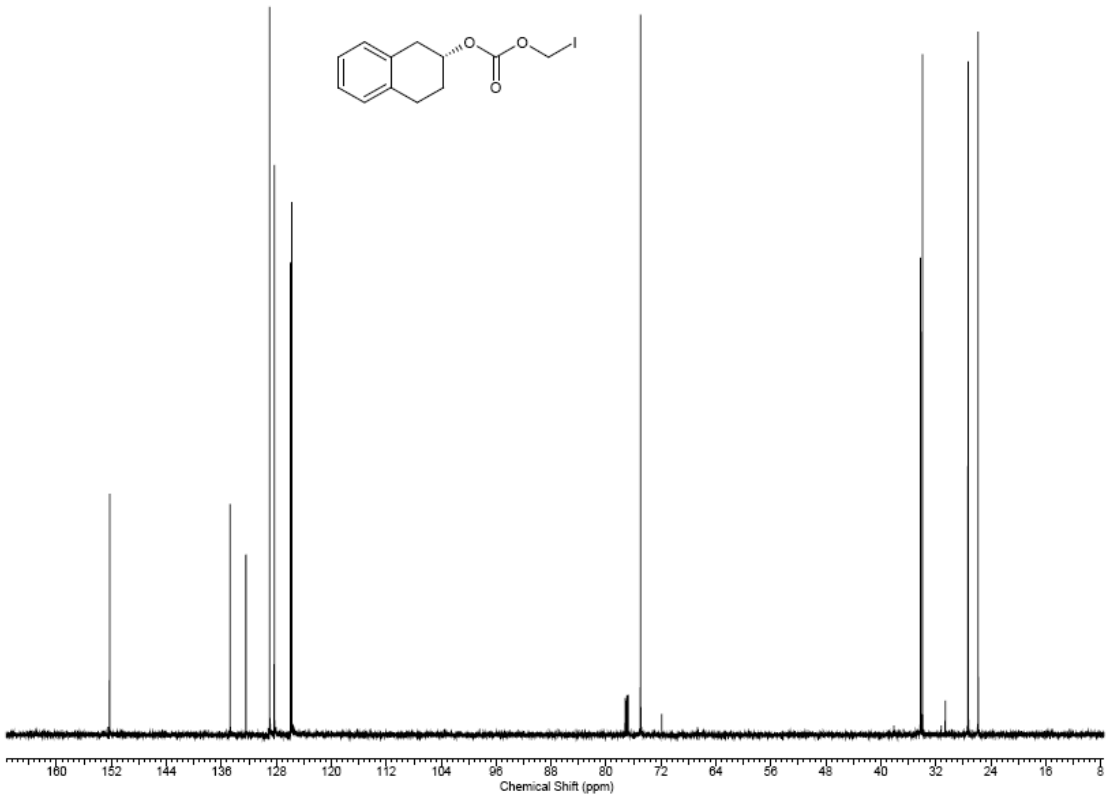

$^{1}$H NMR
Compound **36**

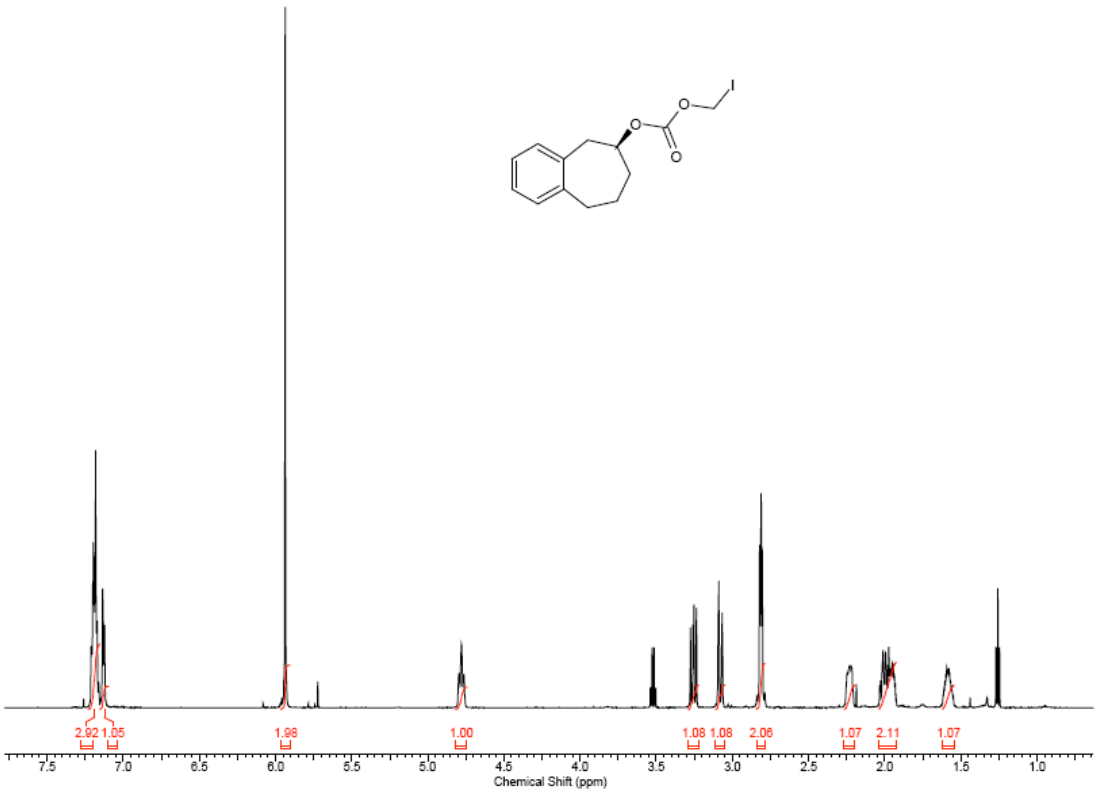

$^{13}$C NMR
Compound **36**

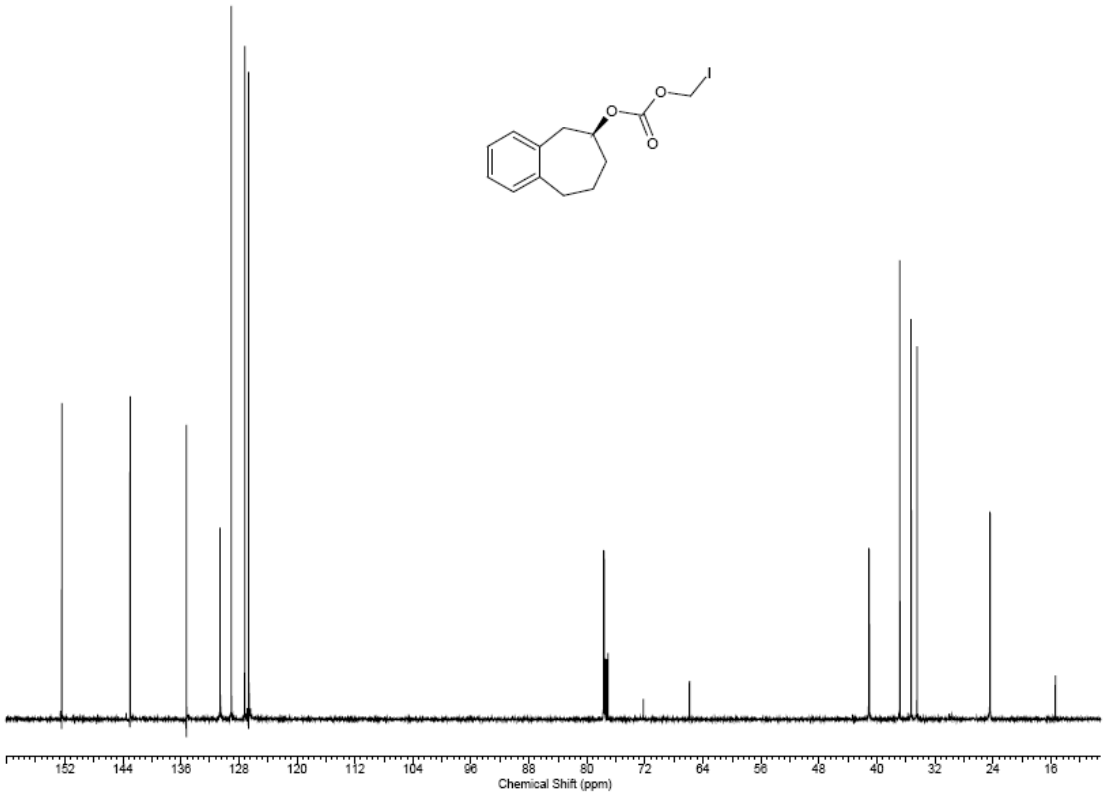

$^{1}$H NMR
Compound **37**

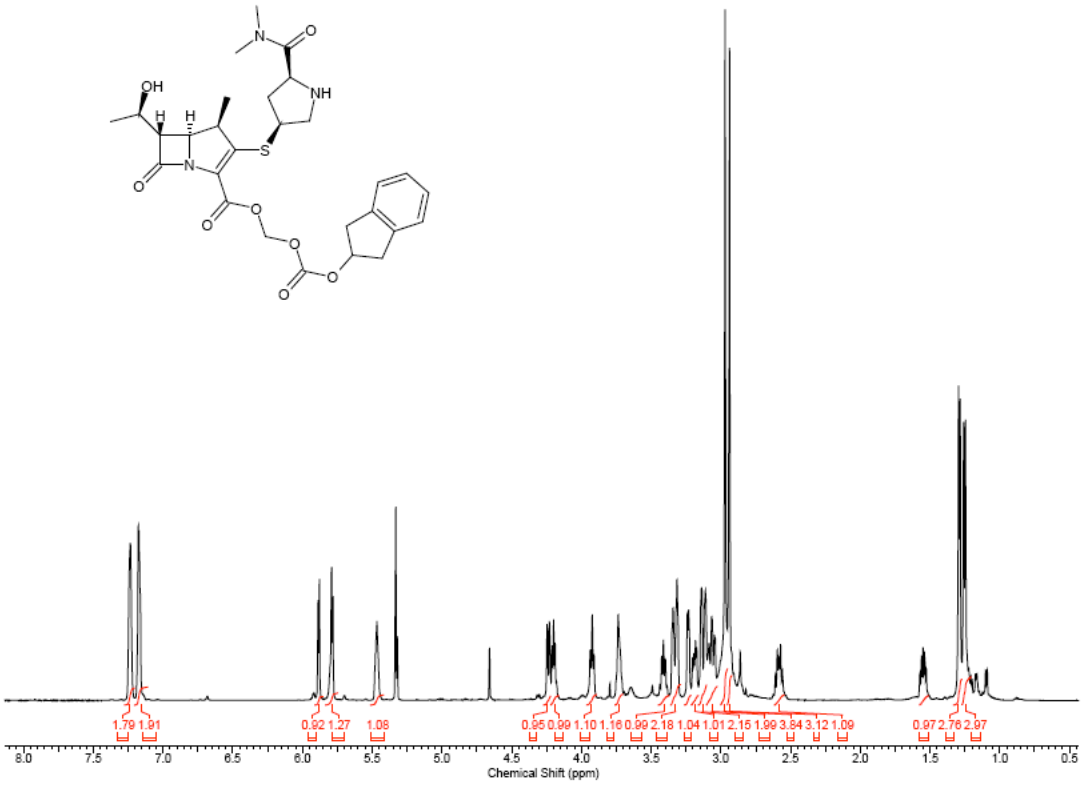

$^{13}$C NMR
Compound **37**

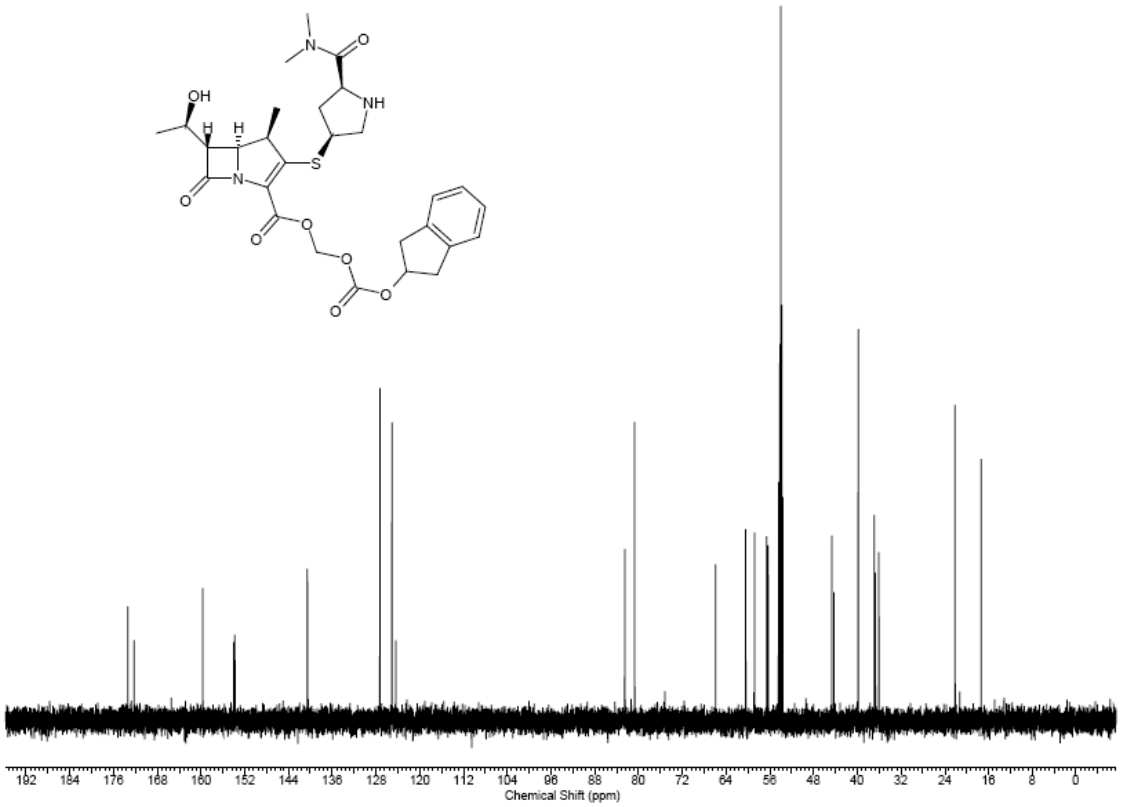

$^{1}$H NMR
Compound **38**

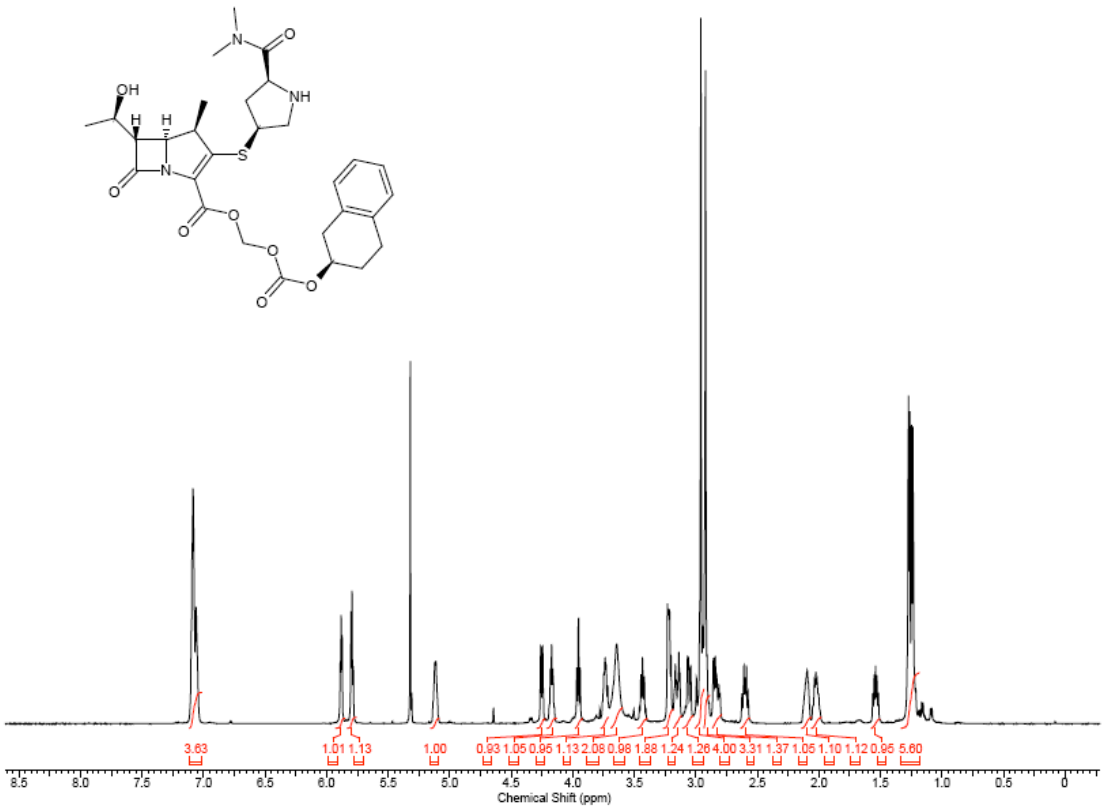

$^{13}$C NMR
Compound **38**

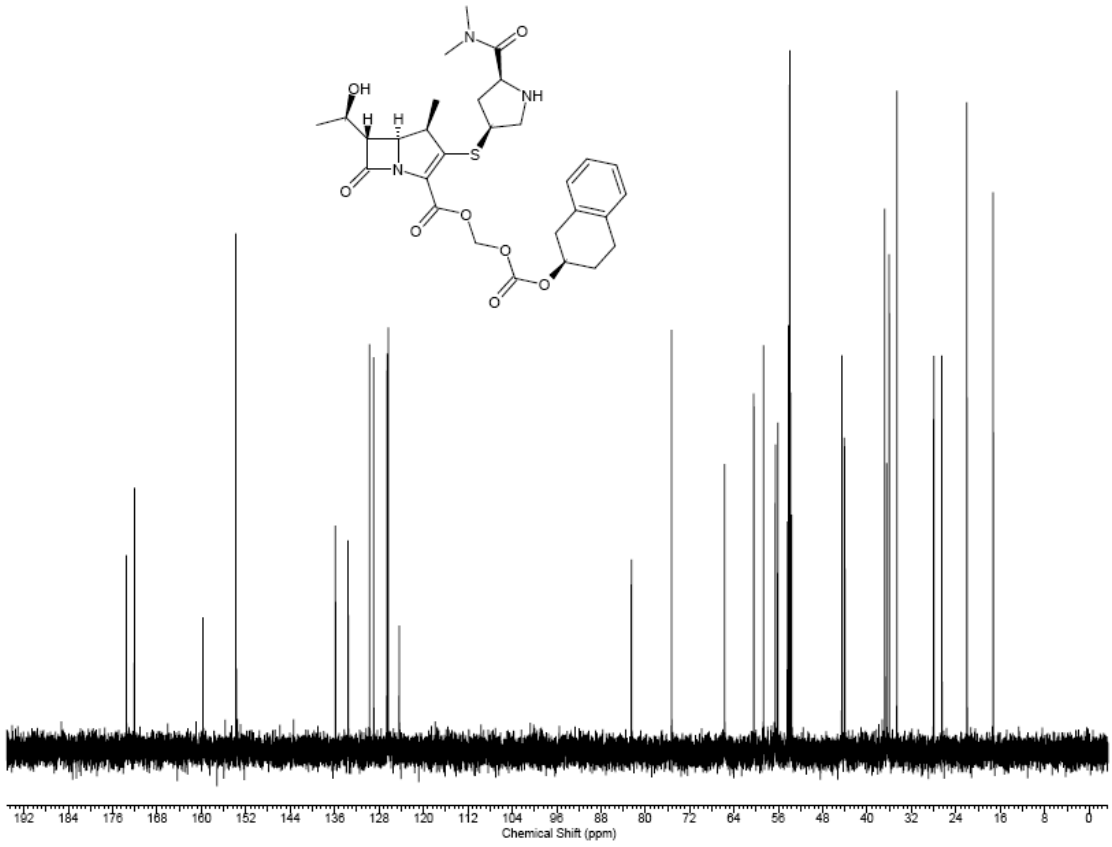

$^{1}$H NMR
Compound **39**

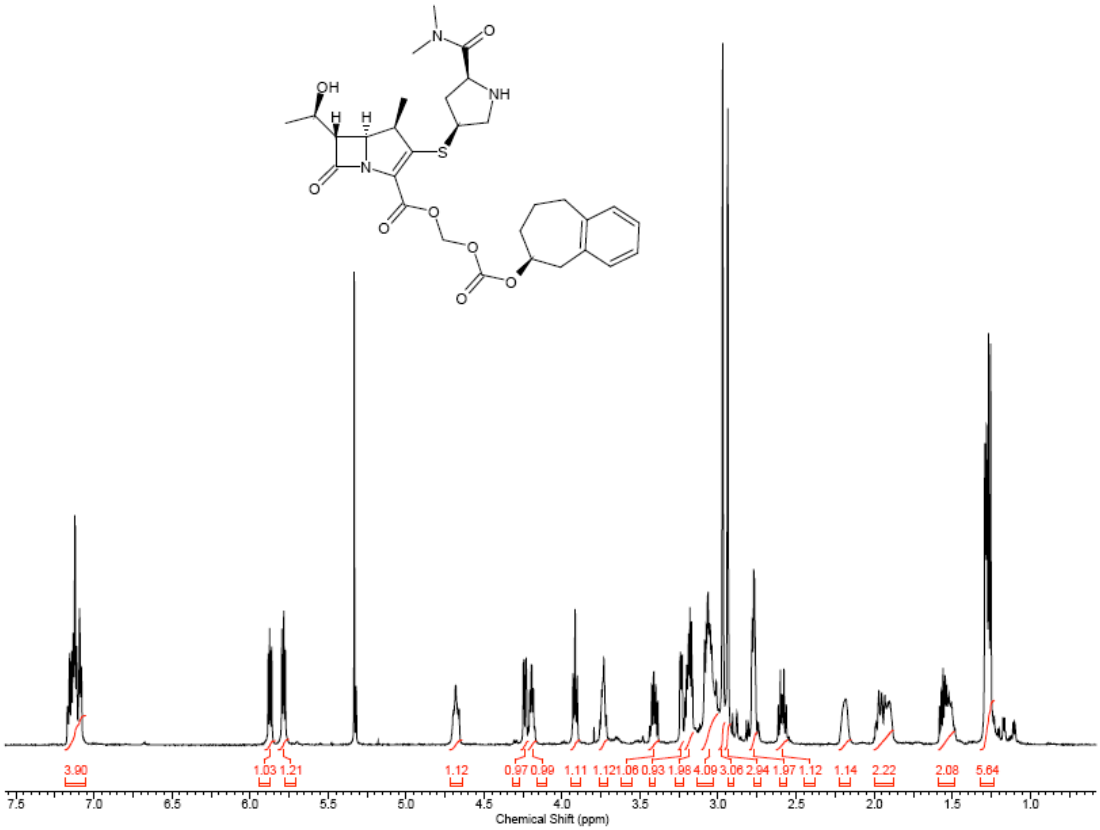

$^{13}$C NMR
Compound **39**

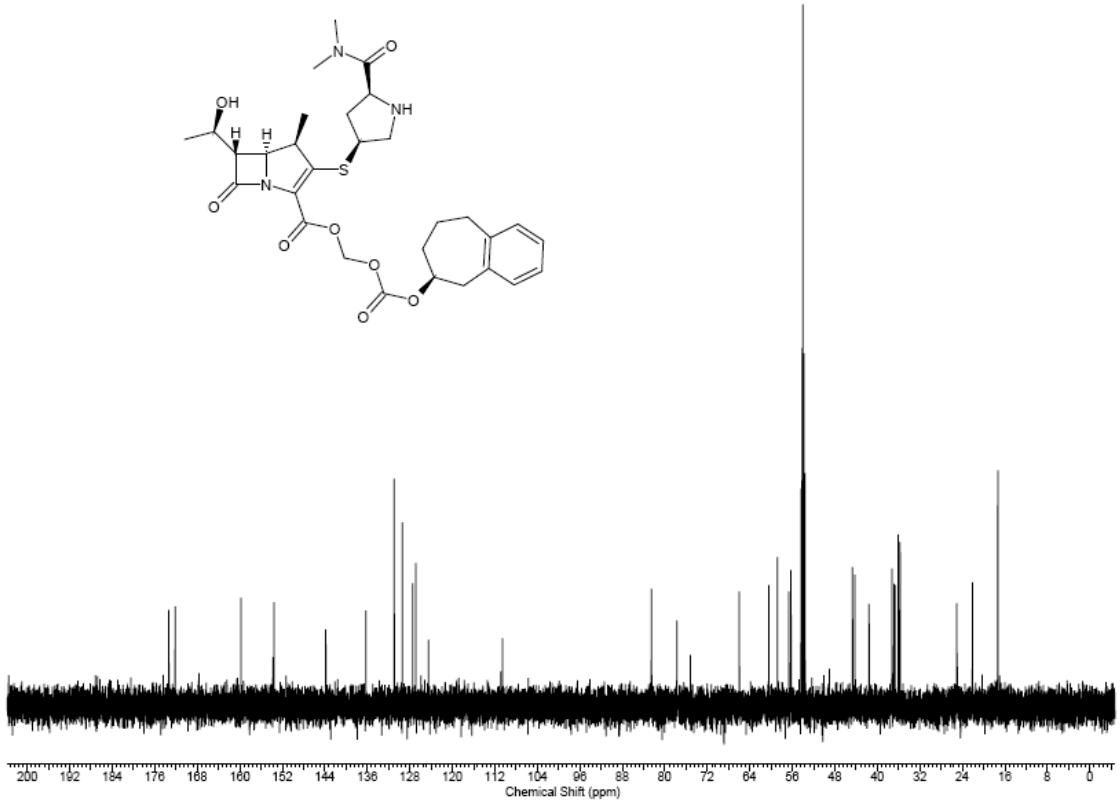

$^{1}$H NMR
Compound **41**

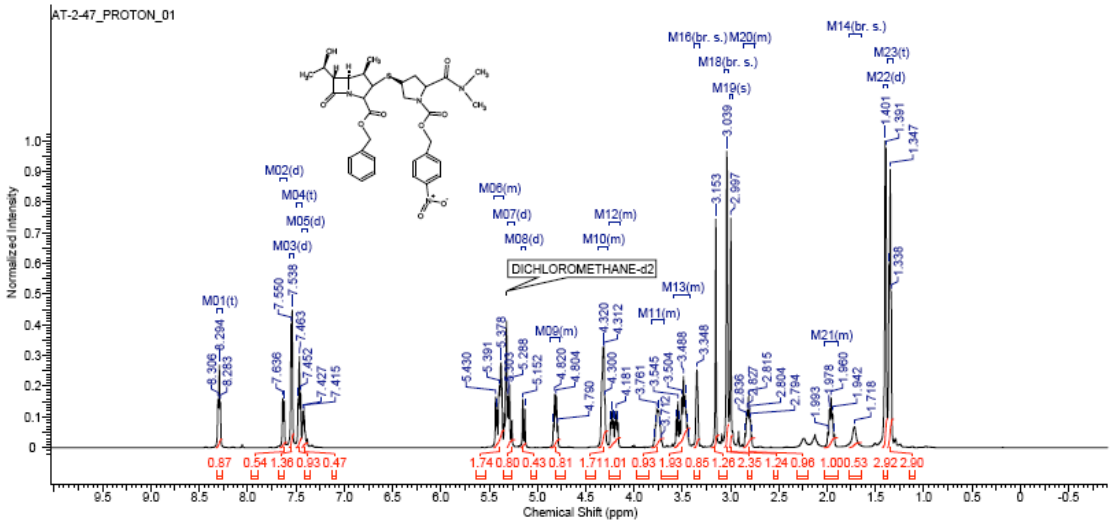

$^{13}$C NMR
Compound **41**

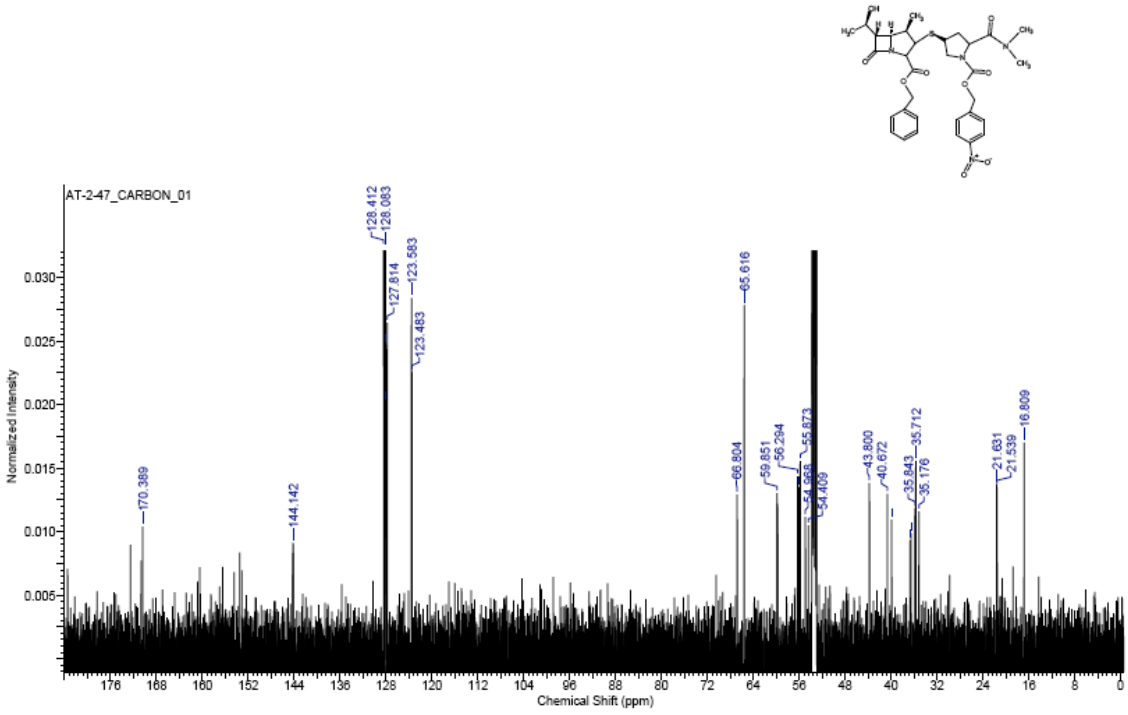

$^{1}$H NMR
Compound **42**

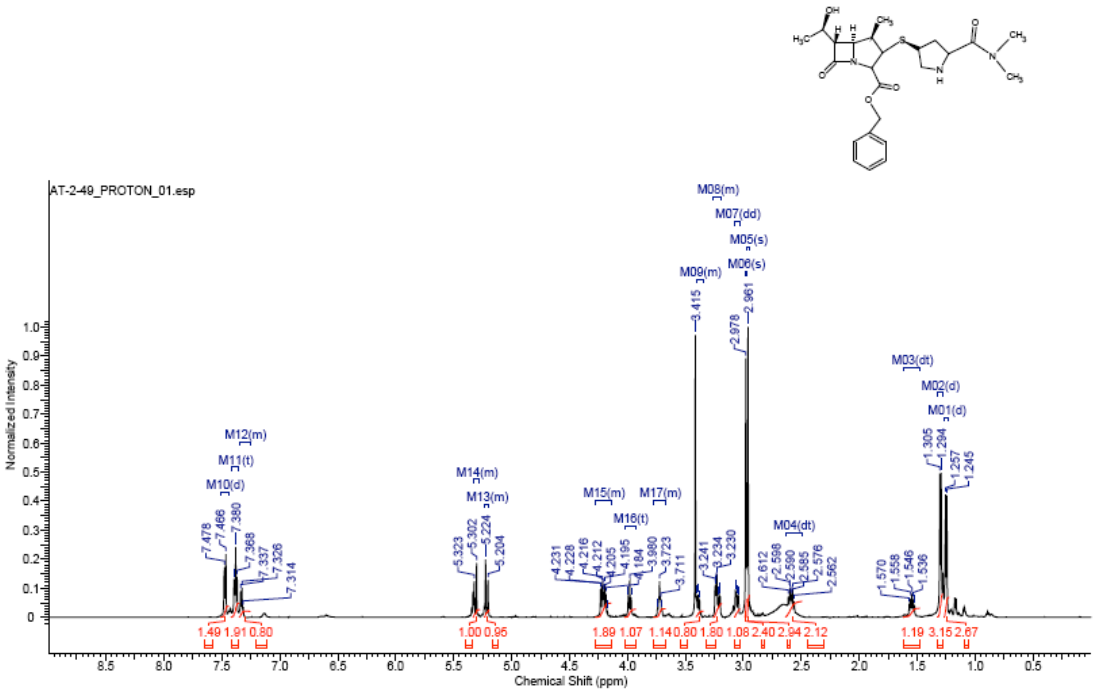

$^{13}$C NMR
Compound **42**